Synthesis and Properties of Tailor-Made Cycloolefin Copolymers Using an *ansa*-Fluorenylamidodimethyltitanium-$[Ph_3C][B(C_6F_5)_4]$ Catalyst System

(*ansa*-フルオレニルアミドジメチルチタン-$[Ph_3C][B(C_6F_5)_4]$ 触媒系を用いた精密構造を持つ環状オレフィンコポリマーの合成と性質)

Haobo Yuan

Polymer Chemistry Laboratory
Department of Applied Chemistry
Graduate School of Engineering
Hiroshima University
March, 2021

Contents

Abbreviations

Ac	acetate
BHT	2,6-di-*tert*-butyl-4-methylphenol
^{t}Bu	*tert*-butyral
^{i}Bu	*iso*-butyral
$C_{29}H_{36}$	octamethyloctahydrodibenzofluorenyl
Cp	cyclopentadienyl
Cy	cyclohexyl
Đ	molecular weight distribution
DCPD	dicyclopentadiene
De	1-decene
dMAO	dried-methylaluminoxane
dMMAO	dried-modified-methylaluminoxane
Do	1-dodecene
DoD	1,11-dodecadiene
DSC	differential scanning calorimetry
E	ethylene
ENB	5-ethylidene-2-norbornene
Et	ethyl
Flu	fluorenyl
GPC	gel permeation chromatography
HD	1,5-hexadiene
Ind	indenyl
IP	isoprene
N	number of polymer chains
N_{arm}	number of arms in star polymer
NB	norbornene
NBD	2,5-norbornadiene
M	central metal
MAO	methylaluminoxane

Me	methyl
MMA	methyl methacrylate
MMAO	modified-methylaluminoxane
M_n	number-average molecular weight
mol%	mol percent
M_w	weight-average molecular weight
NB	norbornene
NBD	2,5-norbornadiene
NMR	nuclear magnetic resonance
O	1-octene
OD	1,7-octadiene
P	propylene
Ph	phenyl
^{i}Pr	*iso*-propyl
r	monomer reactivity ratio
R_3Al	trialkyl aluminum
ROMP	ring-opening metathesis polymerization
SAXS	small-angel X-ray scattering
t	time
T	temperature
T_d	decomposition temperature
T_g	glass-transition temperature
TGA	thermal gravimetric analysis
T_m	melting temperature
TMA	thermomechanical analysis
U-OH	10-undecene-1-ol
VNB	5-vinyl-2-orbornene
WAXD	wide-angle X-ray diffraction
wt.%	weight percent

Chapter 1. Introduction of Norbornene/*α*-olefin Copolymers

1.1. Cycloolefin copolymers

Plastic is an important material widely used to construct the modern world. Since the phenolic resin was first synthesized, new kinds of plastics with better properties have been developed. As a branch of the thermoplastics, polyolefins are so important that their inventers, as well known as Ziegler and Natta, won the 1963's Nobel Prizes. Because olefins are by-products of the petroleum industry, the price of which is low, and polyolefins have excellent properties, the polyolefin industry developed rapidly. Currently, more than half of the plastics produced each year are polyolefins. Although the performance of different types of polyolefins can already meet most of the requirements, researchers keep designing new generation of plastics with unique properties.

Polymers with cyclic structure obtained by addition (coordination-insertion) polymerization of cycloolefins (cyclobutene, cyclopentene, norbornene (NB), tetracyclododecene, etc. **Figure 1-1**) possess excellent properties such as high transparency, low moisture absorption, good thermal stability, low dielectric constant, and good biocompatibility, which are unique compared with conventional polyolefins.[1] However, these so called cycloolefin polymers usually

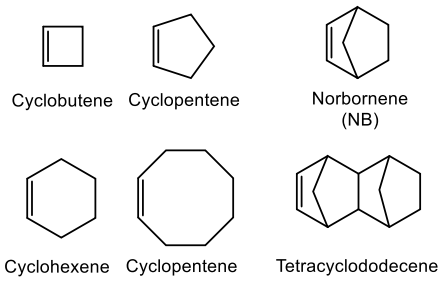

Figure 1-1. Chemical structures of representative cycloolefins.

are brittle and have high melting points (T_m) or high glass transition temperatures (T_g) close to their decomposition temperatures (T_d), which makes their thermoforming difficult and reduces their commercial interest. One simple and effective method to improve their processability is to copolymerize cycloolefins with α-olefins. The resulting products were well known as cycloolefin copolymers (COCs).

Among the cycloolefins, norbornene (NB), which can be easily synthesized from E and cyclopentadiene (Cp) through the Diels-Alder reaction, has relatively high polymerization activity due to its high ring tension and symmetric structure, thus attracted most of researchers' attention. It can be polymerized through ring-opening metathesis polymerization (ROMP), 2,3-addition polymerization and cationic polymerization (**Scheme 1-1**). Both 2,3-addition polymerization and ROMP can happen when the traditional Ziglar-Natta catalyst system was used.[2] In the 1990s, Kaminsky discovered that the zirconocene-methylaluminoxane catalyst system ([Et(Ind)$_2$]ZrCl$_2$-MAO) showed excellent selectivity for the addition polymerization of various cycloolefins

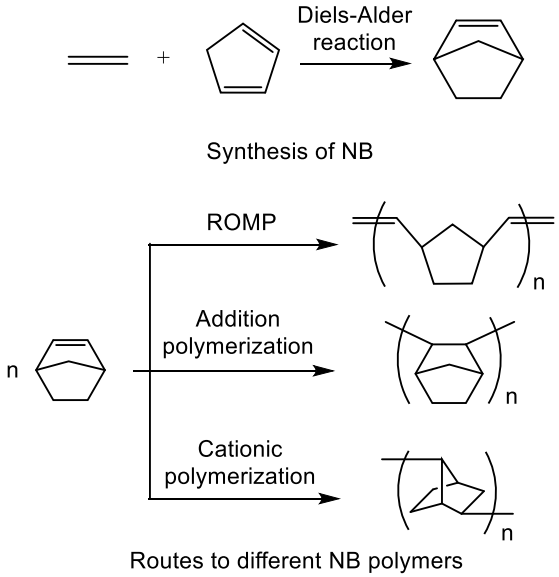

Scheme 1-1. Synthesis of NB and three routes to NB polymers.

including NB, which was a major breakthrough in this field.[3, 4] The zirconocene catalyst systems have high activity compared with traditional Ziegler-Natta and vanadium-based catalysts. More importantly, the structure of the obtained copolymers can be well-controlled by using different catalysts and adjusting the monomer feed ratios.[5, 6] These characteristics of the new catalyst systems have aroused strong interest of researchers.

After 30 years of development, various kinds of complexes including group 4 metallocene complexes, cyclopentadiene-free complexes, group 10 metal complexes, vanadium, chromium, and rare-earth-metal complexes have appeared as a catalyst for NB/α-olefin copolymerization.[1, 7, 8]

This chapter introduced the normal compositions of an organometallic catalyst system, synthesis and functionalization of NB/α-olefin copolymers using organometallic catalyst systems, and the applications of the copolymers.

1.2. Compositions of an organometallic catalyst system

Organometallic catalyst systems are widely used for olefin polymerization. Polymers with high molecular weights (M_ns), narrow molecular weight distributions ($Đ$s) and controllable molecular structures can be obtained in high speed.

An organometallic catalyst system usually includes a complex (pre-catalyst) composed of ligands and a transition metal center, and a cocatalyst (activator). The activation starts from the alkylation of the complex by the cocatalyst (such as MAO), which is replacing the halogen ligands on the metal center with alkyl ligands, and then one of the alkyl ligands leaves the central metal in the form of an anion, giving the coordinatively-unsaturated cationic metal-alkyl complex as an electron-deficient active center. Olefin monomer coordinates in the vacancy of the active center,

and then inserts into the metal-alkyl bond to complete the first step of chain-growth reaction. [9] The subsequent chain-growth reaction is just repeating this process (**Scheme 1-2**). When no chain-transfer reaction and the deactivation of the active center happen during or after the polymerization, which means that the polymerization can be restarted from the polymer chain bonded to the active center by adding further monomer, it is called a living polymerization. Because the cocatalyst is involved in the formation of an ion pair together with the active center, the choice of the cocatalyst can influence the stability of the active center, the activity of the catalyst system and the structure of the obtained polymers.[10-12] MAO, modified-MAO (MMAO) and boron compounds are the typical cocatalysts widely used today (**Figure 1-2**).

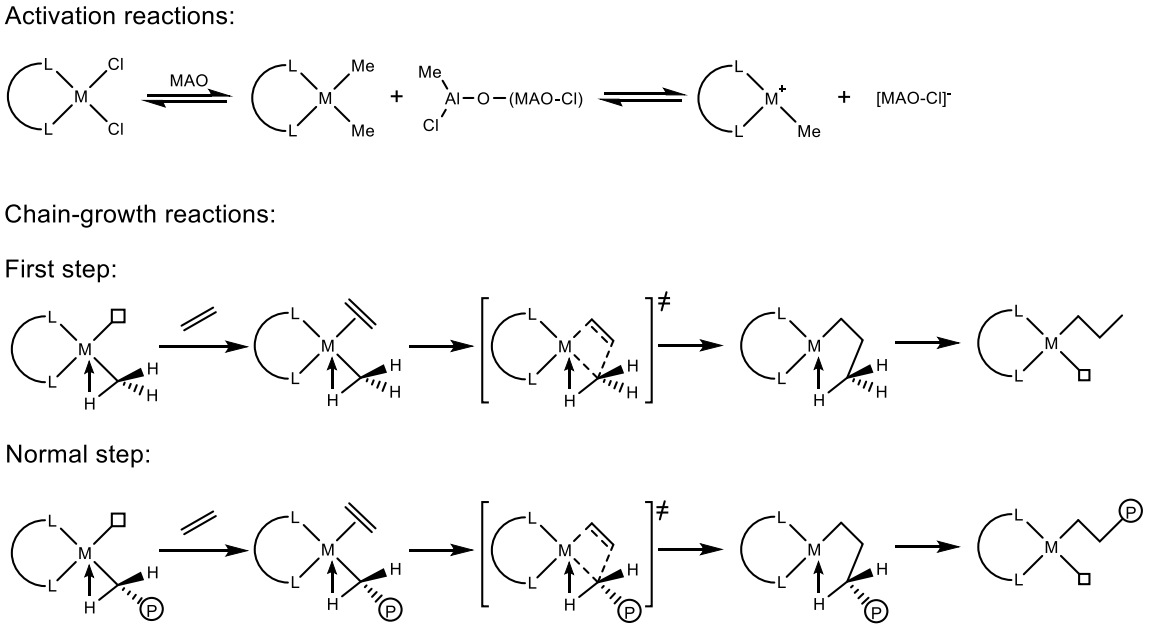

Scheme 1-2. Activation and chain-growth mechanism of E polymerization by an organometallic catalyst system when MAO is used as the cocatalyst.

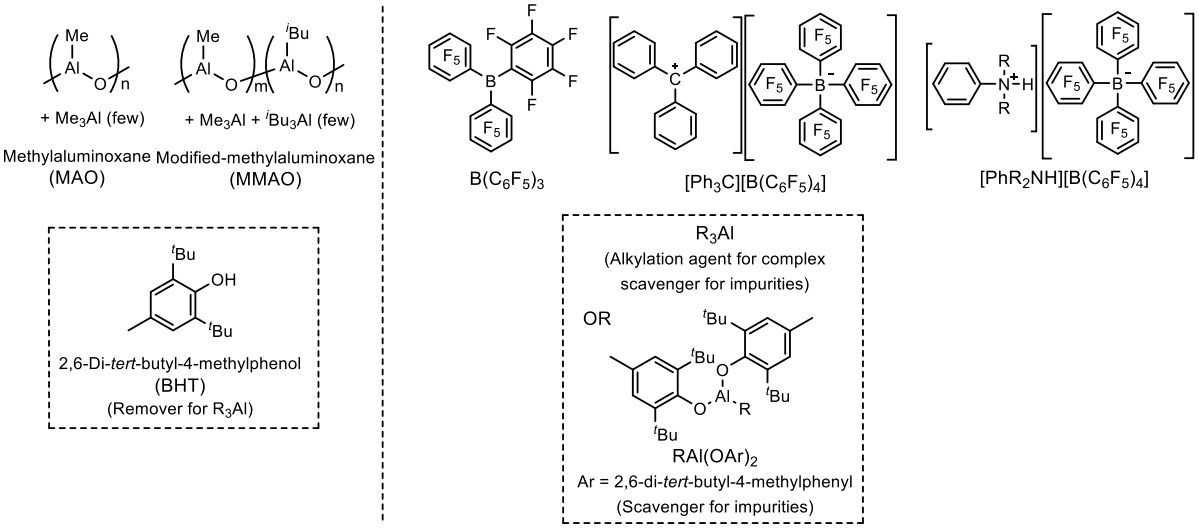

Figure 1-2. Cocatalysts and additives for olefin polymerization by organometallic catalyst systems.

Trialkylaluminums (R_3Als) were once used as the cocatalysts directly for the activation of metallocene, but most of the R_3Al-activated catalyst systems were observed to be inefficient for olefin polymerization. In 1980, H. Sinn and W. Kaminsky invented MAO, which was prepared from Me_3Al and water, and discovered that the MAO-activated metallocene catalysts showed extremely high activity for E polymerization.[13, 14] These results revolutionized the synthesis of polyolefin by metallocene catalyst systems. However, the high-priced MAO had poor solubility, and tended to precipitate from the solution over time to form gels. The reason is still unknown due to the limited understanding of the exact structure of MAO.[15] In order to improve MAO's solubility and stability, a certain proportion of $^{i}Bu_3Al$ was added with Me_3Al during the preparation: the product, called modified-MAO (MMAO), showed better activation efficiency than MAO. Usually a high aluminum adding ratios (Al/M >> 1) is required for the activation of the complexes by MAO or MMAO. Besides, R_3Als, which can work as a chain-transfer agent, are often left in MAO and MMAO solutions. Thus, the elimination of R_3Als is necessary for achieving living polymerization. R_3Als can be removed from MAO or MMAO by drying in vacuum to make dried-

MAO (dMAO) or dried-MMAO (dMMAO) as white solids. The chain transfer ability of R_3Als can also be suppressed by adding 2,6-di-*tert*-butyl-4-methylphenol (BHT)[16].

Boron compounds ($B(C_6F_5)_3$, $[Ph_3C][B(C_6F_5)_4]$ and $[PhNR_2H][B(C_6F_5)_4]$) are another kind of cocatalysts. This kind of cocatalyst also assists the formation of the metal cation as the active center, but the alkylation is completed by additional R_3Als such as $^{i}Bu_3Al$ and Oct_3Al. The R_3Als can also work as a scavenger for impurities, such as H_2O and O_2, in these systems. The boron compound/R_3Al-activated catalyst system usually possesses activity higher than those of the MAO or MMAO-activated ones. However, the chain transfer caused by R_3Als is not neglectable. Fortunately, the alkylation agent is not needed when alkylated complexes are used as a pre-catalyst. In several reports, $RAl(OAr)_2$ (Ar = 2,6-di-*tert*-butyl-4-methylphenyl) compounds were proved to be excellent scavengers without affecting the catalyst performance in the Cp_2ZrMe_2-$B(C_6F_5)_3$ and Cp_2ZrMe_2-$[Ph_3C][B(C_6F_5)_4]$ systems for E homopolymerization, and ($^{t}BuNSiMe_2Flu$)$TiMe_2$-$B(C_6F_5)_3$ for O homopolymerization.[17-20] Thus, it is feasible to achieve fast living polymerization by using $RAl(OAr)_2$ as the scavenger in the alkylated complex-boron compound systems.

Besides, alkylaluminum compounds (R_3Al, R_2AlCl, $RAlCl_2$) are still frequently used as cocatalysts for vanadium complexes.

1.3. Synthesis of norbornene/ethylene copolymers

The T_g of PNB can be efficiently reduced by copolymerizing NB with E. Researchers have designed a variety of organometallic catalysts with high activities for NB/E copolymerization.[1, 7, 8, 21] However, the catalysts which efficiently gave NB/E random copolymers with high molecular weights and high T_g values (NB content > 50 mol%) have been limited. Usually, high E pressure was applied in the copolymerization to improve the activities of the catalysts.

Metallocene complexes (**Figure 1-3**)**:** In the article, where Kaminsky et al. first achieved the NB addition homopolymerization using [Et(Ind)$_2$]ZrCl$_2$ (**2a**)-MAO, NB/E copolymerization was also attempted [4]. The NB/E copolymers successfully obtained had low NB contents (only 2-7 wt.%). Since then, a series of zirconocene complexes with bridged-cyclopentadienyl, indenyl or fluorenyl groups have been developed. The symmetrical structures of the complexes (C_1-, C_s-, C_2- or C_{2v}- symmetry) and the influence of the substituents on the ligands to their activities and the structures of the obtained copolymers were studied in details.[22-29]

Generally, the activities of metallocene catalyst systems for NB/E copolymerization were lower than for the E homopolymerization, and decreased by increasing the initial NB concentration or NB/E ratio in feed. And during the chain growth reaction, when NB was the last inserted unit, the next inserted monomer would be restricted to be E by the huge steric hindrance of NB unit, thus forming an alternating structure of NB and E in the obtained copolymers. This phenomenon made it difficult to synthesize copolymers with NB content over 50 mol%, which have high T_gs with more application value, by most of the metallocene catalyst systems.[7]

Among those metallocene catalyst systems, the complexes with bridged ligands had higher activity.[22] The activities of the complexes with C_s-symmetry were higher than those of the

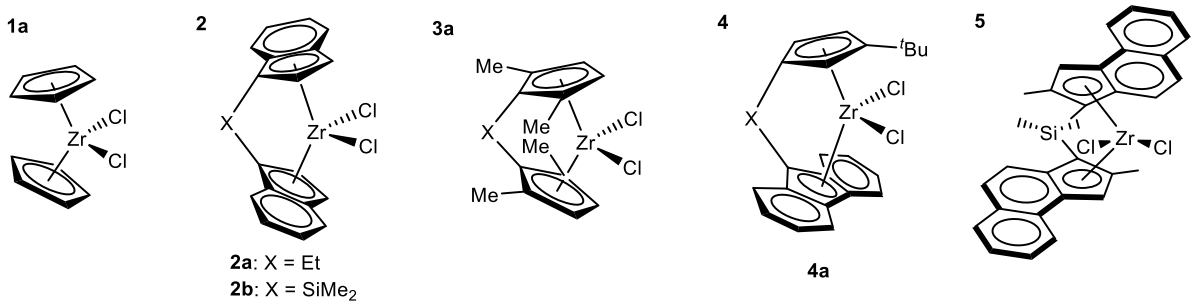

Figure 1-3. Zirconium complexes for NB/E copolymerization.

complexes with other symmetries.[25, 30] The complexes with C_2-symmetry tended to obtain NB/E random copolymers, while the complexes with C_1- or C_s-symmetry tended to obtain NB/E alternating copolymers. The substituents on the complexes had a crucial effect on their stability and catalytic activity, and the comonomer sequence and tacticity of the NB in obtained copolymers could also be influenced.[24, 25, 28, 31, 32] Besides, the stereoregularity of the copolymers, determined by the structure of the catalysts, also influenced their T_g values.

Constrained geometry complexes (Figure 1-4): The catalyst systems with cyclopentadienyl type of constrained geometry complexes (CGCs), such as [^{t}BuNMe$_2$Si(C$_5$Me$_4$)]TiCl$_2$ (**6a**)-MAO, usually show activities for NB/E copolymerization lower than those of zirconocene-MAO systems, and the obtained copolymers contained mainly alternating sequences (NB content < 50 mol%).[24, 33, 34] (^{t}BuNMe$_2$SiInd)TiCl$_2$ (**6b**)-MMAO showed lower activity than that of **6a**-MAO to give the copolymers with mainly alternating sequences under similar copolymerization conditions (NB contents < 35 mol%).[34]

The *ansa*-fluorenylamidodimethyltitanium-based catalysts, in which the coordination way between titanium and the cyclopentadienyl ligand of the complexes were different from other

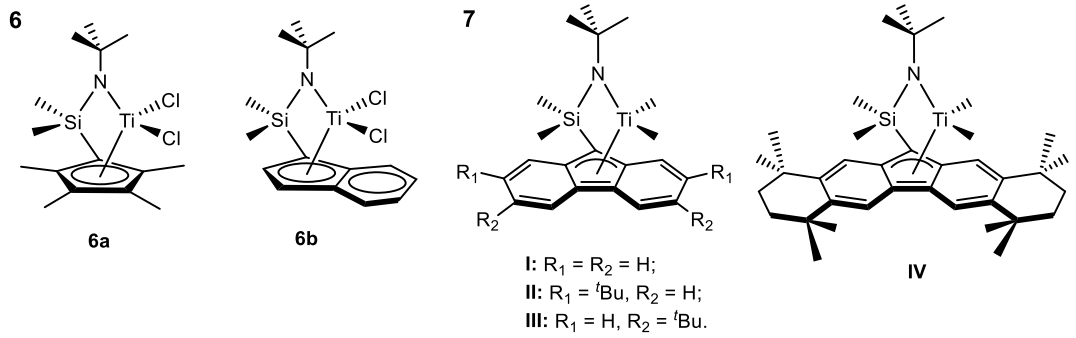

Figure 1-4. Constrained geometry complexes (bridged half metallocene complexes) for NB/E copolymerization.

metallocene complexes, showed remarkable activities for NB/E random copolymerization. (^{t}BuNMe$_2$SiFlu)TiMe$_2$ (**I**)-dMAO had an activity for NB/E copolymerization 10 times higher than that of **6a**-dMAO, and the obtained copolymers had higher NB contents.[35] MMAO and [Ph$_3$C][B(C$_6$F$_5$)$_4$]/Oct$_3$Al were also effective cocatalysts. The NB/E copolymers obtained by **I**-[Ph$_3$C][B(C$_6$F$_5$)$_4$]/Oct$_3$Al in high activity (5220 kg$_{polymer}$/(mol$_{Ti}$ h)) possessed NB contents up to 82 mol% and T_gs up to 237 °C.[35] The NB/E living polymerization was achieved by using **I**-dMAO system under 0 °C and high NB concentration.[36]

Non-bridged half-metallocene catalysts (Figure 1-5): In 2003, the non-bridged (aryloxo)(cyclopentadienyl)titanium complexes (**Figure 1-5, 8a ~ 8d**), the first kind of modified non-bridged half-metallocene catalysts, were used with dMAO for the NB/E copolymerization.[37, 38] Among them, IndTiCl$_2$(O-2,6-^{i}Pr$_2$C$_6$H$_3$) (**8b**)-dMAO showed the highest activity, which is comparable with that of **6a**-dMAO. However, the activities and the molecular weights of the copolymer decreased as the initial NB concentration increased.

When the aryloxo groups were changed to pyrazolato group (^{t}BuCpTiCl$_2$(3,5-^{i}Pr$_2$C$_3$HN$_2$), **8e**), copolymers with higher M_ns and unimodal $Đ$s were obtained in relatively low NB concentration. However, the activities still decreased as the initial NB concentration increased.[39] Cp'TiCl$_2$(N=C^{t}Bu$_2$) (**8f**)-(dMAO or dMMAO) exhibited even more remarkable activity and NB incorporation efficiency for NB/E copolymerization.[40] Different from the previously mentioned catalysts, the activity of this catalyst increased as the initial NB concentration increased. Thus, copolymers with high NB contents (58.8-73.5 mol%) can be obtained under lower E pressure. A linear relationship between T_gs and NB contents of the obtained copolymers was also observed.

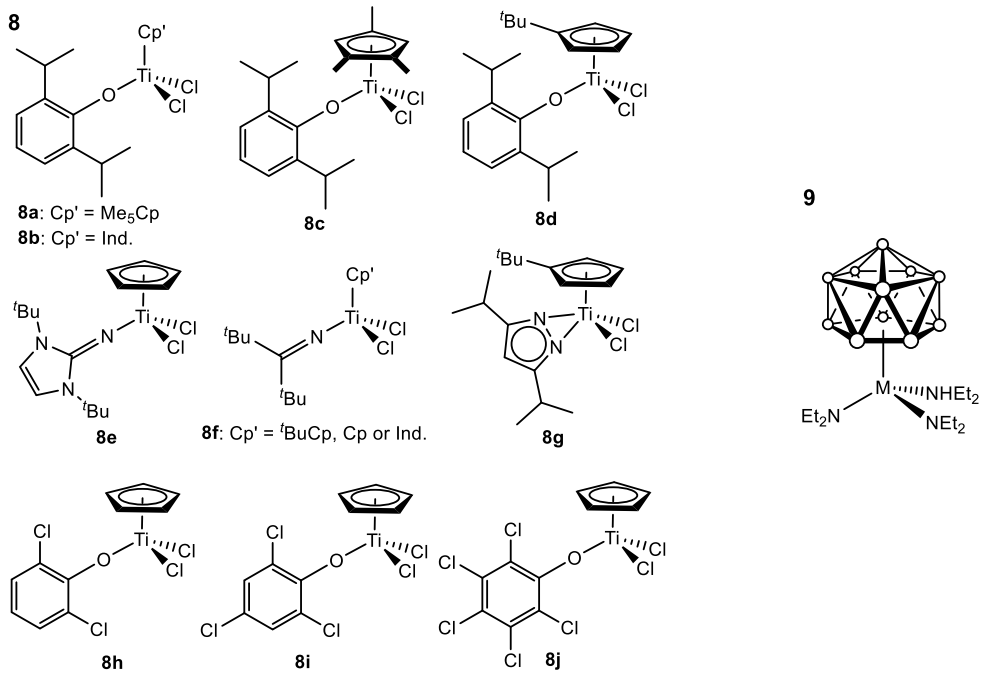

Figure 1-5. Non-bridged half-metallocene complexes for NB/E copolymerization.

$CpTiCl_2$[1,3-^{t}Bu$_2$(CHN)$_2$C=N] (**8g**)-dMAO can be used to synthesize copolymers with high M_ns under lower E pressure.[41]

Recently, $CpTiCl_2(OAr)$ (Ar = 2,6-$Cl_2C_6H_3$, 2,4,6-$Cl_3C_6H_2$ or C_6Cl_5, **8h** ~ **8j**) with dMAO were discovered to show good NB incorporation efficiency (NB content > 65 mol% in random copolymers) than the previously reported catalyst systems.[42]

These examples showed that the ligand substituents significantly influenced both activity and the comonomer incorporation efficiency of the catalyst.[37-42]

Besides, alternating NB/E copolymers can also be produced by the dicarbollide catalysts (η^5-$C_2B_9H_{11}$)M(NEt_2)$_2$($NHEt_2$) (M = Ti or Zr) activated with MAO or other trialkylaluminum compounds (**Figure 1-5, 9**).[43, 44]

Cyclopentadiene-free catalysts (Figure 1-6): Some of the bis(pyrrolide-imine)titanium complexes (PI catalysts) developed by Fujita *et al.* also have activities for NB/E copolymerization, despite they did not have activities for NB homopolymerization. The [2-(RNCH)C_4H_3N]$_2TiCl_2$-MAO (R = Ph (**10a**) or cyclohexyl (Cy) (**10b**)) system achieved NB/E living copolymerization to give highly alternating copolymers with high molecular weights (M_n > 500000), *Đ*s (< 1.20), and NB contents close but not over 50 mol%.[45, 46] The ^{13}C-NMR results showed the copolymers contained over 90% of -NB-E-NB-E-NB- alternating sequence and the rest was isolated NB sequence. The tridentate [O,N,P] titanium (**11a**) and tridentate [O,N,S] titanium (**11b**) complexes, with MAO can also copolymerize NB with E in high activity.[47, 48] The NB contents of the copolymers obtained by these catalysts were not over 40 mol%.

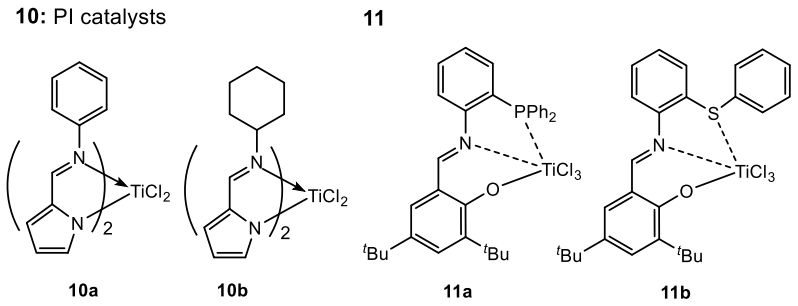

Figure 1-6. Cyclopentadiene-free complexes for NB/E copolymerization.

Vanadium and chromium catalysts (Figure 1-7): There also exist several vanadium complexes, such as (arylimido)(aryloxo)vanadium(V) complexes, vanadium(III) complexes bearing tridentate Schiff base ligands, and [O,N,N]-type amine pyridine(s) phenolate-based oxovanadium(V) complexes, for NB/E copolymerization (**Figure 1-7**, **12-14**).[10, 49-61] R_2AlCl or $RAlCl_2$ was usually used (sometimes with CCl_3COOEt) as a cocatalyst because of their high activation efficiency for these vanadium complexes. These catalyst systems had very high activity for E homopolymerization, but their activity for NB/E copolymerization dropped rapidly as the

initial NB concentration increased. The obtained copolymers mainly contained alternating sequence and isolated NB sequence. By changing the ligand and the substituents on it, the activity of the catalyst was significantly improved. However, the NB content of the obtained copolymers were lower. On the other hand, the activities of the catalysts with good NB insertion efficiency were lower. Highly alternating NB/E copolymers can be obtained by these systems, but the NB contents cannot be over 50 mol%.

The researches about chromium catalysts are rare.[62-67] NB block sequence was observed in the copolymers obtained by some of them.[64, 67] The NB contents in the obtained copolymers were up to 60 mol% for $Cr(CH_2SiMe_3)_4$ (**15b**)-MAO[64] and ranged from 53 to 93 mol% for anilido–imine chromium complexes (**16**)-MAO[67].

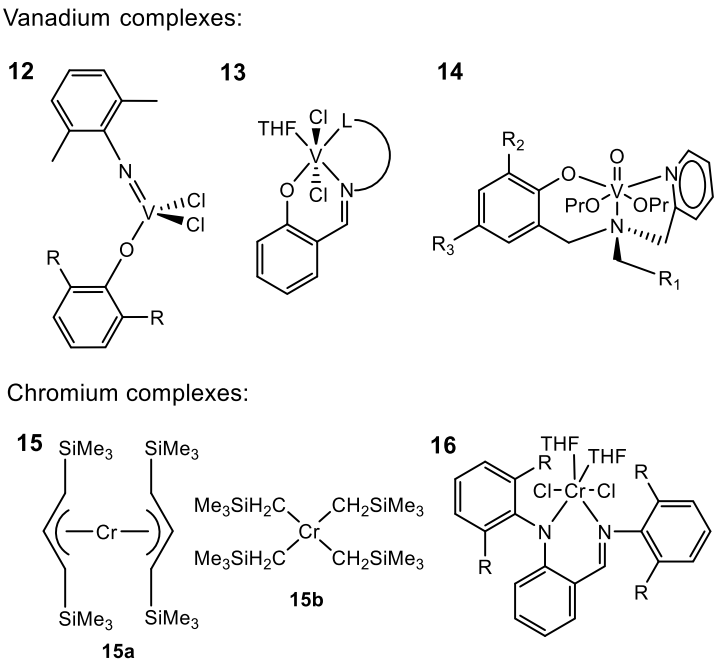

Figure 1-7. Vanadium and chromium complexes for NB/E copolymerization.

Nickle and palladium catalysts (**Figure 1-8**)**:** The high activities of nickel and palladium catalysts for ethylene polymerization is comparable to the most active metallocene catalysts, which has attracted many researchers. As a research hotspot in recent years, new types of nickel and palladium catalysts are emerging fast, some of which are suitable for the NB/E copolymerization.[68-79] The NB/E copolymers obtained by most of the nickel or palladium catalyst systems had either alternating structures[68, 69, 73, 78] or low NB contents[75, 76]. However, NB/E random copolymers with NB contents above 75 mol% were obtained by β-diketiminato nickel complexes (**17**)-MAO.[72] The activity of the catalytic systems increased with increasing the N/E feed ratio. The (anilino)anthraquinone nickel complex-MAO or $B(C_6F_5)_3$ system can produce NB/E random copolymers with NB content above 64 mol%.[79] PE-*b*-PNB copolymers were obtained by an amine–imine nickel complex (**18**)-MMAO system by living polymerization.[74]

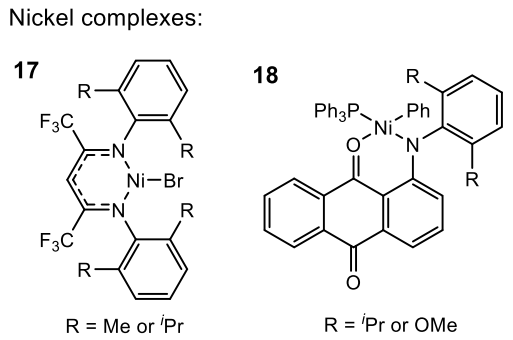

Figure 1-8. Nickle complexes producing NB/E copolymers with NB content over 60 mol%.

Rare-earth catalysts (Figure 1-9): The researches about rare-earth catalysts are rare.[80-83] The first report about the rare-earth catalyst systems (Cp'Sc(CH_2SiMe_3)$_2$(THF) (**19**)-[Ph_3C][$B(C_6F_5)_4$] or -[$PhMe_2NH$][$B(C_6F_5)_4$]) with reactivity for NB/E copolymerization appeared in 2005.[80] Surprisingly, the catalyst systems showed higher activity for NB/E copolymerization than those for E and NB homopolymerizations. NB/E copolymers with alternating structures were obtained and the NB contents were up to 43 mol%. And when the polymerization kept going after full NB consumption, poly(E-*alt*-NB)-*b*-PE block copolymers could form. When the center metal was changed from scandium (Sc) to yttrium (Y), the activity of the catalyst system dropped drastically, and it showed no activity when lutetium (Lu) was applied.[82] The activities of the catalysts were improved by redesigning the structure of the ligand, but the NB content stayed below 50 mol%.[83]

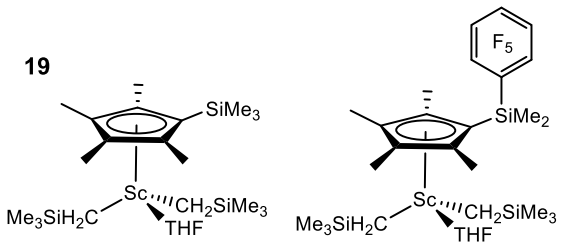

Figure 1-9. Rare-earth complexes for NB/E copolymerization.

1.4. Synthesis of norbornene/propylene copolymers

Since the T_g of PP was higher than that of PE, it was expected that the T_g of NB/P copolymer should be also higher than NB/E copolymers with the same NB content. However, due to the steric hindrance of the methyl group of P, the catalytic systems with good activities for NB/E polymerization had much lower or even no activities for NB/P polymerization. Therefore, the researches about NB/P copolymerization were much fewer.[11, 84-96] However, it is relatively easier to get copolymers with higher NB contents. **Figure 1-10** showed the chemical structures of the complexes for NB/P copolymerization.

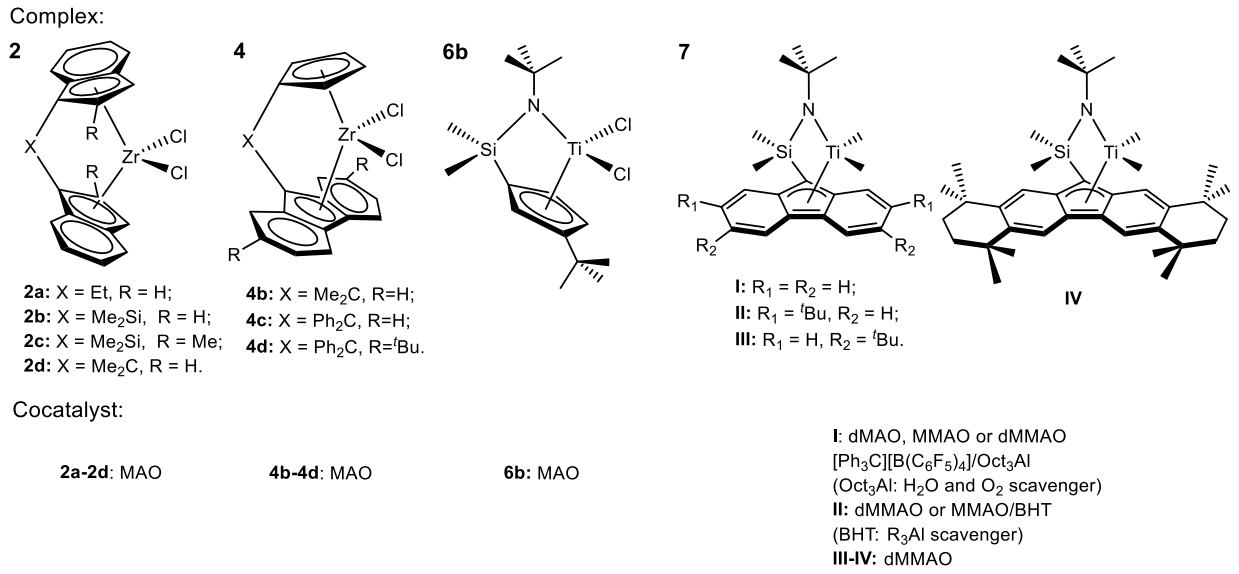

Figure 1-10. Catalyst systems for NB/P copolymerization.

NB/P copolymerization was first succeeded by using $[Me_2Si(Ind)_2]ZrCl_2$ (**2b**)-MAO in 1997.[84] Random copolymers were obtained (r_P = 0.82; r_{NB} = 1.1), and there was a linear relationship between the NB contents (11 – 98 mol%) and T_gs (-13 – 255 °C) of the copolymers. However, the monomer conversion and the activity of the catalyst dropped drastically as the NB/P adding ratio increased, which was also true for other sandwich-structured zirconocene catalysts. Such zirconocene catalysts usually have relatively large steric hindrance which can strongly affect

the insertion of NB and P. The symmetric structure of the catalyst (C_2- or C_s-symmetry) can affect their activities and the stereoregularity of the P segments in the obtained copolymers. For example, NB/P copolymerization results by C_2-symmetric [Et(Ind)$_2$]ZrCl$_2$ (**2a**)-MAO, **2b**-MAO, and C_s-symmetric [Me$_2$C(Cp)(Flu)]ZrCl$_2$ (**4b**)-MAO showed that the activity of the C_s-symmetric catalyst was higher than those of the two C_2-symmetric catalysts due to the steric hindrance, and the P segments in the copolymers obtained by the C_s-symmetric catalyst had higher stereoregularity.[85] The NB content in the obtained copolymer was up to 40 mol% with a T_g up to 140 °C. The type and structure of the bridge connecting the ligands can decide the space size of the metal center for the monomer insertion. In the NB/P copolymerization by **2a**-MAO, the presence of 1,3-propene misinsertions happened more frequently as the NB/P ratio in feed increased. When NB was the last inserted unit, it was difficult for the next P to insert, causing low polymerization activities, molecular weights, and T_g values.[86] Recent studies on zirconocene catalysts were focusing on the effects of polymerization conditions on their activity and the structure of the products.[92-94]

The CGCs can also be applied for NB/P copolymerization. The activity of [^{t}BuNSiMe$_2$(3-^{t}BuCp)]TiCl$_2$ (**6b**)-MAO for NB/P copolymerization was much lower than that of [Ph$_2$C(Cp)(2,7-^{t}Bu$_2$Flu)]ZrCl$_2$ (**4d**)-MAO, and the activity of both systems dropped as the NB/P ratio in feed increased.[89] The NB contents of the obtained copolymers were in a range from 0 to 77 mol%. The *ansa*-fluorenylamidodimethyltitanium-based catalysts showed excellent activities for NB/P copolymerization under normal P pressure. **I**-dMAO showed far higher activity for NB/P copolymerization under high NB/P ratio in feed compared to those for the zirconocene catalyst systems described so far to give random copolymers with NB content up to 71 mol% and T_gs up to 249 °C in high NB efficiency (NB conversion > 90%).[11] When the cocatalyst was changed to MMAO, or [Ph$_3$C][B(C$_6$F$_5$)$_4$]/Oct$_3$Al, the activity of the catalyst system furtherly increased. The

T_g value of the obtained NB/P copolymer, which can be precisely controlled by adjusting the NB/P ratio in feed, had a linear relationship with the NB content and was about 30 °C higher than that of the NB/E copolymer with the same NB content. These results have met all the past expectations for the properties of the NB/P random copolymer.

The reports about NB/P living copolymerization were very limited.[95] The **I**, [^{t}BuNSiMe$_2$(2,7-^{t}Bu$_2$Flu)]TiMe$_2$ (**II**), [^{t}BuNSiMe$_2$(3,6-^{t}Bu$_2$Flu)]TiMe$_2$ (**III**), and [^{t}BuNSiMe$_2$($C_{29}H_{36}$)]TiMe$_2$ ($C_{29}H_{36}$: octamethyloctahydrodibenzofluorenyl, **IV**) -dMMAO systems showed a living manner for the NB/P copolymerization obtaining copolymers with high M_ns and narrow $Đ$s.[97] By introducing alkyl groups on the Flu ligand, the activity significantly increased, and **IV**-dMMAO showed the highest activity, which was eight times as high as that of **I**-dMMAO. Taking the advantage of the living manner of **III**-dMMAO for both P and NB/P polymerization, *syndiotactic* PP (*s*PP)-*b*-poly(P-*ran*-NB) block copolymers were successfully synthesized. Both the T_m of *s*PP sequence and the T_g of NB/P random copolymer sequence can be detected by DSC.[88] By adding P before full NB consumption, poly(NB-*b*-P) with a short poly(NB-*ran*-P) sequence between the two blocks was successfully synthesized in high speed with 100 % monomer efficiency using the same catalyst system.[91] When ^{i}Bu$_3$Al was used as a chain-transfer agent, this process was repeatable with multiple addition of the same amount of NB and P in one pot resulting in the catalytic synthesis of monodisperse block copolymer (**Scheme 1-3**). The poly(NB-*b*-P-*b*-MMA) terpolymer was also successfully synthesized by (^{t}BuNSiMe$_2$Flu)TiMe$_2$-MMAO/BHT.[96]

Although the thermal properties of the obtained polymers were studied with the synthesis of NB/P copolymers, there is no systematic study about their mechanical properties.

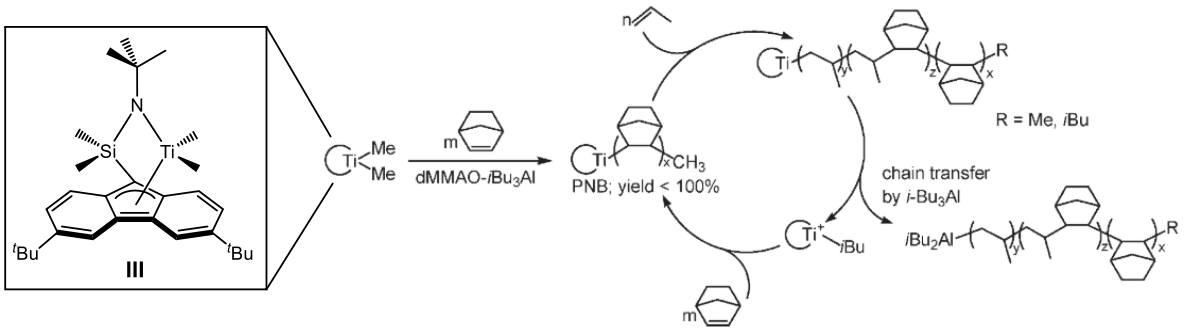

Scheme 1-3. Repeatable process of NB/P living block copolymerization in one pot using [^{t}BuNSiMe$_2$(3,6-^{t}Bu$_2$Flu)]TiMe$_2$-dMMAO with ^{i}Bu$_3$Al as a chain-transfer agent.

1.5. Synthesis of norbornene/higher *α*-olefin copolymers

Since the difference between the structures of higher *α*-olefins is small, the same catalyst system is usually active for the copolymerization of NB with different higher *α*-olefins. There only exists a few catalytic systems suitable for NB/*α*-olefin copolymerization now (**Figure 1-11**).[8, 12, 19, 20, 97-111] Therefore, it is still a challenge to find catalytic systems with high activity and high catalytic efficiency, and the catalytic systems with ability for NB/*α*-olefin living polymerization are extremely rare. Moreover, the difference in the reactivity ratio between the NB and higher *α*-olefin can cause the changes in the structure of the obtained copolymer.

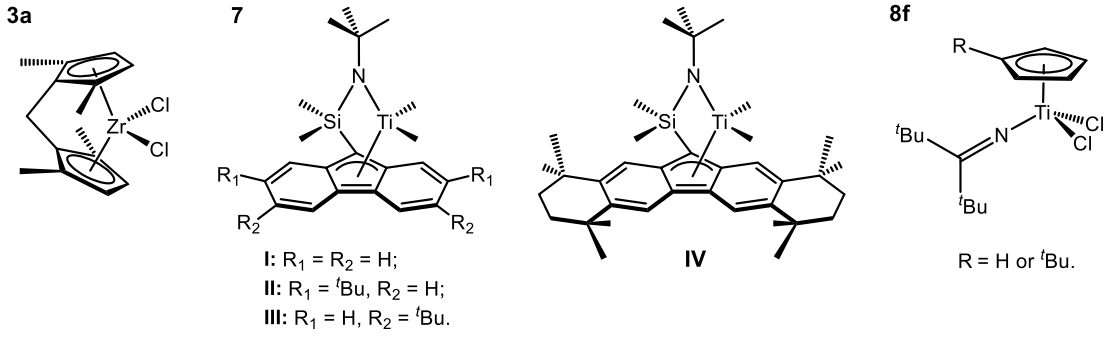

Figure 1-11. Complexes for NB/higher *α*-olefin copolymerization.

$[H_2C(2,5\text{-}Me_2C_5H_2)_2]ZrCl_2$ (**3a**)-MAO was the first system applied for NB/*α*-olefin (1-hexcene (H) or 1-octene (O)) copolymerization.[98] The T_g value of the obtained NB/H copolymer with a H content from 9.5 to 35.6 mol% decreased from 224 to 98 °C, while The T_g value of the obtained NB/O copolymer with an O content from 12.5 to 34.4 mol% decreased from 208 to 85 °C. The relationship between T_g values of NB/higher *α*-olefin copolymers and NB content are shown in **Figure 1-12**.

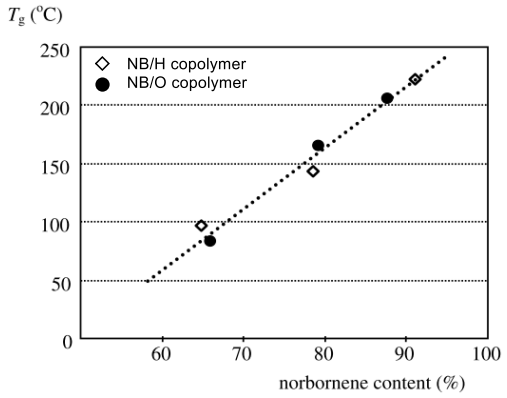

Figure 1-12. Relationship between T_g values of NB/higher *α*-olefin copolymers and NB content.

The *ansa*-fluorenylamidodimethyltitanium-based catalysts showed excellent activities for NB/higher *α*-olefin copolymerization. Copolymerizations of NB with H, O or 1-decene (De) were achieved by **I**-$[Ph_3C][B(C_6F_5)_4]$/Oct_3Al with reasonable activities.[99] However, the chain-transfer caused by Oct_3Al was not neglectable. The obtained copolymers had high T_g values (~ 296 °C) and high M_n (129000 kg/mol). The O content of NB/O copolymer was up to 58 mol%. Copolymer films with a thickness about 120 μm had transmittance values over 80%. The **I**, **II**, **III**, and **IV**-dMMAO systems which showed a living manner for the NB/P copolymerization also showed a living manner for the NB/higher *α*-olefin copolymerization.[97] Further studies on the NB/O copolymerization reaction showed that the monomer reactivity ratios of NB and O ($r_{NB} > 1 > r_O$) depended on the Ti complex used, so the slope of the T_gs versus NB content plot varies slightly.

The **IV**-MMAO/BHT can be used for the terpolymerization NB, O and isoprene (IP).[107] The obtained terpolymers had good thermostability and strong enough to form transparent films. The IP content in the obtained terpolymer was up to 7 mol %, and the incorporated IP was mainly inserted in 1,4-addition.

The living nature of the *ansa*-fluorenylamidodimethyltitanium-based catalysts let them be able to synthesize various block copolymers. By using **II**-MMAO/BHT, poly(NB-*co*-O)-*b*-PP-*b*-poly(NB-*co*-O), an A-B-A block copolymer, and poly(NB-*co*-O)-*b*-PMMA were successfully synthesized.[103] The films of the triblock copolymers were successfully prepared by solution casting method and the elongation test results showed that these block copolymers had better mechanical properties than poly(NB-*co*-O).

In 2016, the Cp'$TiCl_2$(N=C^tBu_2)-MAO (Cp' = ^{t}BuC_5H_4 or C_5H_5 (**8f**)) systems were found to show good activities for NB/*α*-olefin (H, O or 1-dodecene (Do)) copolymerization.[106] $CpTiCl_2$(N=C^tBu_2)-dMAO showed both higher activity and NB incorporation efficiency than the other. Copolymers with a NB content ranging from 9.6 to 84.1 mol% were obtained.

Recently, some nickel and palladium catalysts were also found to show activity for NB/*α*-olefin copolymerization (**Figure 1-13**). The Ni[$CR_3C(O)CHC[N(naphthyl)]CH_3]_2$ (**20a**)-B(C_6F_5)$_3$ system can catalyze the copolymerization of NB and H, O, or De.[100] This catalyst showed great activity for the homopolymerization of NB, but almost no activity for the homopolymerization of higher *α*-olefins. Thus, the activities of the catalyst systems for NB/higher *α*-olefin copolymerization and the polymer yield decreased as the NB/*α*-olefin ratio in feed decreased. The reactivity ratios determined by the Kelen–Tüdös method were r_O = 0.009 O and r_{NB} = 13.461 for

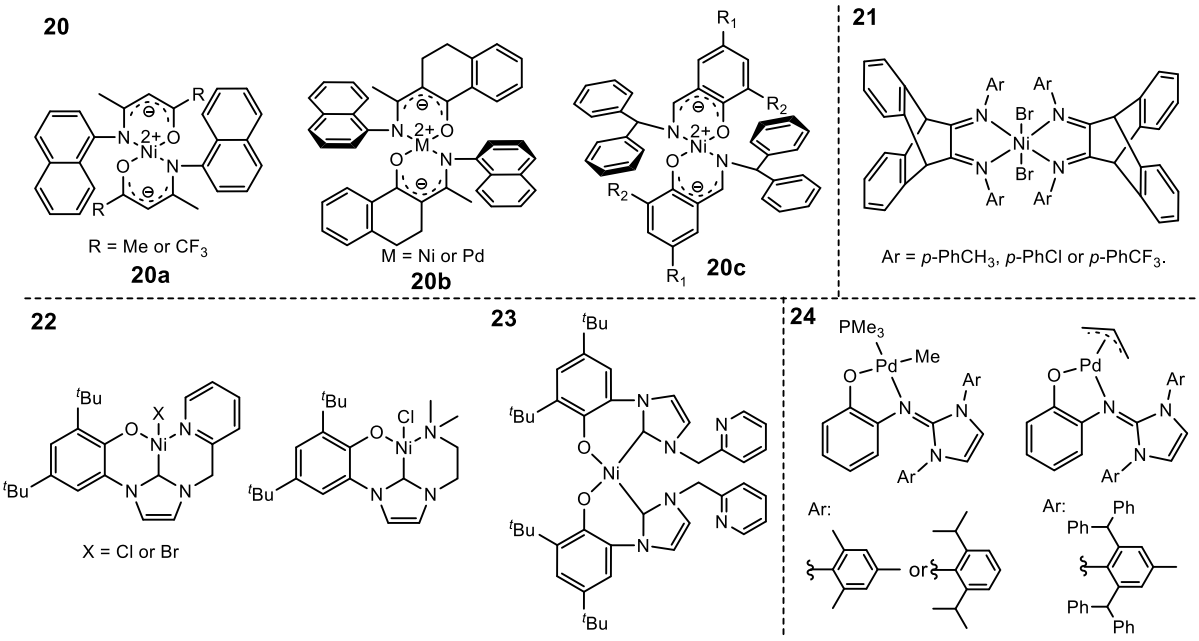

Figure 1-13. Nickel and palladium complexes for NB/higher α-olefin copolymerization.

the **20a**-$B(C_6F_5)_3$ system. The copolymers showed T_ds over 400 °C, and their T_gs were over 200 °C because of the low α-olefin contents (< 15 mol%). The activity of the catalyst system was improved by changing the structure of the ligand or adding new substituents onto the ligand (**Figure 1-13, 20b** and **20c**).[101, 108, 111]

Nickel complexes with bulky bis(α-diimine) ligands (**Figure 1-13, 21**) or *o*-aryloxide-N-heterocyclic carbene ligands (**Figure 1-13, 22, 23**), and neutral palladium complexes bearing aryloxide imidazolin-2-imine ligands (**Figure 1-13, 24**) were also found to show activities for NB/higher α-olefin copolymerization.[105, 109, 110] However, the activities of these nickel or palladium catalyst systems usually decrease rapidly with the increase of the α-olefin/NB addition ratio, and the α-olefin conversion and the α-olefin content in the obtained copolymers were low. At present, there is still no report about nickel or palladium catalyst system that can achieve NB/α-olefin living polymerization.

In summary, the *ansa*-fluorenylamidodimethyltitanium-based catalyst systems are the only kind which can achieve all the living copolymerization of NB with E, P, or higher α-olefins. However, it's still necessary to improve their copolymerization activities by the use of simple catalytic systems because one active center is necessary for one polymer chain. It is also important to explore the structures and the mechanical properties of NB/α-olefin block copolymers which can only be synthesize by these catalyst systems.

1.6. Functionalization of norbornene/α-olefin copolymers

The functionalization of polyolefins by copolymerization is an important method of polyolefin modification. The comonomers can be dienes and olefins with hydroxyl, ether, and ester groups and so on. At present, most of the functionalized NB/α-olefin copolymers are copolymers of NB derivatives and E, but there also exist a few researches on the copolymerization of NB and long-chain polar monomers. The chemical structures of dienes and comonomers applied for functionalization of NB/α-olefin copolymers are shown in **Figure 1-14**.

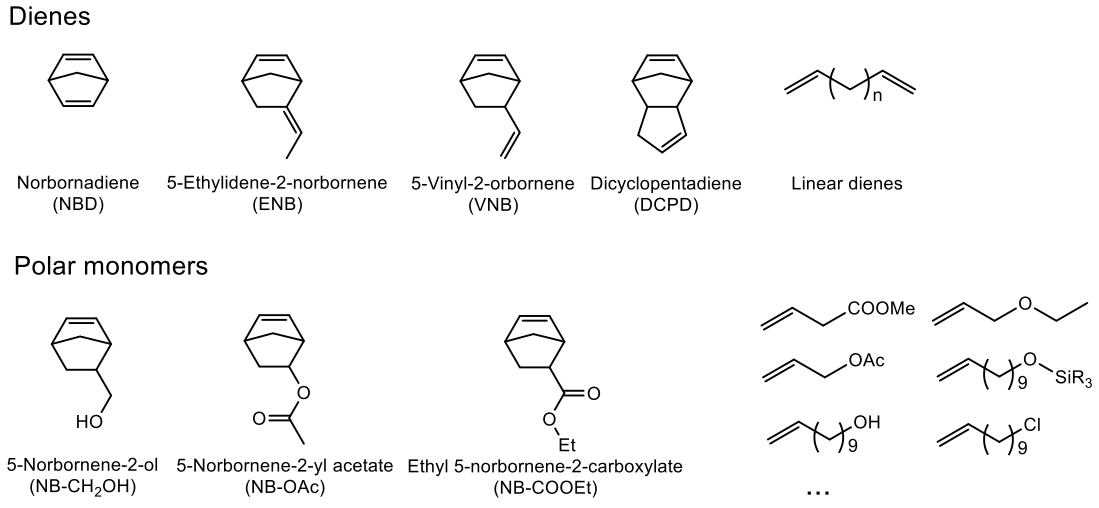

Figure 1-14. Chemical structures of representative dienes and polar monomers for functionalization of NB/α-olefin copolymers.

Copolymerization with dienes: Pendant carbon-carbon double bonds can be introduced to polymers by copolymerizing dienes. Most of the catalysts are much more tolerant to dienes than to other functional groups with heteroatoms. In addition, the carbon-carbon double bonds remained in the polymer can be converted into various groups as well as being used in crosslinking reactions, and polymerization to generate block, branched and star polymers.[112]

The researches about the copolymerization of norbornadiene (NBD) are limited. Cross-linking reactions can happen between the copolymer chains due to the relatively high reactivity of the second double bonds in NBD units which was used for synthesis of star polymer.[113] **1a**-, $(BuCp)_2ZrCl_2$ (**1b**)-, **2a**-, and $Me_2SiCp_2ZrCl_2$ (**3b**)-MAO showed activity for NBD/E copolymerization (**Figure 1-15**).[114, 115] When **1**-MAO was used, copolymers with NBD contents up to 19 mol% were obtained. It was confirmed that copolymerization of NBD occurred via both double bonds of NBD, but cross-linking only happened when **3b**-MAO was used. The copolymerization of H and NBD by **1**-MAO system produced oligomers.[116] Cross-linking structures were observed in the NBD/E copolymers obtained by the **6a**-MAO system.[117] The NBD content was up to 9.5 mol%.

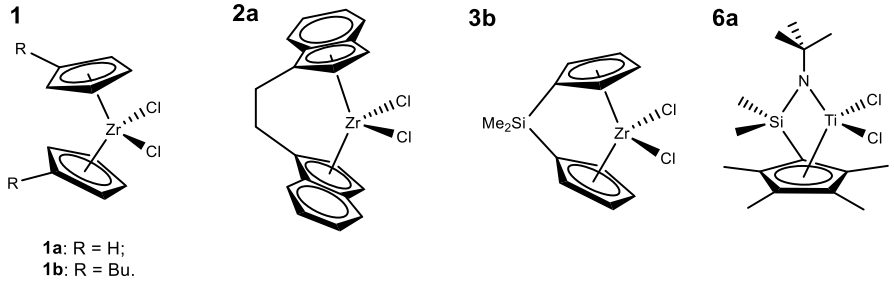

Figure 1-15. Complexes for NBD/E copolymerization.

The copolymers of E, P and other NB diene-derivatives, including ENB[52, 118, 119], VNB[58, 112, 120], and DCPD[58, 120, 121] can be obtained by zirconium and vanadium catalyst systems. The copolymers obtained by the vanadium catalyst systems had higher contents of NB derivatives.

Polymers obtained by short non-conjugated dienes usually have cyclic structural units.[122] [123] Cross-linking reaction can happen in the copolymerization with long-chain dienes. Thus, there are only a few reports about efficient introduction of double bonds to polymers by linear dienes. NB/O/OD terpolymerization was achieved by **8f**-dMAO.[106] Terpolymers with high M_ns and unimodal molecular weight distributions were obtained without cross-linking. NB/HD copolymerization by **I**-MMAO/BHT gave the copolymers with pendant vinyl groups up to 9.5 mol%, which can be used for further functionalization.[123]

Copolymerization of NB with polar monomers: The introduction of hydroxyl groups, a common polar group, can improve the hydrophilicity and dyeability of the polymers and be used to bind other groups. However, the hydroxyl groups are usually toxic for early-transition-metal catalysts. Therefore, the hydroxyl groups on the monomers need to be protected by, for example, $^{i}Bu_3Al$ before use. The formed $^{i}Bu_2AlO$- groups can be returned to hydroxyl groups during the quenching procedure by methanolic HCl. By using this method, poly(norbornene-*co*-10-undecene-1-ol) (P(NB-*co*-U-OH)) was obtained using **I**-[Ph_3C][$B(C_6F_5)_4$]-$^{i}Bu_3Al$ or -MMAO/BHT.[124] The content of hydroxyl group in the copolymers was up to 17 mol%. Taking the advantage of the living manner of **I** -MMAO/BHT, PE-*b*-P(NB-*co*-U-OH), *s*PP-*b*-P(NB-*co*-U-OH)[124] and PNB-*b*-PP-*b*-P(NB-*co*-U-OH)[125] were synthesized successfully. PNB-*b*-PP-*b*-P(NB-*co*-U-OH), an A-B-C type olefin block copolymer, showed remarkable elastic properties and high transparency.

One kind of aryloxide imidazolin-2-imine ligated neutral nickel(II) complex-$B(C_6F_5)_3$ system had activity for the copolymerization of NB with various polar monomers, although the content of polar monomer in the obtained copolymers was low (< 5 mol%).[126]

Copolymerization of polar NB derivatives with olefins: The Lewis acidity of nickel and palladium catalysts are weaker than that of early-transition-metal catalysts, which gives them better tolerance to polar groups.[127, 128] They can be used to directly copolymerize E, P with various polar NB derivatives (for example, 5-norbornene-2-ol (NB-CH_2OH), 5-norbornene-2-yl acetate (NB-OAc) and ethyl 5-norbornene-2-carboxylate (NB-COOEt)), although the content of the NB derivatives in the obtained copolymers were low (< 30 mol%).[69, 73, 77, 129] One kind of anilinonaphthoquinone-ligated palladium-MMAO system achieved copolymerization of E and NB-OAc to give the copolymers with a NB-OAc content ranging from 36 to 81 mol%.[130] The surface properties of these polar functionalized copolymers were improved.

Copolymerization of NB with other functionalized monomers: The hydroxyl group in the polymer can also be obtained by the oxidation reaction of other groups. Poly(NB-*co*-O-*co*-7-octene-1-ol) was obtained using **I**-[Ph_3C][$B(C_6F_5)_4$] by copolymerization of NB and 7-octenyldiisobutylaluminium or terpolymerization of NB, O and 7-octenyldiisobutylaluminium followed by quenching with oxygen.[131] The content of 7-octene-1-ol in copolymers was up to 26 mol%. Poly(NB-*co*-7-octene-1-ol) was obtained using **I**-[Ph_3C][$B(C_6F_5)_4$]/$^{i}Bu_3Al$ or -MMAO/BHT by copolymerization of NB and 9-(7-octenyl)-borabicyclo[3.3.1]nonane followed by quenching with H_2O_2, where the **I**-MMAO/BHT system conducted the copolymerization in a living manner.[132]

Boronic acid end-functionalized NB/O copolymers were successfully obtained by using **I**-$B(C_6F_5)_3$ with $^{i}BuAl(OAr)_2$ (Ar = 2,6-bis(1,1-dimethylethyl)-4-methylphenyl) as a scavenger.[19, 20] The copolymers with the boronic acid functional groups were transformed into star-shaped

polymers in the presence of amine by a reversable process, where the number of arms was controllable (**Scheme 1-4**).

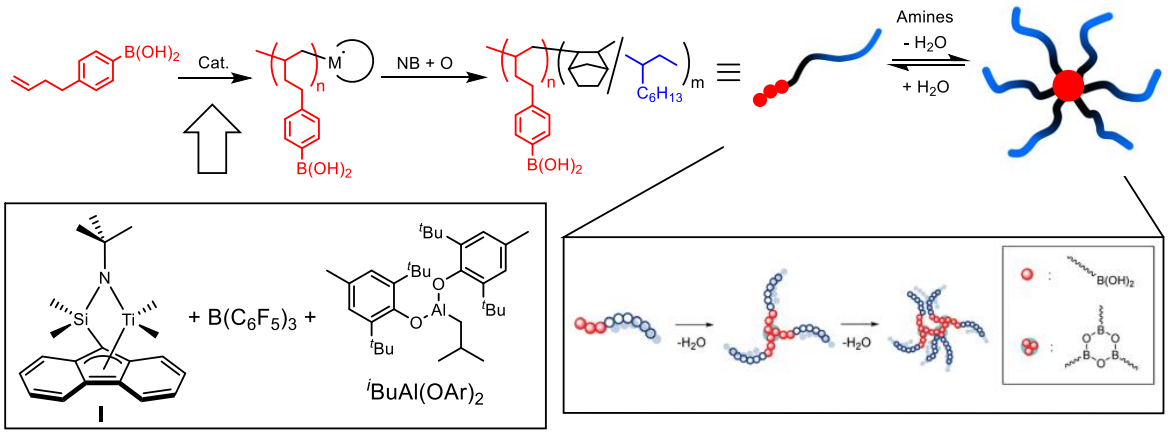

Scheme 1-4. Synthesis of star polymers with NB/O segment arms by (^{t}BuNSiMe$_2$Flu)TiMe$_2$-B(C$_6$F$_5$)$_3$/scavenger system.

1.7. Applications

Currently, most of the COCs on the market are amorphous NB/E copolymers. These copolymers have some common features, such as high optical transparency, low water absorption, high thermal stability, low dielectric constants and good resistance to polar solvents.[133] However, the copolymers with different NB contents have different applications: Copolymers with low NB contents have low T_gs, and easier to be processed. These copolymers are more flexible, and have higher elongation at break with lower strength. Such materials can be used for packing food and drugs. The copolymers with high NB contents have higher strength. They are more suitable for making microtiter plates for genomics, medical test tubes and disposable syringes, optical lenses, capacitor films and so on. These copolymers with better properties must have a wider range of applications in the future.

Aim of this work

NB/α-olefin copolymers, a kind of cycloolefin copolymers, possess high transparency, low water uptake, excellent thermal stability, and good biocompatibility. These α-olefins were introduced to reduce the high T_g of PNB for processability and improve the mechanical properties.

The NB/E copolymers with different microstructures have been synthesized by various kinds of catalyst systems, and produced in industrial scale for optical, electronic, and medical applications. However, the copolymerization of NB with P is difficult to be achieved because of the steric hindrance of the methyl group of P. The copolymerization of NB and higher α-olefins is more difficult due to the higher steric hindrance of the side chain of α-olefins and the catalyst systems for the copolymerization is very limited.

The (^{t}BuNSiMe$_2$Flu)TiMe$_2$-MMAO/BHT system was proved to have a living manner for NB/α-olefin copolymerization. The copolymerization was promoted in a moderate rate. When the cocatalyst was changed to [Ph$_3$C][B(C$_6$F$_5$)$_4$] with ^{i}Bu$_3$Al as a scavenger, the catalyst system showed much higher activity. However, ^{i}Bu$_3$Al caused chain-transfer reactions which was a problem for achieving living copolymerization. The living NB/α-olefin copolymerization can also be achieved in high speed by using alkyl-modified (^{t}BuNSiMe$_2$Flu)TiMe$_2$-based complexes with dMMAO. However, because the catalyst activation efficiency was unstable, it was difficult to precisely control the molecular weight of the obtained copolymer.

Recently, ^{i}BuAl(OAr)$_2$ (Ar = 2,6-di-*tert*-butyl-4-methylphenyl), made from BHT and ^{i}Bu$_3$Al, was proved to be a good scavenger keeping the living nature in the NB/O copolymerization by the (^{t}BuNSiMe$_2$Flu)TiMe$_2$-B(C$_6$F$_5$)$_3$ system. Thus, in this thesis, a solution of mixture containing RAl(OAr)$_2$ (Ar = 2,6-di-*tert*-butyl-4-methylphenyl, R = ^{i}Bu or Oct) (R$_3$Al/BHT) as an average composition formula was prepared by mixing R$_3$Al with 2 equivalents of BHT in toluene

and applied it as a scavenger in NB/α-olefin copolymerization with (^{t}BuNSiMe$_2$Flu)TiMe$_2$-[Ph$_3$C][B(C$_6$F$_5$)$_4$] aiming at achieving a high speed living polymerization by a simple catalytic system (**Figure 1-16**). Tailor-made COCs with different molecular structures were successfully synthesized, and the mechanical properties of the obtained copolymers were investigated for evaluating such materials as potential practical thermoplastics.

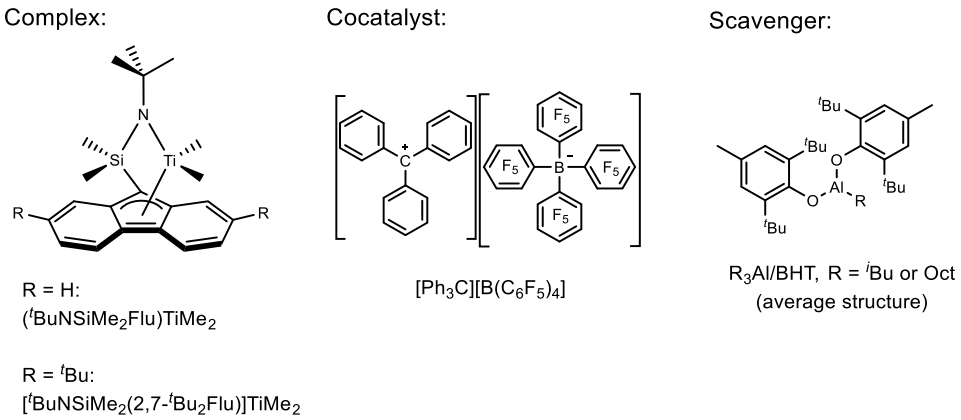

Figure 1-16. Composition of the catalyst system used in this thesis.

In Chapter 2, high speed living NB/α-olefin copolymerization was achieved by using (^{t}BuNSiMe$_2$Flu)TiMe$_2$-[Ph$_3$C][B(C$_6$F$_5$)$_4$] with R$_3$Al/BHT (R = ^{i}Bu or Oct) as a scavenger. The obtained copolymers were found to possess a gradient structure as was expected from the monomer reactivity ratios of NB and α-olefin. NB/α-olefins (O, De or Do) copolymers with different NB contents were synthesized and their mechanical properties were investigated in detail.

In Chapter 3, the high-speed catalytic system found in Chapter 2 was applied for the synthesis of NB/α-olefin (O or Do) block copolymers with a gradient structure in each block after confirming the pseudo-living nature of the copolymerization. A series of block copolymers such as the same molecular weight with different number of blocks were synthesized and their mechanical properties were investigated in detail.

In Chapter 4, NBD homopolymerization and NBD/O/NB terpolymerization were conducted aiming at synthesizing COP and COC possessing reactive norbornenyl structure in the polymer chain which can be used for further reactions. Four combinations of titanium complex, (^{t}BuNSiMe$_2$Flu)TiMe$_2$ or [^{t}BuNSiMe$_2$(2,7-^{t}Bu$_2$Flu)]TiMe$_2$, with cocatalyst, MMAO/BHT or [Ph$_3$C][B(C$_6$F$_5$)$_4$]/^{i}Bu$_3$Al/BHT, were tested and compared for both the homopolymerization and the terpolymerization.

In Chapter 5, NBD/E or 1,11-dodecadiene (DoD) was added at the end of NB/O copolymerization by (^{t}BuNSiMe$_2$Flu)TiMe$_2$-[Ph$_3$C][B(C$_6$F$_5$)$_4$]/R$_3$Al/BHT aiming at synthesizing star polymers with NB/O gradient copolymer segment arms and cross-linked polymer cores. The star polymer would have NB-rich segments far from the cores and O-rich segments close to the cores. The thermal and mechanical properties of the obtained polymers were investigated and compared with those of the gradient copolymers and star polymers with opposite gradient structures in their arms.

References

1 X. Li and Z. Hou, *Coord. Chem. Rev.*, 2008, **252**, 1842-1869.
2 T. Tsujino, T. Saegusa and J. Furukawa, *Die Makromolekulare Chemie*, 1965, **85**, 71-79.
3 W. Kaminsky and R. Spiehl, *Makromol. Chem.*, 1989, **190**, 515-526.
4 W. Kaminsky, A. Bark and M. Arndt, *Makromol. Chem. Macromol. Symp.*, 1991, **47**, 83-93.
5 W. Kaminsky, O. Sperber and R. Werner, *Coord. Chem. Rev.*, 2006, **250**, 110-117.
6 I. Tritto, L. Boggioni and D. R. Ferro, *Coord. Chem. Rev.*, 2006, **250**, 212-241.
7 L. Boggioni and I. Tritto, in *Polyolefins: 50 years after Ziegler and Natta II*, ed. K. Walter, Springer-Verlag Berlin Heidelberg, 2013, ch. 217, pp. 117-141.
8 W. Zhao and K. Nomura, *Catalysts*, 2016, **6**, 175.
9 J. Hu, B. Zhu, J. Yi and J. Wang, in *Organometallic Olefin Polymerization Catalysts and Polyolefins*, Chemical Industry Press Co., Ltd., 2010, ch. 2, pp. 21-25.
10 W. Wang and K. Nomura, *Macromolecules*, 2005, **38**, 5905-5913.
11 T. Hasan, T. Ikeda and T. Shiono, *Macromolecules*, 2005, **38**, 1071-1074.
12 T. Shiono, *Polym. J.*, 2011, **43**, 331-351.
13 W. Kaminsky, *Macromolecules*, 2012, **45**, 3289-3297.
14 H. Sinn, W. Kaminsky, H. J. Vollmer and R. Woldt, *Angew. Chem. Int. Ed. Engl.*, 1980, **19**, 390-392.
15 F. Ghiotto, C. Pateraki, J. Tanskanen, J. R. Severn, N. Luehmann, A. Kusmin, J. Stellbrink, M. Linnolahti and M. Bochmann, *Organometallics*, 2013, **32**, 3354-3362.
16 V. Busico, R. Cipullo, F. Cutillo, N. Friederichs, S. Ronca and B. Wang, *J. Am. Chem. Soc.*, 2003, **125**, 12402-12403.
17 V. C. Williams, C. Dai, Z. Li, S. Collins, W. E. Piers, W. Clegg, M. R. J. Elsegood and T. B. Marder, *Angew. Chem. Int. Ed.*, 1999, **38**, 3695-3698.
18 V. C. Williams, G. J. Irvine, W. E. Piers, Z. Li, S. Collins, W. Clegg, M. R. J. Elsegood and T. B. Marder, *Organometallics*, 2000, **19**, 1619-1621.
19 R. Tanaka, N. Tonoko, S.-i. Kihara, Y. Nakayama and T. Shiono, *Polym. Chem.*, 2018, **9**, 3774-3779.
20 T. Kida, R. Tanaka, K.-h. Nitta and T. Shiono, *Polym. Chem.*, 2019, **10**, 5578-5583.
21 H. Makio and T. Fujita, *Acc. Chem. Res.*, 2009, **42**, 1532-1544.
22 H. L.asarov, K. Monkkonen and T. T. Pakkanen, *Macromol. Chem. Phys.*, 1998, **199**, 1939-1942.
23 D. Ruchatz and G. Fink, *Macromolecules*, 1998, **31**, 4669-4673.
24 D. Ruchatz and G. Fink, *Macromolecules*, 1998, **31**, 4674-4680.
25 D. Ruchatz and G. Fink, *Macromolecules*, 1998, **31**, 4681-4683.
26 D. Ruchatz and G. Fink, *Macromolecules*, 1998, **31**, 4684-4686.
27 W. Kaminsky, I. Beulich and M. Arndt-Rosenau, *Macromol. Symp.*, 2001, **173**, 211-225.
28 J. Forsyth, J. M. Perena, R. Benavente, E. Perez, I. Tritto, L. Boggioni and H. H. Brintzinger, *Macromol. Chem. Phys.*, 2001, **202**, 614-620.
29 I. Tritto, C. Marestin, L. Boggioni, M. C. Sacchi, H.-H. Brintzinger and D. R. Ferro, *Macromolecules*, 2001, **34**, 5770-5777.
30 M. Amdt and I. Beulich, *Macromol. Chem. Phys.*, 1998, **199**, 1221-1232.
31 B. Y. Lee, Y. H. Kim, Y. C. Won, C. B. Shim, D. M. Shin and Y. K. Chung, *J. Organomet. Chem.*, 2002, **660**, 161-166.

32 E. S. Cho, U. G. Joung, B. Y. Lee, H. Lee, Y.-W. Park, C. H. Lee and D. M. Shin, *Organometallics*, 2004, **23**, 4693-4699.
33 B. A. Harrington and D. J. Crowther, *Journal of Molecular Catalysis a-Chemical*, 1998, **128**, 79-84.
34 A. L. McKnight and R. M. Waymouth, *Macromolecules*, 1999, **32**, 2816-2825.
35 T. Hasan, T. Ikeda and T. Shiono, *Macromolecules*, 2004, **37**, 8503-8509.
36 T. Hasan, T. Shiono and T. Ikeda, *Macromol. Symp.*, 2004, **213**, 123-130.
37 K. Nomura, M. Tsubota and M. Fujiki, *Macromolecules*, 2003, **36**, 3797-3799.
38 W. Wang, T. Tanaka, M. Tsubota, M. Fujiki, S. Yamanaka and K. Nomura, *Adv. Synth. Catal.*, 2005, **347**, 433-446.
39 K. Nomura, H. Fukuda, S. Katao, M. Fujiki, H. J. Kim, D.-H. Kim and I. Saeed, *Macromolecules*, 2011, **44**, 1986-1998.
40 K. Nomura, W. Wang, M. Fujiki and J. Liu, *Chem. Commun.*, 2006, 2659-2661.
41 W. Apisuk, A. G. Trambitas, B. Kitiyanan, M. Tamm and K. Nomura, *J. Polym. Sci., Part A: Polym. Chem.*, 2013, **51**, 2575-2580.
42 W. Zhao, Q. Yan, K. Tsutsumi and K. Nomura, *Organometallics*, 2016, **35**, 1895-1905.
43 P. Altamura and A. Grassi, *Macromolecules*, 2001, **34**, 9197-9200.
44 A. Grassi, G. Maffei, S. Milione and R. F. Jordan, *Macromol. Chem. Phys.*, 2001, **202**, 1239-1245.
45 Y. Yoshida, J. Saito, M. Mitani, Y. Takagi, S. Matsui, S. Ishii, T. Nakano, N. Kashiwa and T. Fujita, *Chem. Commun.*, 2002, 1298–1299.
46 Y. Yoshida, J. Mohri, S. Ishii, M. Mitani, J. Saito, S. Matsui, H. Makio, T. Nakano, H. Tanaka, M. Onda, Y. Yamamoto, A. Mizuno and T. Fujita, *J. Am. Chem. Soc.*, 2004, **126**, 12023-12032.
47 W.-Q. Hu, X.-L. Sun, C. Wang, Y. Gao, Y. Tang, L.-P. Shi, W. Xia, J. Sun, H.-L. Dai, X.-Q. Li, X.-L. Yao and X.-R. Wang, *Organometallics*, 2004, **23**, 1684-1688.
48 C. Wang, X.-L. Sun, Y.-H. Guo, Y. Gao, B. Liu, Z. Ma, W. Xia, L.-P. Shi and Y. Tang, *Macromol. Rapid Commun.*, 2005, **26**, 1609-1614.
49 K. Nomura, A. Sagara and Y. Imanishi, *Macromolecules*, 2002, **35**, 1583-1590.
50 W. Wang and K. Nomura, *Adv. Synth. Catal.*, 2006, **348**, 743-750.
51 J.-Q. Wu, L. Pan, Y.-G. Li, S.-R. Liu and Y.-S. Li, *Organometallics*, 2009, **28**, 1817-1825.
52 K. Nomura, B. K. Bahuleyan, S. Zhang, P. M. Veeresha Sharma, S. Katao, A. Igarashi, A. Inagaki and M. Tamm, *Inorg. Chem.*, 2014, **53**, 607-623.
53 J. B. Wang, L. P. Lu, J. Y. Liu and Y. S. Li, *Dalton Trans.*, 2014, **43**, 12926-12934.
54 J.-B. Wang, L.-P. Lu, J.-Y. Liu, H.-l. Mu and Y.-S. Li, *J. Mol. Catal. A: Chem.*, 2015, **398**, 289-296.
55 K. Nomura, M. Oshima, T. Mitsudome, H. Harakawa, P. Hao, K. Tsutsumi, G. Nagai, T. Ina, H. Takaya, W. H. Sun and S. Yamazoe, *ACS Omega*, 2017, **2**, 8660-8673.
56 W. Ochędzan-Siodłak, A. Bihun-Kisiel, D. Siodłak, A. Poliwoda and B. Dziuk, *Eur. Polym. J.*, 2018, **106**, 148-155.
57 G. Zanchin, I. Pierro, E. Parisini, J. Martí-Rujas, G. Ricci and G. Leone, *J. Organomet. Chem.*, 2018, **861**, 142-150.
58 G. Zanchin, L. Vendier, I. Pierro, F. Bertini, G. Ricci, C. Lorber and G. Leone, *Organometallics*, 2018, **37**, 3181-3195.
59 W. Ochędzan-Siodłak, D. Siodłak, A. Piontek and K. Doležal, *Catalysts*, 2019, **9**, 1041.

60 M. van der Ende, P. M. Hauser, C. Lienert, D. Wang, W. Frey and M. R. Buchmeiser, *ChemCatChem*, 2019, **11**, 744-752.
61 G. Zanchin, A. Gavezzoli, F. Bertini, G. Ricci and G. Leone, *Molecules*, 2019, **24**, 2088.
62 U. Peucker and W. Heitz, *Macromol. Rapid Commun.*, 1998, **19**, 159-162.
63 U. Peucker and W. Heitz, *Macromol. Chem. Phys.*, 2001, **202**, 1289-1297.
64 T. J. Woodman, Y. Sarazin, S. Garratt, G. Fink and M. Bochmann, *J. Mol. Catal. A: Chem.*, 2005, **235**, 88-97.
65 J.-Y. Liu, P. Tao, Y.-X. Wang and Y.-S. Li, *RSC Adv.*, 2014, **4**, 19433-19439.
66 P. Tao, J.-Y. Liu, Y.-S. Li and Y.-G. Li, *J. Organomet. Chem.*, 2015, **798**, 422-428.
67 L. Pei, Y. Tang and H. Gao, *Polymers*, 2016, **8**, 69.
68 F. M. Bauers and S. Mecking, *Macromolecules*, 2001, **34**, 1165-1171.
69 G. M. Benedikt, E. Elce, B. L. Goodall, H. A. Kalamarides, L. H. McIntosh, L. F. Rhodes, K. T. Selvy, C. Andes, K. Oyler and A. Sen, *Macromolecules*, 2002, **35**, 8978-8988.
70 K. L. Makovetskii, V. I. Bykov and E. S. Finkel'shtein, *Kinet. Catal.*, 2006, **47**, 241-244.
71 P. Wehrmann, M. Zuideveld, R. Thomann and S. Mecking, *Macromolecules*, 2006, **39**, 5995-6002.
72 Y. Li, M. Gao, H. Gao and Q. Wu, *Eur. Polym. J.*, 2011, **47**, 1964–1969.
73 A. Ravasio, L. Boggioni and I. Tritto, *Macromolecules*, 2011, **44**, 4180-4186.
74 H. Gao, Y. Liu, G. Li, Z. Xiao, G. Liang and Q. Wu, *Polym. Chem.*, 2014, **5**, 6012-6018.
75 M. Chen, W. Zou, Z. Cai and C. Chen, *Polym. Chem.*, 2015, **6**, 2669-2676.
76 Y. P. Zhang, W. W. Li, B. X. Li, H. L. Mu and Y. S. Li, *Dalton Trans.*, 2015, **44**, 7382-7394.
77 Y. Na, D. Zhang and C. Chen, *Polym. Chem.*, 2017, **8**, 2405-2409.
78 K. H. Yu, S. L. Huang, Y. H. Liu, Y. Wang, S. T. Liu, Y. C. Cheng, Y. F. Lin and J. T. Chen, *Molecules*, 2017, **22**.
79 H. Cheng and Z. Cai, *ChemCatChem*, 2018, **10**, 497-500.
80 X. Li, J. Baldamus and Z. Hou, *Angew. Chem. Int. Ed. Engl.*, 2005, **44**, 962-965.
81 Z. Hou, Y. Luo and X. Li, *J. Organomet. Chem.*, 2006, **691**, 3114-3121.
82 A. Ravasio, C. Zampa, L. Boggioni, I. Tritto, J. Hitzbleck and J. Okuda, *Macromolecules*, 2008, **41**, 9565-9569.
83 B. Wang, T. Tang, Y. Li and D. Cui, *Dalton Trans.*, 2009, 8963-8969.
84 O. Henschke, F. Köller and M. Arnold, *Macromol. Rapid Commun.*, 1997, **18**, 617-623.
85 L. Boggioni, I. Tritto, M. Ragazzi, P. Carbone and D. R. Ferro, *Macromol. Symp.*, 2001, **169**, 39-50.
86 L. Boggioni, F. Bertini, G. Zannoni, I. Tritto, P. Carbone, M. Ragazzi and D. R. Ferro, *Macromolecules*, 2003, **36**, 882-890.
87 N. Naga and Y. Imanishi, *J. Polym. Sci., Part A: Polym. Chem.*, 2003, **41**, 441–448.
88 Z. Cai, Y. Nakayama and T. Shiono, *Macromolecules*, 2006, **39**, 2031-2033.
89 W. Kaminsky, S. Derlin and M. Hoff, *Polymer*, 2007, **48**, 7271-7278.
90 L. Boggioni, C. Zampa, A. Ravasio, D. R. Ferro and I. Tritto, *Macromolecules*, 2008, **41**, 5107-5115.
91 Z. Cai, Y. Nakayama and T. Shiono, *Macromol. Rapid Commun.*, 2008, **29**, 525-529.
92 L. Boggioni, A. Ravasio, A. C. Boccia, D. R. Ferro and I. Tritto, *Macromolecules*, 2010, **43**, 4543-4556.
93 L. Boggioni, A. Ravasio, C. Zampa, D. R. Ferro and I. Tritto, *Macromolecules*, 2010, **43**, 4532-4542.
94 M. E. Vanegas, R. Quijada and G. B. Galland, *Polymer*, 2010, **51**, 4627-4631.

95 Z. Cai, H. Su and T. Shiono, *Chin. J. Polym. Sci.*, 2013, **31**, 541-549.
96 R. Tanaka, Y. Nakayama and T. Shiono, *Polym. Chem.*, 2013, **4**, 3974.
97 Z. Cai, R. Harada, Y. Nakayama and T. Shiono, *Macromolecules*, 2010, **43**, 4527-4531.
98 H. Jung, S. Hong, M. Jung, H. Lee and Y. Park, *Polyhedron*, 2005, **24**, 1269-1273.
99 T. Shiono, M. Sugimoto, T. Hasan, Z. Cai and T. Ikeda, *Macromolecules*, 2008, **41**, 8292-8294.
100 Y. Xing, Y. Chen, X. He and H. Nie, *J. Appl. Polym. Sci.*, 2012, **124**, 1323-1332.
101 Y. Liu, M. Ouyang, X. He, Y. Chen and K. Wang, *J. Appl. Polym. Sci.*, 2013, **128**, 216-223.
102 T. Shiono, in *Polyolefins: 50 years after Ziegler and Natta II*, Springer-Verlag Berlin Heidelberg, 2013, ch. 211, pp. 143-161.
103 R. Tanaka, T. Suenaga, Z. Cai, Y. Nakayama and T. Shiono, *J. Polym. Sci., Part A: Polym. Chem.*, 2014, **52**, 267-271.
104 P. Huo, W. Liu, X. He and G. Mei, *J. Polym. Res.*, 2015, **22**, 1-7.
105 X. He, Y. Deng, Z. Han, Y. Yang and D. Chen, *J. Polym. Sci., Part A: Polym. Chem.*, 2016, **54**, 3495-3505.
106 W. Zhao and K. Nomura, *Macromolecules*, 2016, **49**, 59-70.
107 R. Tanaka, R. Matsuzaki, Y. Nakayama and T. Shiono, *J. Polym. Sci., Part A: Polym. Chem.*, 2017, **55**, 2136-2140.
108 X. He, G. Tu, F. Zhang, S. Huang, C. Cheng, C. Zhu, Y. Duan, S. Wang and D. Chen, *RSC Advances*, 2018, **8**, 36298-36312.
109 D. Yang, J. Dong and B. Wang, *Dalton Trans.*, 2018, **47**, 180-189.
110 M. Li, H. Zhang, Z. Cai and M. S. Eisen, *Polym. Chem.*, 2019, **10**, 2741-2748.
111 X. He, Y. Duan, Y. Guo, K. Wang, B. Wu, Y. Wen, J. Zou, C. Zhu, S. Huang and D. Chen, *J. Organomet. Chem.*, 2020, **915**.
112 Y. Sarazin, G. Fink, K. Hauschild and M. Bochmann, *Macromol. Rapid Commun.*, 2005, **26**, 1208-1213.
113 E. Landry and Z. Ye, *Macromol. Rapid Commun.*, 2013, **34**, 1493-1498.
114 K. Monkkonen and T. T. Pakkanen, *Macromol. Chem. Phys.*, 1999, **200**, 2623-2628.
115 K. Radhakrishnan and S. Sivaram, *Macromol. Chem. Phys.*, 1999, **200**, 858-862.
116 M. J. Yanjarappa and S. Sivaram, *Macromol. Chem. Phys.*, 2004, **205**, 2055-2063.
117 N. Naga, *J. Polym. Sci., Part A: Polym. Chem.*, 2005, **43**, 1285-1291.
118 A. Malmberg and B. Lofgren, *J. Appl. Polym. Sci.*, 1997, **66**, 35-44.
119 H. Arabi, H. S. Mobarakeh, Z. Balzadeh and G.-R. Nejabat, *J. Appl. Polym. Sci.*, 2013, **129**, 3047-3053.
120 K. Wang, J. Wang, Y. Li, L. Pan and Y. Li, *Polymers*, 2017, **9**, 353.
121 Y. Liu, H. X. Xiang, K. T. Wang, G. Wu and Y. B. Li, *Macromol. Chem. Phys.*, 2019, **220**, 1900008.
122 D. Takeuchi and K. Osakada, *Polymer*, 2008, **49**, 4911-4924.
123 R. Tanaka, A. Sasaki, T. Takenaka, Y. Nakayama and T. Shiono, *Polymer*, 2018, **136**, 109-113.
124 X. Song, L. Yu, T. Shiono, T. Hasan and Z. Cai, *Macromol. Rapid Commun.*, 2017, **38**, 1600815.
125 X. Song, L. Cao, R. Tanaka, T. Shiono and Z. Cai, *ACS Macro Lett.*, 2019, **8**, 299-303.
126 M. Li, Z. Cai and M. S. Eisen, *Organometallics*, 2018, **37**, 4753-4762.
127 C. Chen, *Nature Reviews Chemistry*, 2018, **2**, 6-14.
128 C. Tan and C. Chen, *Angew. Chem. Int. Ed. Engl.*, 2019, **58**, 7192-7200.

129 R. Wang, M. Zhao and C. Chen, *Polym. Chem.*, 2016, **7**, 3933-3938.
130 L. Ding, H. Cheng, Y. Li, R. Tanaka, T. Shiono and Z. Cai, *Polym. Chem.*, 2018, **9**, 5476-5482.
131 T. Shiono, M. Sugimoto, T. Hasan and Z. Cai, *Macromol. Chem. Phys.*, 2013, **214**, 2239-2244.
132 R. Tanaka, T. Ikeda, Y. Nakayama and T. Shiono, *Polymer*, 2015, **56**, 218-222.
133 R. Mulhaupt, *Macromol. Chem. Phys.*, 2003, **204**, 289–327.

Chapter 2. Synthesis and Properties of Norbornene/Higher *α*-Olefin Gradient Copolymers by an *ansa*-Fluorenylamidodimethyltitanium-$[Ph_3C][B(C_6F_5)_4]$ Catalyst System

2.1. Introduction

Norbornene (NB)-based olefin copolymers, the most common cycloolefin copolymers (COCs), have excellent thermal, chemical resistance, high transparency and good biocompatibility.[1] The choice of comonomer, comonomer composition, and comonomer sequence distribution controlled the properties of NB-based copolymers. The NB/ethylene (E) copolymerization by zirconocene catalyst systems first appeared in 1991.[2] Since then, researches have designed many types of complexes[3-12], including (^{t}BuNSiMe$_2$Flu)TiMe$_2$ (**I**)[13, 14], which have high activity for NB/E copolymerization when activated by a suitable cocatalyst.[15-17] Some of these catalyst systems also showed activity for NB/propylene (P) copolymerization, despite their activities are much lower than those of the NB/E copolymerization.[18-23]

The catalysts for NB/higher *α*-olefin copolymerization have also been well searched. Beside the early-transition-metal complexes, such as methylene-bridged *ansa*-zirconocenes[24] and half-titanocenes[25], late-transition-metal complexes[26-30] were also reported to show activity for NB/*α*-olefin copolymerization. However, when these complexes are used, the yield of NB/*α*-olefin copolymer usually decreases significantly as the amount of *α*-olefin in the feed increased.

Our group have achieved the living copolymerization of NB and higher *α*-olefins using **I** and its derivatives with dried modified-methylaluminoxane (MMAO) or 2,6-di-*tert*-butyl-4-

methylphenol (BHT)-treated MMAO as a cocatalyst. Moreover, it was discovered that the activity could be improved by introducing alkyl groups (*tert*-butyl (^{t}Bu)) to the fluorenyl ligand.[31, 32]

We have also investigated the NB/higher α-olefin copolymerization by **I**-[Ph_3C][$B(C_6F_5)_4$] with R_3Al (tri-*i*-butylaluminum (^{i}Bu_3Al) or tri-*n*-octylaluminum (Oct_3Al)) as a scavenger. This catalytic system showed high activity, but the chain-transfer by R_3Al was inevitable.[33] Several papers reported about the E homopolymerization with Cp_2ZrMe_2 activated by $B(C_6F_5)_3$ or [Ph_3C][$B(C_6F_5)_4$] using $RAl(OAr)_2$ (Ar = 2,6-di-*tert*-butyl-4-methylphenyl) as a scavenger.[34, 35] We have also reported the synthesis of polyolefins with functionalized chain-ends using the living nature of the **1**-$B(C_6F_5)_3$/^{i}$BuAl(OAr)_2$ system.[36, 37] These examples indicate that $RAl(OAr)_2$ should be a completely qualified scavenger with no chain transfer ability.

In this chapter, a mixture of R_3Al and BHT (R_3Al: BHT = 1:2; R = ^{i}Bu or Oct) (**Figure 2-1**) was prepared and used as the scavenger with **1**-[Ph_3C][$B(C_6F_5)_4$] for NB/α-olefin copolymerization to prevent the occurrence of chain transfer reaction. It was found that the NB/α-olefin (1-octene (O), 1-decene (De), or 1-dodecene (Do)) copolymerization proceeds in a 'living' manner quantitatively to produce the copolymers with gradient structures at high speed. The

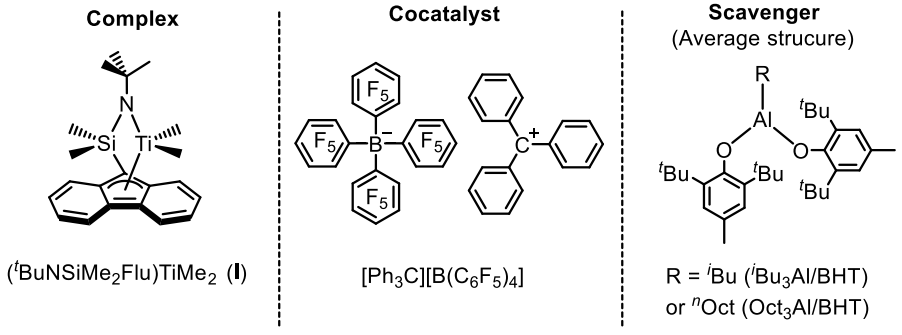

Figure 2-1. Chemical structures of **I**, [Ph_3C][$B(C_6F_5)_4$] (cocatalyst), and aluminum compounds (scavengers for water).

physical properties of these copolymers with novel structures synthesized by the **I**-$[Ph_3C][B(C_6F_5)_4]$/R_3Al/BHT system were investigated in details.

2.2. Experimental section

Materials. Standard Schlenk-line techniques were used and all operations were performed under nitrogen atmosphere. The titanium complex **I** was synthesized according to the method in a previous report.[38] $[Ph_3C][B(C_6F_5)_4]$ (Tosoh Finechem Co.), tri-*i*-butylaluminum ($^{i}Bu_3Al$; 13.6 wt.% Al; Tosoh Finechem Co.), tri-*n*-octylaluminum (Oct_3Al; 7.3 wt.% Al; Tosoh Finechem Co.), and 2,6-bis(1,1-dimethylethyl)-4-methylphenol (BHT; FUJIFILM Wako Pure Chemical Co.) were used as received. The R_3Al/BHT mixture (R = ^{i}Bu or Oct; 0.4 M in toluene) was prepared by adding BHT to R_3Al (R_3Al/BHT = 1/2) in toluene at room temperature. Norbornene (NB), 1-octene (O), 1-decene (De), and 1-dodecene (Do) (Tokyo Chemical Industry Co.) were dried by CaH_2 and distilled, and toluene (Kanto Chemical Co.) was dried by sodium metal and distilled before use.

Copolymerization. All the copolymerization reactions were operated in a 100 mL-glass flask with a magnetic stirrer bar under nitrogen atmosphere. The reactor was heated with a hot air gun under reduced pressure to remove a trace of moisture and charged with nitrogen gas first. Then prescribed amounts of toluene, NB (5.3 M in toluene) and α-olefin liquid were added in turn. After R_3Al/BHT (R = ^{i}Bu or Oct; 0.4 M in toluene) was added, the solution was stirred in room temperature for 30 min and then cooled down to 0 °C by an ice-water bath. At last, toluene solution of $[Ph_3C][B(C_6F_5)_4]$ (18.6 mg, 20 μmol in 4 mL) and **I** (7.4 mg, 20 μmol in 1 mL) were added to start the copolymerization. After the reaction completed (10 min), the solution was quenched by ethanol with 5 wt.% of concentrated hydrochloric acid and poured into methanol. The precipitated

copolymer was filtered, and dried at 60 °C under reduced pressure for 3 hours. The yields (%) were calculated from the weights of copolymers and monomers charged.

Preparation of Sample Films. Polymer solids were heated to 210 °C in a mold and pressed at 20 MPa for 5 minutes. Then the mold was quenched in ice water bath to successfully prepare the sample films (thickness: ~ 200 μm), which were used for the measurements of thermal and mechanical properties.

Analytical Procedures. The number-average molecular weights (M_n) and molecular weight distributions ($Đ$s) were measured by gel permeation chromatography (GPC HLC-8320, Tosoh Co., Tokyo, Japan). Polystyrene standards were used for calibration with THF as the solvent at 40 °C. ^{13}C NMR (125.40 MHz) spectra were measured by a JNM-LA500 spectrometer (JEOL Ltd., Tokyo, Japan) in pulse Fourier transform mode at 130 °C. The pulse angle was 45°, and 10000 scans were accumulated with a pulse repetition time of 3.0 s. The copolymer sample solutions (> 20 wt.%) were prepared with 1,1,2,2-tetrachloroethane-d_2 as a solvent. The central peak (74.47 ppm) of the solvent was used as the internal reference. Thermal gravimetric analysis (TGA) traces (temperature range: 30-500 °C; heating rate: 10 °C/min) were measured on a SII TG/DTA 6300 (Hitachi High-technologies Co., Tokyo, Japan) in nitrogen gas. Differential scanning calorimetry (DSC) traces were measured on a SII DSC 6220 (Hitachi High-technologies Co., Tokyo, Japan) in nitrogen gas using a heating and a cooling rate of 10 °C/min and 20 °C/min, respectively. The glass transition temperatures (T_gs) of the polymers were determined from the middle point of the phase transition of the second heating scan (temperature range: -80-350 °C). The elongation tests of copolymer films were done by a tensile-testing machine (Model 4466, INSTRON Japan, Kanagawa, Japan) with an elongation rate of 10 mm/min at room temperature (25 °C). Samples with the same dumbbell-shape (width: 4 mm; length: 10 mm; thickness: ~ 200μm)

were cut from the copolymer films. Young's modulus values were determined as the slope of the straight line in the first 2 to 5% of elastic region of the stress-strain curve, and the strength and strain at break were determined from the strain at break point of the sample. The visible light transmittance curves of the copolymer films were measured by a SHIMADZU UV-2600 UV/vis spectrophotometer between 350 nm and 800 nm.

Calculation methods. The experimental NB distribution of the NB/O copolymer chain was calculated with Microsoft Excel as follows: "NB′$_n$%", the NB mol% in the NB/O copolymer chain synthesized during the n^{th} minute, was calculated using the following equation:

$$\mathrm{NB'}_n\% = \frac{(\mathrm{conv.}_{\mathrm{NB},n+1} - \mathrm{conv.}_{\mathrm{NB},n})\mathrm{n}_{\mathrm{NB}}}{(\mathrm{conv.}_{\mathrm{NB},n+1} - \mathrm{conv.}_{\mathrm{NB},n})\mathrm{n}_{\mathrm{NB}} + (\mathrm{conv.}_{\mathrm{O},n+1} - \mathrm{conv.}_{\mathrm{O},n})\mathrm{n}_{\mathrm{O}}} \qquad (2-1)$$

where conv.$_{NB,n}$ is the total NB conversion after n minutes, n_{NB} the total amount of NB in the feed, conv.$_{O,n}$ the total O conversion after n minutes, and n_O the total amount of O in the feed. The average total monomer conversion during the n^{th} minute, "conv.′$_n$", is given by the following equation:

$$\mathrm{conv.'}_n = \frac{(\mathrm{conv.}_{\mathrm{NB},n+1} + \mathrm{conv.}_{\mathrm{O},n+1}) - (\mathrm{conv.}_{\mathrm{NB},n} + \mathrm{conv.}_{\mathrm{O},n})}{2} \qquad (2-2)$$

"NB′$_n$%" was plotted as a function of "conv.′$_n$".

The curves of the NB distributions in the copolymers were calculated using the Mayo-Lewis equation based on the monomer reactivity ratios (r_{NB} and $r_{\alpha\text{-olefin}}$) determined using the Fineman-Ross method and the comonomer feed ratio as follows: Assuming that p =

[NB]/([NB]+[α-olefin]) in the feed, P = [NB]/([NB]+[α-olefin]) in the copolymer, and conv.$_{tot.}$ = total monomer conversion, when [NB]/[α-olefin] = 1:1 and thus p_0 = 1:2.

$$p_0 = \frac{1}{2}, P_0 = P(p_0) = \frac{r_{\mathrm{NB}} p_0^2 + p_0(1-p_0)}{r_{\mathrm{NB}} p_0^2 + 2p_0(1-p_0) + r_{\mathrm{olefin}}(1-p_0)^2}, \mathrm{conv.}_{tot.} = 0. \quad (2-3)$$

$$p_1 = p(P_0) = \frac{1 - \frac{2}{n} P_0}{2 - \frac{2}{n}}, P_1 = P(p_1), \mathrm{conv.}_{tot.} = \frac{1}{n}. \quad (2-4)$$

$$p_2 = p(P_1), P_2 = P(p_2), \mathrm{conv.}_{tot.} = \frac{2}{n}. \quad (2-5)$$

…

$$p_n = p(P_{n-1}), P_n = P(p_n), \mathrm{conv.}_{tot.} = \frac{n}{n} = 1. \quad (2-6)$$

In this calculation, 1000 points were applied.

2.3. Results and discussion

Synthesis and structure of the copolymers. At first, the effects of cocatalyst/(scavenger) were investigated in NB/O copolymerization (NB/O = 5/5 mmol/mmol) by **I**. The results shown in **Table 2-1** indicate that the **I**-[Ph_3C][$B(C_6F_5)_4$]/R_3Al/BHT system had the highest activity among these combinations.

Then, the effects of scavenger in NB/O copolymerization using **I**-[Ph_3C][$B(C_6F_5)_4$] were investigated and the results are shown in **Table 2-2** (NB/O = 5.4/5.4 mmol/mmol, T = 0 °C, t = 1 h). When Oct_3Al was used, the copolymer with a M_n of 27 kg/mol and a $Đ$ of 1.66 was obtained

Table 2-1. Results of NB/O copolymerization using **I** with various cocatalyst/scavenger combinations [a]

sample	cocat.	cat./cocat.	scavenger	yield [b] (%)	M_n [c] (kg/mol)	$Đ$ [c]
O-1	MMAO	200	-	11	5	1.4
O-2	dMMAO	200	-	12	5	1.5
O-3[d]	MMAO/BHT	200	-	40	28	1.2
O-4[e]	$B(C_6F_5)_3$	1	$^{i}Bu_3Al$/BHT	<1	4	1.1
O-5[e]	$[Ph_3C][B(C_6F_5)_4]$	1	$^{i}Bu_3Al$/BHT	98	44	1.2

[a] Conditions: Ti = 20 μmol, solvent = toluene, total volume = 33 mL, NB = O = 5 mmol, T = 0 °C, t = 60 min. [b] Calculated from the weight of the obtained copolymer and the total mass of monomer in feed. [c] Determined by GPC (THF, 40 °C, polystyrene standards). [d] BHT = 300 μmol. [e] $^{i}Bu_3Al$/BHT = 400 μmol.

Table 2-2. Results of NB/O copolymerization using **I**-$[Ph_3C][B(C_6F_5)_4]$ with Oct_3Al, $^{i}Bu_3Al$/BHT or Oct_3Al/BHT scavengers [a]

sample	scavenger	yield [b] (%)	M_n [c] (kg/mol)	$Đ$ [c]	N [d] (μmol)
O-6	Oct_3Al	96	27	1.66	40
O-7	$^{i}Bu_3Al$/BHT	100	48	1.20	23
O-8	Oct_3Al/BHT	100	55	1.20	20

[a] Conditions: Ti = 20 μmol, Ti/B/Al = 1/1/10, NB = O = 5.4 mmol, solvent = toluene, total volume = 30 mL, T = 0 °C, t = 60 min. [b] Calculated from the weight of the obtained copolymer and the total mass of monomer in feed. [c] Determined by GPC using monodisperse polystyrene standards (THF, 40 °C, polystyrene standards). [d] Number of copolymer chains calculated based on the weight and M_n of the obtained copolymers.

in 96% yield. On the other hand, copolymers were obtained in 100% yield when $^{i}Bu_3Al$/BHT (M_n = 48 kg/mol; $Đ$ = 1.20) or Oct_3Al/BHT (M_n = 55 kg/mol; $Đ$ = 1.20) was used as the scavenger.

The number of polymer chains (N), a parameter for initiation efficiency and chain-transfer frequency, was calculated from the M_n and the weight of the obtained copolymer. In the system using Oct_3Al as the scavenger, the N value (40 μmol) was twice the number of complex **1** used (20 μmol), which indicated that chain transfer reaction occurred. On the contrary, the N values were close to 20 μmol for the systems with R_3Al/BHT, indicating low chain-transfer ability of R_3Al/BHT. The reason for the difference between the M_n values of sample 2-7 and 2-8 was thought

to be the experimental error: the error in the amount of **I** added and/or partial deactivation of **I** could have caused the different initiation efficiency. The presence of a low-molecular-weight fraction was observed in the GPC curve of the copolymer obtained by the system with Oct_3Al scavenger (**Figure 2-2**), which was absent in the curves of the copolymers obtained by the systems with R_3Al/BHT scavenger.

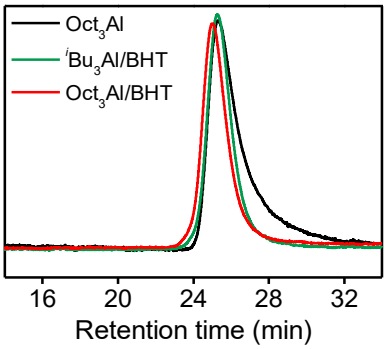

Figure 2-2. GPC curves of the NB/O copolymers obtained by **I**-$[Ph_3C][B(C_6F_5)_4]$ with Oct_3Al, $^{i}Bu_3Al$/BHT or Oct_3Al/BHT as a scavenger.

Next, NB/O copolymerization reactions were further conducted using **I**-$[Ph_3C][B(C_6F_5)_4]$/R_3Al/BHT by changing the amount of monomers added (NB/O = 1/1) (**Table 2-3**). As a result, the copolymers were obtained in 100% yields within 10 minutes irrespective of the type of scavenger used and the amount of monomers added. A linear relationship between the amount of monomers and the M_n values of the obtained copolymers was observed while the $Đ$s remained narrow (**Figure 2-3**). The Ns of the copolymers (19-21 μmol) were close to the number of complex **I** used. The above results lead to the conclusion that the NB/O copolymerization by **I**-$[Ph_3C][B(C_6F_5)_4]$ proceeds in a 'living' manner when $^{i}Bu_3Al$/BHT or Oct_3Al/BHT are used as a scavenger. No significant difference was observed between $^{i}Bu_3Al$/BHT and Oct_3Al/BHT in the scavenger ability for the copolymerization. Therefore, Oct_3Al/BHT was used in the subsequent copolymerization experiments.

Table 2-3. Results of NB/α-olefin copolymerization using **I**-[Ph_3C][$B(C_6F_5)_4$]/R_3Al/BHT [a]

sample	scavenger	NB/α-olefin (mmol/mmol)	yield [b] (%)	M_n [c] (kg/mol)	$Đ$ [c]	N [d] (μmol)
O-9	^{i}Bu_3Al/BHT	2.7/2.7	99	29	1.21	19
O-10	^{i}Bu_3Al/BHT	5.4/5.4	100	60	1.20	19
O-11	^{i}Bu_3Al/BHT	10.8/10.8	100	107	1.20	21
O-12	Oct_3Al/BHT	2.7/2.7	99	29	1.19	19
O-13	Oct_3Al/BHT	5.4/5.4	100	60	1.26	19
O-14	Oct_3Al/BHT	10.8/10.8	100	104	1.24	21
O-15	Oct_3Al/BHT	14.4/7.2	100	112	1.20	19
O-16	Oct_3Al/BHT	7.2/14.4	100	101	1.25	23
O-17	Oct_3Al/BHT	10.8/16.2	100	141	1.27	20
De-1 [e]	Oct_3Al/BHT	10.8/10.8	100	112	1.30	22
Do-1 [f]	Oct_3Al/BHT	10.8/10.8	100	124	1.28	23

[a] Conditions: Ti = 20 μmol, Ti/B/Al = 1/1/10, α-olefin = O, solvent = toluene, total volume = 30 mL, T = 0 °C, t = 10 min. [b] Calculated from the weight of the obtained copolymer and the total mass of monomer in feed. [c] Determined by GPC using monodisperse polystyrene standards (THF, 40 °C, polystyrene standards). [d] Number of copolymer chains calculated from the weight and M_n of the obtained copolymers. [e] α-Olefin = De. [f] α-Olefin = Do.

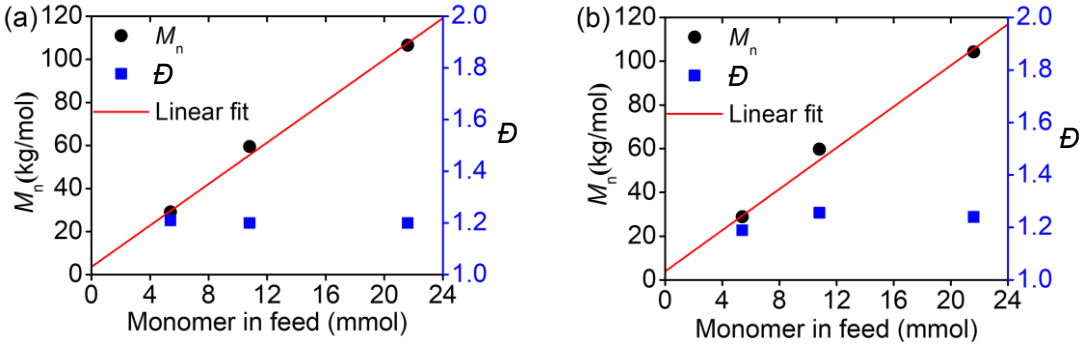

Figure 2-3. M_n and $Đ$ of NB/O copolymers obtained by **1**-[Ph_3C][$B(C_6F_5)_4$]/R_3Al/BHT as a function of the monomer content in the feed, NB/O = 1/1 (mol/mol). (a) Scavenger = ^{i}Bu_3Al/BHT. (b) Scavenger = Oct_3Al/BHT.

Previous study showed that the monomer reactivity ratios of NB and O (r_{NB} and r_O) in the copolymerization by **I**-dMMAO were 8.23 and 0.42, respectively; these ratios suggest that there should exist a gradient structure in the obtained NB/O copolymer.[31] It was expected that the NB/O copolymer obtained by **I**-[Ph_3C][$B(C_6F_5)_4$]/R_3Al/BHT would also have a similar gradient structure. To prove this point, the monomer reactivity ratios of NB/O copolymerization (r_{NB} and r_O) and NB/Do copolymerization (r_{NB} and r_{Do}) by **I**-[Ph_3C][$B(C_6F_5)_4$]/Oct_3Al/BHT were determined by a

series of copolymerizations at different monomer feed ratios (NB:α-olefin = 1:1–1:2.5) in low conversion (**Table 2-4)**.

Table 2-4. Results of NB/α-olefin copolymerization using **I**-[Ph_3C][$B(C_6F_5)_4$]/Oct_3Al/BHT with different monomer ratios in the feed [a]

sample	α-olefin	NB/α-olefin (mmol/mmol)	yield [b] (%)	M_n [c] (kg/mol)	$Đ$ [c]	cont.$_{NB}$ [d] (mol%)
O-18	O	10.8/10.8	7	9	1.30	83
O-19	O	10.8/16.2	14	24	1.19	74
O-20	O	10.8/21.6	11	26	1.20	68
O-21	O	10.8/27.0	15	34	1.15	62
Do-2	Do	10.8/10.8	10	20	1.20	83
Do-3	Do	10.8/16.2	8	24	1.18	78
Do-4	Do	10.8/21.6	10	29	1.19	70
Do-5	Do	10.8/27.0	13	41	1.18	69

[a] Conditions: Ti = 20 μmol, Ti/B/Al = 1/1/1, solvent = toluene, total volume = 30 mL, T = 0 °C, t = 1 min. [b] Calculated from the weight of the obtained copolymer and the total mass of monomer in feed. [c] Determined by GPC (THF, 40 °C, polystyrene standards). [d] Norbornene molar content calculated from the ^{13}C NMR spectra of the copolymers ($CDCl_2CDCl_2$, 125 MHz, 130 °C, 10000 scans).

The NB molar contents (cont.$_{NB}$) of the copolymers obtained were determined by ^{13}C NMR spectroscopy (**Figure 2-4**). The NB contents (in mol%) of the NB/O copolymers were calculated from the integration values of O7 (22.97 ppm), O8 (14.22 ppm) and the total peaks (I_{O7}, I_{O8} and $I_{tot.}$) by eq. 2-7:

$$\text{NB mol\%} = \left[1 - \frac{\frac{I_{O7} + I_{O8}}{2}}{\frac{I_{O7} + I_{O8}}{2} + (I_{tot.} - \frac{I_{O7} + I_{O8}}{2} \times 8)/7}\right] \times 100\% \qquad (2-7)$$

The NB contents (in mol%) of the NB/Do copolymers were calculated from the integration values of Do11 (22.92 ppm), Do12 (14.21 ppm) and the total peaks (I_{Do11}, I_{Do12} and $I_{tot.}$) by eq. 2-8:

$$\text{NB mol\%} = \left[1 - \frac{\frac{I_{\text{Do11}} + I_{\text{Do12}}}{2}}{\frac{I_{\text{Do11}} + I_{\text{Do12}}}{2} + (I_{\text{tot.}} - \frac{I_{\text{Do11}} + I_{\text{Do12}}}{2} \times 12)/7}\right] \times 100\% \qquad (2-8)$$

The monomer reactivity ratios were determined from the monomer molar contents in the copolymers and the monomer feed ratios using the Fineman-Ross method (**Figure 2-4**).[31]

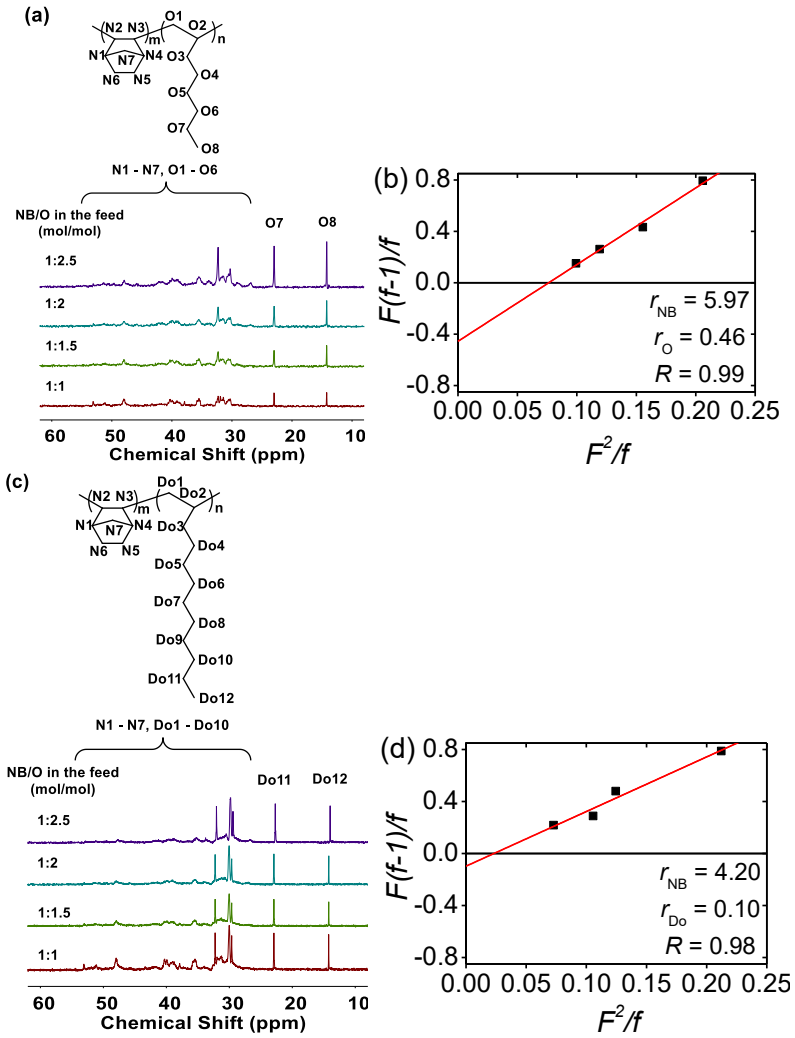

Figure 2-4. (a) ^{13}C NMR spectra of NB/O copolymers obtained using various monomer feed ratios ($CDCl_2CDCl_2$, 125 MHz, 130 °C, 10000 scans). (b) Fineman-Ross plots for NB/O copolymerization: F = [NB]/[O] ratio in the feed, f = [NB]/[O] ratio in the copolymer, R = correlation coefficient. (c) ^{13}C NMR spectra of the NB/Do copolymers obtained using different monomer feed ratios. (d) Fineman-Ross plots for the NB/Do copolymerization, F = [NB]/[Do] in the feed, f = [NB]/[Do] in the copolymer, R = correlation coefficient.

The reactivity ratios of NB and O in the NB/O copolymerization, 5.97 (r_{NB}) and 0.46 (r_O), are higher than those in the NB/Do copolymerization (r_{NB} = 4.20; r_{Do} = 0.10). The monomer reactivity ratios in the NB/De copolymerization were expected to be close to those of NB/O and NB/Do. These results indicate that the obtained NB/α-olefin copolymers should possess a gradient structure starting form a NB-rich head to an α-olefin-rich tail.

The characterization of the specific gradient structure in the NB/O copolymer started from the analysis of a series of copolymers obtained within different reaction times (**Table 2-5**), and the composition profile of the copolymer was determined. The monomer conversion in each interval was calculated from the NB molar contents in the obtained copolymer calculated from ^{13}C NMR spectrum and the copolymer yield (**Figures 2-5** and **2-6** a). The polymerization completed within 6 minutes (monomer conversion = 100%). The NB molar content (NB mol%) was plotted as a function of the monomer total conversion (Conv.$_{tot.}$) in **Figures 2-6** b. The NB molar content of the copolymer gradually decreased from approximately 80 to 0 mol% as the copolymerization proceeded, and the experimental points were close to the curve calculated by the Mayo-Lewis

Table 2-5. Results of NB/O copolymerization using **1**-[Ph_3C][$B(C_6F_5)_4$]/Oct_3Al/BHT with various reaction times [a]

entry	NB/O (mmol/mmol)	t (min)	yield [b] (%)	M_n [c] (kg/mol)	$Đ$ [c]	cont.$_{NB}$ [d] (mol%)
O-22	2.7/2.7	1	10	3	1.23	73
O-23	2.7/2.7	2	24	9	1.20	72
O-24	2.7/2.7	3	44	15	1.16	70
O-25	2.7/2.7	4	59	19	1.15	67
O-26	2.7/2.7	5	74	24	1.16	58
O-27	2.7/2.7	6	99	25	1.17	50

[a] Conditions: Ti = 20 μmol, Ti/B/Al =1/1/1, solvent = toluene, total volume = 30 mL, T = 0 °C. [b] Calculated from the weight of the obtained copolymer and the total mass of monomer in feed. [c] Determined by GPC (THF, 40 °C, polystyrene standards). [d] Norbornene molar content was calculated from the ^{13}C NMR spectra of the copolymers ($CDCl_2CDCl_2$, 125 MHz, 130 °C, 10000 scans).

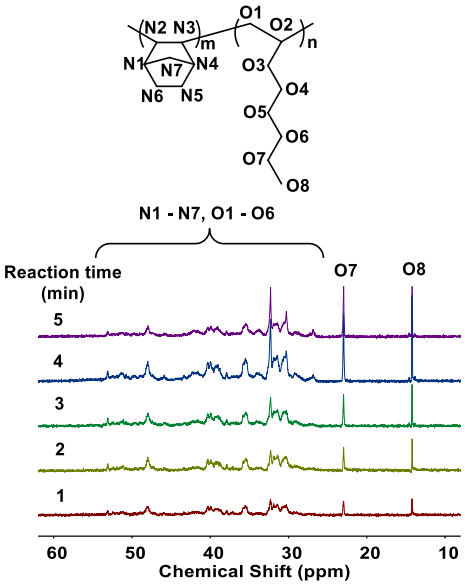

Figure 2-5. ^{13}C NMR spectra of the NB/O copolymers obtained using **I**-[Ph_3C][$B(C_6F_5)_4$]/Oct_3Al/BHT and different reaction times ($CDCl_2CDCl_2$, 125 MHz, 130 °C, 10000 scans).

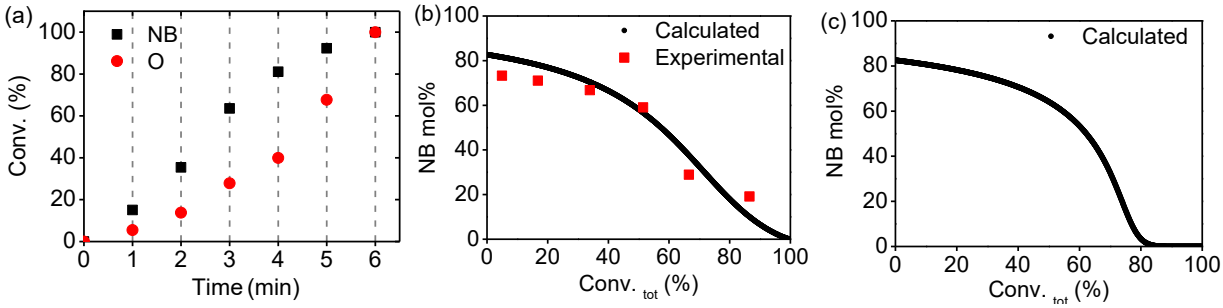

Figure 2-6. (a) NB and O conversion as a function of the reaction time. (b) NB mol% in the NB/O copolymer chain as a function of the total monomer conversion, and the calculated composition profile curve. (c) Calculated composition profile curve of the NB/Do copolymer.

equation: the details of the calculation method were described in the experimental section. Moreover, a slight difference was observed between the composition profile curves of the NB/Do and NB/O copolymers: the NB mol% in the NB/Do copolymer changed more rapidly in the late stage of the copolymerization, and pure Do block was formed at the end of the copolymer chain (**Figure 2-6** c).

In addition to the NB/O gradient copolymers with different chain lengths (sample O-9 to O-14, NB = 50 mol%), the NB/O gradient copolymers with different NB mol% (67 mol% for O-15 and 33 mol% for O-16) were also synthesized for investigating the influence of the molecular structures of the copolymers on their thermal and mechanical properties as shown in **Table 2-3**. NB/De and NB/Do copolymers were also synthesized from the same amounts of comonomers with sample O-14 (sample De-1 and Do-1). The copolymers were obtained in 100% yield within 10 minutes for all the copolymerization without any influence from the amount of comonomer or the type of α-olefin added. A NB/O copolymer with a M_n value and NB weight content similar to those of the NB/Do copolymer (Do-1) was also synthesized (O-17, 36 wt.% of NB). The influence of the side chain length of the α-olefin units on the physical and mechanical properties of these gradient copolymers were investigated in the following sections.

Thermal and tensile properties. The thermal properties of the copolymer films prepared by a melt-pressing procedure at 210 °C were measured by TGA and DSC, the curves were shown in **Figure 2-7** and **2-8**. **Table 2-6** summarized the decomposition temperatures ($T_{d(10\%)}$) and glass transition temperatures (T_g) of the copolymers. All the copolymers showed the $T_{d\ (10\%)}$ values approximately 400 – 415 °C except sample O-15, which had the highest NB content (66 mol%) and showed a higher $T_{d\ (10\%)}$ (424 °C). Only one T_g was observed from -11.7 °C to -18.4 °C in the DSC curves of the /O and NB/De copolymers with 50 mol% of NB, which belonged to the O- or De-rich segment. The NB/Do copolymer possessed a T_g (-47.9 °C) obviously lower than those of the other copolymers, which should be ascribed to almost pure PDo block at the termination of the NB/Do copolymer (**Figure 2-6** c). In addition, the NB/Do copolymer showed a melting point at -32.5 °C caused by the side-crystallization of the PDo block (**Figure 2-8**).

Table 2-6. Thermal and tensile properties of the NB/α-olefin copolymer films

sample	M_n [a] (kg/mol)	$T_{d\,(10\%)}$ [b] (°C)	T_g [c] (°C)	Young's modulus (MPa) [d]	strength (MPa) [d]	strain at break [d]
O-11	107	412	-11.7	298 ± 28	6.8 ± 0.9	0.03 ± 0.01
O-12 [e]	29	407	- [g]	- [g]	- [g]	- [g]
O-13	60	415	-15.6	375 ± 13	9.3 ± 0.6	0.03 ± 0.01
O-14	104	408	-16.5	327 ± 14	6.5 ± 0.2	0.03 ± 0.01
O-15 [f]	112	424	-14.1	- [g]	- [g]	- [g]
O-16	101	412	(-48.6, -9.4, 303.9)	97 ± 12	3.0 ± 0.4	0.27 ± 0.11
O-17	141	400	-18.4	312 ± 3	9.7 ± 0.3	0.11 ± 0.05
De-1	112	412	-16.6	154 ± 12	3.8 ± 0.9	0.04 ± 0.01
Do-1	124	414	-47.9	158 ± 15	4.8 ± 0.2	0.22 ± 0.10

[a] Number-average molecular weights were determined by GPC (THF, 40 °C, polystyrene standards). [b] Decomposition temperature (10 wt.%) determined by TGA. [c] Glass transition temperatures were determined by DSC. [d] Determined by elongation tests. [e] This copolymer film could not be tested due to its brittleness. [f] This copolymer did not form a film. [g] Not determined.

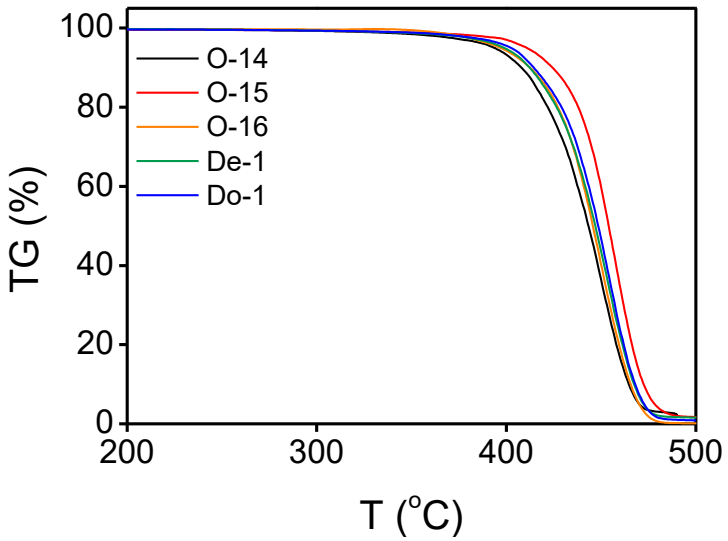

Figure 2-7. TGA curves of the NB/α-olefin copolymers (30 °C – 500 °C, heating rate = 10 °C/min).

It is worth noting that although the observed T_gs were much lower than 0 °C, all the sample films had good strength at room temperature. This phenomenon suggested that there should be a second T_g above room temperature for the copolymers. Considering that the copolymers can be molded into sample films at 210 °C, the second T_g should also be below 210 °C. Besides, three T_g

values were identified in the curve of the NB/O copolymer with 33 mol% of NB, (O-16, **Figure 2-8**). On the other hand, only one T_g was detected for the NB/α-olefin copolymers obtained by non-bridged half-titanocene catalysts (135 °C for NB/O copolymer with 49.2 mol% of NB and 100 °C for NB/Do copolymer with 55.0 mol% of NB).[25] The difference of the thermal properties between these copolymers also indicated that the NB/α-olefin copolymers obtained by **I**-[Ph_3C][$B(C_6F_5)_4$]/R_3Al/BHT had gradient structures.

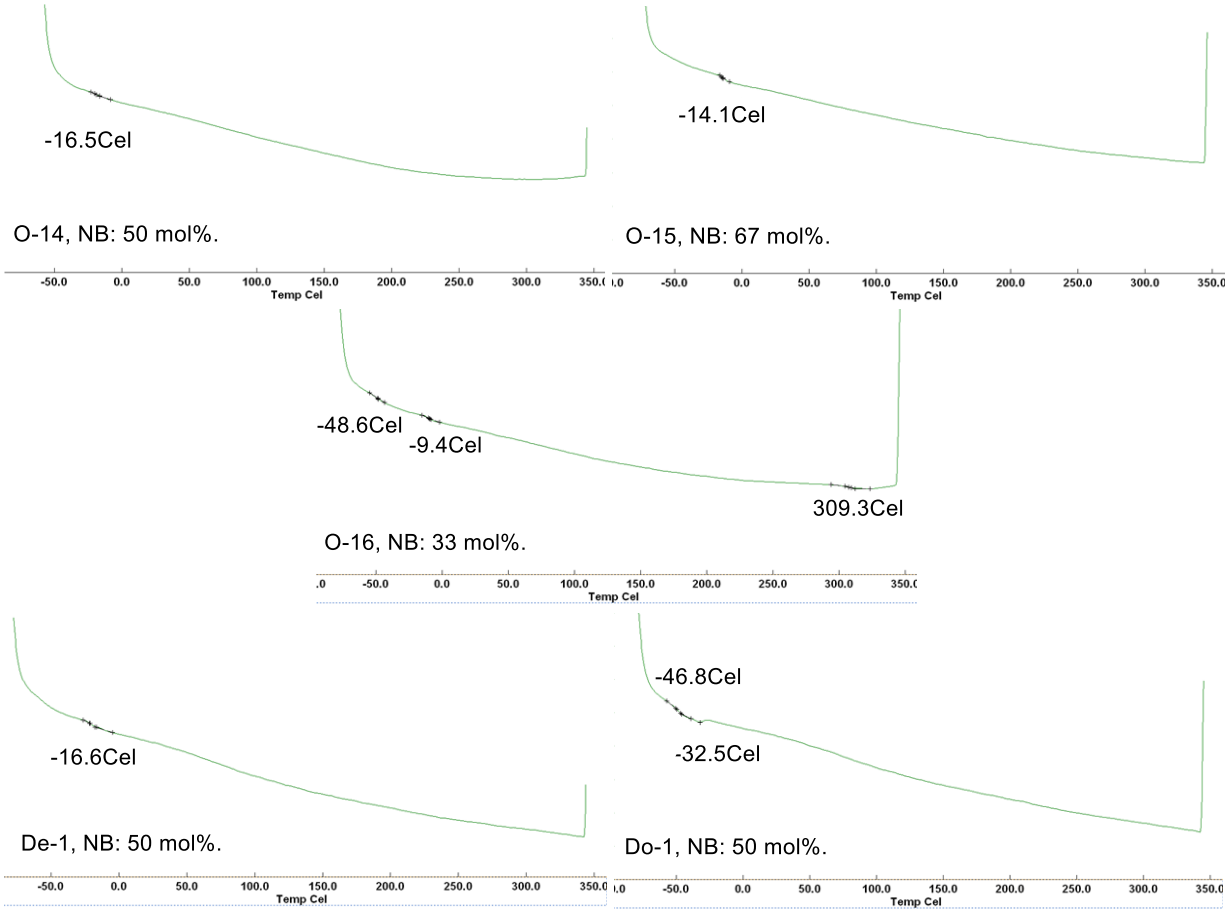

Figure 2-8. Second heating scan of the DSC curves of NB/O copolymers with different NB molar contents, and NB/De and NB/Do copolymers (-80 °C – 350 °C, heating rate = 10 °C/min, cooling rate = 20 °C/min.

The data of tensile properties of the copolymer films are also listed in **Table 2-6**. The difference between the tensile properties of O-11 and O-14 were tiny, indicating that the R_3Al/BHT scavenger used for copolymerization did not influence the structure of obtained NB/O copolymers. The stress-strain curves of the NB/O copolymers with different chain length are shown in **Figure 2-9**a. The film of sample O-12, which had the lowest M_n, was too brittle for the tensile test. Sample O-13 and O-14 had almost the same strain at break value, suggesting that when the M_n value was over 60 kg/mol, the chain length of the gradient copolymer had no influence on the strain at break.

The stress-strain curves for NB/O copolymers with different NB molar contents are shown in **Figure 2-9**b. Sample O-15 with the highest NB molar content (66 mol%), could not be melt-pressed into a film at 210 °C because of its high T_g. The stress-strain curve of NB/O copolymer

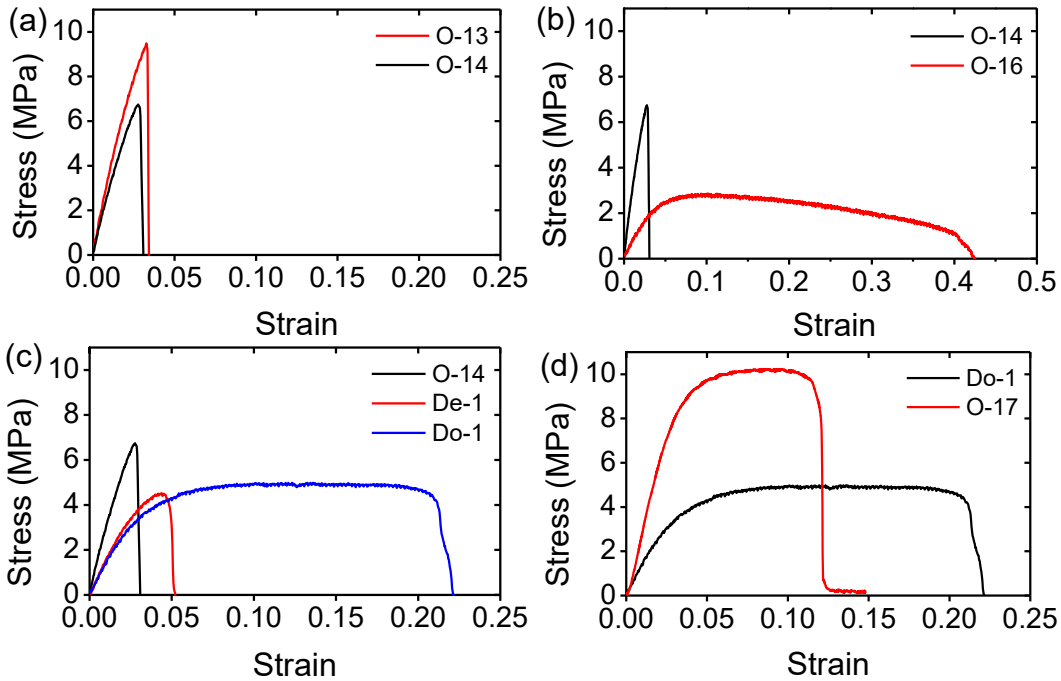

Figure 2-9. Elongation test results for (a) NB/O copolymer films with different chain length, (b) NB/O copolymer films with different NB mol%, (c) NB/α-olefin copolymer films with different α-olefins (O, De or Do). (d) NB/O and NB/Do copolymer films with identical NB weight content and similar molecular weights.

drastically changed by the NB content: the copolymer with the lowest NB content of 33 mol% was elastomeric, whereas the copolymer with 50 mol% of NB was brittle. Specifically, the strain at break for sample O-16 was almost 10 times higher than that of O-14. When the NB molar content in the copolymer increased, the length of the hard NB-rich segment increased and that of the soft O-rich segment decreased, resulting in a brittle material. On the contrary, decreasing the NB molar content led to an increase of the O-rich segment length, resulting in the improvement of strain at break and a loss of strength.

When the comonomer was changed from O to Do keeping the NB molar content in copolymers at 50 mol%, the weight content of NB decreased from 46 wt.% to 36 wt.%. The film of NB/longer *α*-olefin copolymer had higher strain at break with lower strength (**Figure 2-9**c). Surprisingly, the strain at break of NB/Do copolymer (sample Do-1) was about 5 times that of NB/De copolymer (sample De-1), even though the alkyl side chain of *α*-olefin unit was only two carbon atoms longer. These results indicate that the mechanical properties of the gradient copolymers were strongly influenced by the length of the side chain. The mechanical properties of the NB/O and NB/Do copolymer films with the same NB wt.% and similar molecular weights (sample O-17 and Do-1) were also compared (**Figure 2-9**d). The strain at break of O-17 was lower than those of Do-1, but the strength was higher.

These elongation test results fully indicates that the mechanical properties of the gradient poly(NB-*co*-*α*-olefin) copolymers can be well controlled with an excellent balance between drawability and strength by changing the type of *α*-olefin, the comonomer content and the chain length of the copolymer.

The visible-light transmittance of the well-made NB/α-olefin copolymer films (sample O-13, O-14, De-1, and Do-1) was up to 80% (**Figure 2-10**).

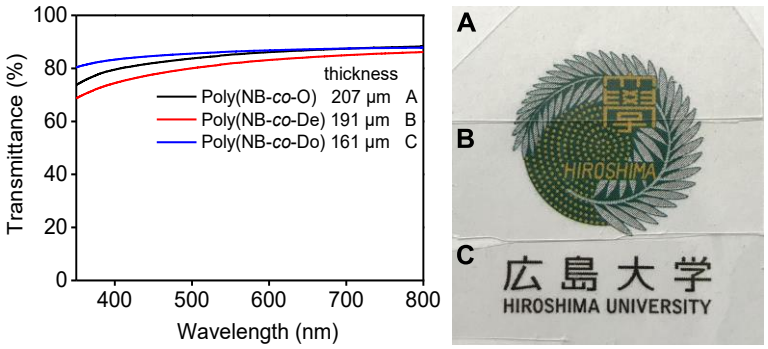

Figure 2-10. Visible-light transmittance curves (350 – 800 nm) and a photograph of the NB/α-olefin copolymer films (NB = 50 mol%) fabricated using melt-pressing and quenching procedures.

2.4. Conclusions

The copolymerization of norbornene (NB) and 1-octene (O) using (^{t}BuNSiMe$_2$Flu)TiMe$_2$ (**I**)-[Ph$_3$C][B(C$_6$F$_5$)$_4$] with 2,6-di-*tert*-butyl-4-methylphenol-treated tri-*i*-butylaluminum (*i*Bu$_3$Al/BHT) or tri-*n*-octylaluminum (Oct$_3$Al/BHT) as a scavenger proceeded in high speed with a 'living' manner. Copolymers with controllable number-average molecular weights (M_n) and narrow molecular weight distributions ($Đ$s) were quantitively obtained. Copolymers of NB with 1-decene (De) or 1-dodecene (Do) were also synthesized. All copolymerization reactions completed within 10 minutes. The difference between the monomer reactivity ratios of the NB/O copolymerization (r_{NB} = 5.97; r_O = 0.46) and the NB/Do copolymerization (r_{NB} = 4.20; r_{Do} = 0.10) suggested the gradient structures in NB/α-olefin copolymers were slightly different. The copolymers possessed decomposition temperatures ($T_{d\,(10\%)}$) of 400–424 °C. The NB/O and NB/De copolymers with 50 mol% of NB showed one glass transition temperature (T_g) between -11.7 °C and 18.4 °C, whereas the NB/Do copolymer with 50 mol% of NB showed a lower T_g (-47.9 °C).

The melt-pressed copolymer films had high transparency. The mechanical properties of the films were controlled by the choice of comonomer, the comonomer content, and the chain length of the copolymers.

References

1 P. S. Nunes, P. D. Ohlsson, O. Ordeig and J. P. Kutter, *Microfluid Nanofluidics*, 2010, **9**, 145-161.
2 W. Kaminsky, A. Bark and M. Arndt, *Makromol. Chem. Macromol. Symp.*, 1991, **47**, 83-93.
3 X. Li, J. Baldamus and Z. Hou, *Angew. Chem. Int. Ed. Engl.*, 2005, **44**, 962-965.
4 H. Terao, A. Iwashita, S. Ishii, H. Tanaka, Y. Yoshida, M. Mitani and T. Fujita, *Macromolecules*, 2009, **42**, 4359-4361.
5 B. Wang, T. Tang, Y. Li and D. Cui, *Dalton Trans.*, 2009, 8963-8969.
6 W. Apisuk, A. G. Trambitas, B. Kitiyanan, M. Tamm and K. Nomura, *J. Polym. Sci., Part A: Polym. Chem.*, 2013, **51**, 2575-2580.
7 P. Xiang and Z. Ye, *J. Polym. Sci., Part A: Polym. Chem.*, 2013, **51**, 672-686.
8 G. Leone, I. Pierro, G. Zanchin, A. Forni, F. Bertini, A. Rapallo and G. Ricci, *J. Mol. Catal. A: Chem.*, 2016, **424**, 220-231.
9 Y. Yoshida, J. Mohri, S. Ishii, M. Mitani, J. Saito, S. Matsui, H. Makio, T. Nakano, H. Tanaka, M. Onda, Y. Yamamoto, A. Mizuno and T. Fujita, *J. Am. Chem. Soc.*, 2004, **126**, 12023-12032.
10 G. M. Benedikt, E. Elce, B. L. Goodall, H. A. Kalamarides, L. H. McIntosh, L. F. Rhodes, K. T. Selvy, C. Andes, K. Oyler and A. Sen, *Macromolecules*, 2002, **35**, 8978-8988.
11 A. Ravasio, L. Boggioni and I. Tritto, *Macromolecules*, 2011, **44**, 4180-4186.
12 M. Chen, W. Zou, Z. Cai and C. Chen, *Polym. Chem.*, 2015, **6**, 2669-2676.
13 T. Hasan, T. Ikeda and T. Shiono, *Macromolecules*, 2004, **37**, 8503-8509.
14 T. Hasan, T. Shiono and T. Ikeda, *Macromol. Symp.*, 2004, **213**, 123-130.
15 X. Li and Z. Hou, *Coord. Chem. Rev.*, 2008, **252**, 1842-1869.
16 L. Boggioni and I. Tritto, in *Polyolefins: 50 years after Ziegler and Natta II*, ed. K. Walter, Springer-Verlag Berlin Heidelberg, 2013, ch. 217, pp. 117-141.
17 W. Zhao and K. Nomura, *Catalysts*, 2016, **6**, 175.
18 O. Henschke, F. Köller and M. Arnold, *Macromol. Rapid Commun.*, 1997, **18**, 617-623.
19 N. Naga and Y. Imanishi, *J. Polym. Sci., Part A: Polym. Chem.*, 2003, **41**, 441–448.
20 T. Hasan, T. Ikeda and T. Shiono, *Macromolecules*, 2005, **38**, 1071-1074.
21 Z. Cai, Y. Nakayama and T. Shiono, *Macromolecules*, 2006, **39**, 2031-2033.
22 L. Boggioni, A. Ravasio, C. Zampa, D. R. Ferro and I. Tritto, *Macromolecules*, 2010, **43**, 4532-4542.
23 M. E. Vanegas, R. Quijada and G. B. Galland, *Polymer*, 2010, **51**, 4627-4631.
24 H. Jung, S. Hong, M. Jung, H. Lee and Y. Park, *Polyhedron*, 2005, **24**, 1269-1273.
25 W. Zhao and K. Nomura, *Macromolecules*, 2016, **49**, 59-70.
26 Y. Xing, Y. Chen, X. He and H. Nie, *J. Appl. Polym. Sci.*, 2012, **124**, 1323-1332.
27 Y. Liu, M. Ouyang, X. He, Y. Chen and K. Wang, *J. Appl. Polym. Sci.*, 2013, **128**, 216-223.
28 P. Huo, W. Liu, X. He and G. Mei, *J. Polym. Res.*, 2015, **22**, 1-7.
29 X. He, Y. Deng, Z. Han, Y. Yang and D. Chen, *J. Polym. Sci., Part A: Polym. Chem.*, 2016, **54**, 3495-3505.
30 M. Li, H. Zhang, Z. Cai and M. S. Eisen, *Polym. Chem.*, 2019, **10**, 2741-2748.
31 Z. Cai, R. Harada, Y. Nakayama and T. Shiono, *Macromolecules*, 2010, **43**, 4527-4531.
32 R. Tanaka, T. Suenaga, Z. Cai, Y. Nakayama and T. Shiono, *J. Polym. Sci., Part A: Polym. Chem.*, 2014, **52**, 267-271.

33 T. Shiono, M. Sugimoto, T. Hasan, Z. Cai and T. Ikeda, *Macromolecules*, 2008, **41**, 8292-8294.
34 V. C. Williams, C. Dai, Z. Li, S. Collins, W. E. Piers, W. Clegg, M. R. J. Elsegood and T. B. Marder, *Angew. Chem. Int. Ed.*, 1999, **38**, 3695-3698.
35 V. C. Williams, G. J. Irvine, W. E. Piers, Z. Li, S. Collins, W. Clegg, M. R. J. Elsegood and T. B. Marder, *Organometallics*, 2000, **19**, 1619-1621.
36 R. Tanaka, N. Tonoko, S.-i. Kihara, Y. Nakayama and T. Shiono, *Polym. Chem.*, 2018, **9**, 3774-3779.
37 T. Kida, R. Tanaka, K.-h. Nitta and T. Shiono, *Polym. Chem.*, 2019, **10**, 5578-5583.
38 H. Hagihara, T. Shiono and T. Ikeda, *Macromolecules*, 1998, **31**, 3184-3188.

Chapter 3. Synthesis and Properties of Block Copolymers Composed of Norbornene/Higher α-Olefin Gradient Segments Using an *ansa*-Fluorenylamidodimethyltitanium–$[Ph_3C][B(C_6F_5)_4]$ Catalyst System

3.1. Introduction

A variety of polymers with different properties can be obtained from limited olefin monomers through copolymerization.[1-5] The properties of copolymers can be controlled by the choice of comonomers and the content of comonomers.[6, 7] The comonomer sequence distribution in copolymers, i.e., random, alternating, gradient, and block, also strongly influences the properties of copolymers. For block copolymers, unique properties can be given by the design of the structure of each block segment. For example, multi-block polymers formed by alternately connecting polyethylene (PE) and *isotactic* polypropylene (*i*PP) segments have outstanding mechanical properties. [8] The multiblock copolymers with isoprene/4-methylstyrene tapered segments were proved to be good thermoplastic elastomers.[9]

In Chapter 2, by using (^{t}BuNSiMe$_2$Flu)TiMe$_2$ (**I**)–$[Ph_3C][B(C_6F_5)_4]$ with 2,6-di-*tert*-butyl-4-methylphenol (BHT)-treated tri-*i*-butylaluminum (^{i}Bu$_3$Al/BHT) or tri-*n*-octylaluminum (Oct$_3$Al/BHT) as a scavenger, NB/higher α-olefin copolymerization (1-octene (O), 1-decene (De) or 1-dodecene (Do)) was achieved with a "living" manner in high speed. The obtained copolymers were discovered possessing gradient structures: with NB-rich heads and O-rich tails. The copolymers were melt-pressed into transparent films under 210 °C, and the strain at break behavior

of the copolymer films increased as length of the alkyl group of the α-olefin increasing, while the strength decreased.

In this chapter, the copolymerization of NB and higher α-olefins (O or Do) was conducted by **I**–$[Ph_3C][B(C_6F_5)_4]$/Oct_3Al/BHT to verify the "living" nature of the system, and synthesize di- and triblock NB/α-olefin copolymers with gradient segments. The mechanical properties of the obtained block copolymers were investigated and compared to those of the corresponding gradient copolymers (**Scheme 3-1**).

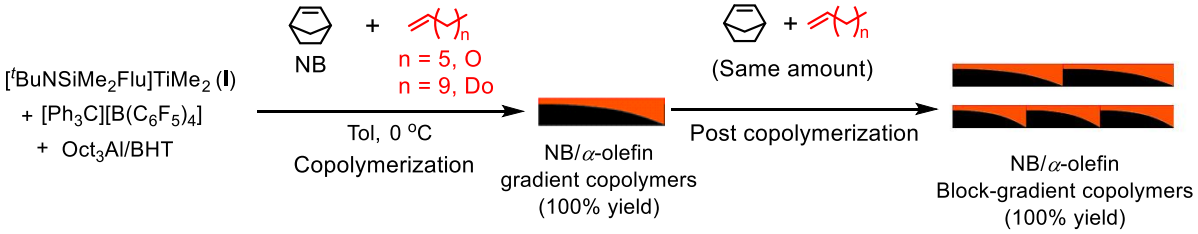

Scheme 3-1 Synthesis of NB/α-olefin (O or Do) block-gradient copolymers using **I**–$[Ph_3C][B(C_6F_5)_4]$/Oct_3Al/BHT.

3.2. Experimental section

Materials. All operations were performed under nitrogen gas using standard Schlenk-line techniques. Titanium complex **I** was synthesized according to a previously reported method.[10] $[Ph_3C][B(C_6F_5)_4]$ (Tosoh Finechem Co.), BHT (Fujifilm Wako Pure Chemical Co.), and Oct_3Al (7.3 wt.% Al; Tosoh Finechem Co.) were used as received. The Oct_3Al/BHT toluene solution (0.4 mol/L), was prepared by adding two equivalents of BHT into Oct_3Al in toluene. Toluene (Kanto Chemical Co.) was dried with sodium metal and distilled before use. NB, O, and Do (Tokyo Chemical Industry Co.) were dried over CaH_2, distilled, and made into toluene solutions before use.

Copolymerization. A toluene solution of NB and α-olefin mixture (NB/α-olefin = 1/1 (mol/mol)) was prepared. All the copolymerization reactions were performed in a 100-mL glass reactor with a magnetic stirrer bar under the nitrogen atmosphere. First, the reactor was heated by hot air gun under reduced pressure to remove a trace of moisture and then charged with nitrogen gas. Then prescribed amounts of toluene, NB/α-olefin and Oct_3Al/BHT solutions were added in this order into the reactor. The solution was stirred at room temperature for 30 min and then cooled down to 0 °C by an ice-water bath. Finally, $[Ph_3C][B(C_6F_5)_4]$ (18.6 mg, 20 μmol in 4 mL toluene) and **I** (7.4 mg, 20 μmol in 1 mL toluene) were added successively to start the polymerization. After the first stage of copolymerization had been completed, the same amount of NB/α-olefin toluene solution was added to start block copolymerization. This process was repeated when synthesizing the triblock copolymers. (total volume of the solution = 30 mL) After the polymerization was completed, the copolymerization reaction was quenched using methanol with 5 wt.% of concentrated hydrochloric acid. The copolymers were washed with methanol, filtered, and dried at 60 °C under reduced pressure for 3 h. The yields (%) were calculated from the copolymer weights and the weight of the monomer charged.

Preparation of Sample Films. Polymer films were made by a melt-pressing procedure under 210 °C. After the copolymers were pressed under 20 MPa for 5 min, they were quenched in ice water and separated from the mold. Then the polymer films were annealed in an oven at 100 °C for 3 h and cooled to room temperature in air to prepare sample sheets (thickness: ~200 μm) for thermal and tensile measurements.

Analytical Procedures. The number-average molecular weights (M_ns) and molecular weight distributions ($Đ$s) were determined by gel permeation chromatography (GPC HLC-8320,

Tosoh Co., Tokyo, Japan) at 40 °C with THF as the solvent. Polystyrene standards were used for calibration. ^{13}C NMR (125.40 MHz) spectra were recorded at 130 °C by a JNM-LA500 spectrometer (JEOL Ltd., Tokyo, Japan) in pulsed-Fourier-transform mode. The pulse angle was 45°, and 10000 scans were accumulated with a pulse repetition time of 3.0 s. The copolymer solutions were prepared with 1,1,2,2-tetrachloroethane-d_2 as the solvent (concentration > 20 wt.%). The central peak (74.47 ppm) of the solvent was used as the internal reference. Thermal gravimetric analysis (TGA) (30 – 500 °C; 10 °C/min) was performed using a SII TG/DTA 6300 (Hitachi High-technologies Co., Tokyo, Japan). Differential scanning calorimetry (DSC) was performed in nitrogen gas using a SII DSC 6220 (Hitachi High-technologies Co., Tokyo, Japan) with a heating rate of 10 °C/min and a cooling rate of 20 °C/min. The T_g values were determined from the middle point of the phase transition of the second heating scan. Dynamic mechanical analysis (DMA) of the films was performed from -100 to 200 °C at 10 Hz with a heating rate of 2 °C/min using a dynamic mechanical analyzer (DVE-V4, UBM Co. Ltd, Kyoto, Japan) and rectangular specimens (width, 5 mm; gauge length, 30 mm) cut from the copolymer sheets. Stress–strain curves were recorded using a tensile-testing machine (Model 4466, Instron Japan, Kanagawa, Japan) at 25 °C with an elongation rate of 10 mm/min. Dumbbell-shaped specimens with a width of 4 mm and a gauge length of 10 mm were cut from the sample sheets. Young's modulus values were determined as the slope of the straight line in the first 2 to 5% of elastic region of the stress-strain curve, and the strength and strain at break were determined from the strain at break point of the sample. The light transmittances of the copolymer films were measured using a Shimadzu UV-2600 UV/vis spectrophotometer with a light wavelength ranging from 350 nm to 800 nm. One-dimensional small-angle X-ray scattering (SAXS) measurements were performed using a Nano-Viewer SAXS system (Rigaku, Japan) with Cu*Ka* radiation (40 kV and 30 mA). SAXS patterns

were measured using an imaging plate with an exposure time of 30 min. Scanning probe microscope (SPM) measurements were performed on a Dimension Icon SPM system (Bruker, America) with a RTESPA-300 probe using standard peak force quantitative nanomechanical mapping (QNM) mode (in air). The scan size was 3 μm, and the scan rate was 0.5 Hz. The samples were prepared as followed: The copolymer films made by a melt-pressing procedure were first covered by a two-component epoxy resin adhesive, then the samples were cut from the films by a cryomicrotome under -115 °C.

3.3. Results and discussion

Synthesis of block copolymers. As was described in Chapter 2, the NB/O copolymerization reactions (NB/O = 1/1 (mol/mol)) using **I**–[Ph_3C][$B(C_6F_5)_4$]/Oct_3Al/BHT quantitatively produced copolymers in 6 min regardless the amount of the monomers added (**Table 3-1**, P(NB-*co*-O)-1, P(NB-*co*-O)-2, P(NB-*co*-O)-3). Based on these results, post copolymerization reactions were performed by adding the same amount of NB/O after the first polymerization for 6 min to obtain diblock copolymers (**Table 3-1**, P(NB-*co*-O)$_2$-1, P(NB-*co*-O)$_2$-2, P(NB-*co*-O)$_2$-3). The second copolymerization lasted another 5–6 min for reaching 100% monomer conversion. Triblock copolymers were also quantitatively obtained by repeating this process (**Table 3-1**, P(NB-*co*-O)$_3$-1, P(NB-*co*-O)$_3$-2).

The GPC curves of the gradient and block NB/O copolymers were compared (**Figure 3-1**). **Figure 3-1**a shows the GPC curves of the diblock copolymer (P(NB-*co*-O)-4), the corresponding gradient copolymer (P(NB-*co*-O)$_2$-3), and the prepolymer (P(NB-*co*-O)-3) obtained in the first stage. The main peak in the GPC curve of the diblock copolymer coincided well that of the

Table 3-1. Results of NB/α-olefin copolymerization and block copolymerization [a]

sample	NB/α-olefin (mmol/mmol)	t (min)	yield [b] (%)	M_n [c] (kg/mol)	$Đ$ [c]	N [d] (μmol)	$T_{d(10\%)}$ [e] (°C)	T_g [f] (°C)
P(NB-*co*-O)-1	2.7/2.7	6	99	25	1.17	22	– [i]	– [i]
P(NB-*co*-O)-2	3.6/3.6	6	99	35	1.16	21	– [i]	– [i]
P(NB-*co*-O)-3	5.4/5.4	6	100	57	1.17	19	415	-15.6
P(NB-*co*-O)-4 [g]	10.8/10.8	10	100	104	1.24	21	408	-16.5
P(NB-*co*-O)$_2$-1	2.7/2.7 × 2	6 + 5	100	53	1.32	21	415	-13.2
P(NB-*co*-O)$_2$-2	3.6/3.6 × 2	6 + 5	100	76	1.27	20	418	-11.1
P(NB-*co*-O)$_2$-3	5.4/5.4 × 2	6 + 6	100	94	1.35	24	412	– [j]
P(NB-*co*-O)$_3$-1	2.7/2.7 × 3	6 + 5 + 5	100	75	1.46	22	413	-18.0
P(NB-*co*-O)$_3$-2	3.6/3.6 × 3	6 + 5 + 6	100	103	1.45	22	412	-11.8
P(NB-*co*-O)$_n$ [h]	10.8/10.8	10 (7.5)	100	106	1.43	21	412	– [j]
P(NB-*co*-O)-5 [g]	10.8/16.2	10	100	141	1.27	20	400	-18.4
P(NB-*co*-O)$_2$-4	5.4/8.1 × 2	6 + 6	100	125	1.46	23	395	-13.2
P(NB-*co*-Do) [g]	10.8/10.8	10	100	124	1.28	23	414	-46.8
P(NB-*co*-Do)$_2$	5.4/5.4 × 2	6 + 6	100	114	1.44	25	412	-13.6
P(NB-*co*-Do)$_n$ [h]	10.8/10.8	10 (7.5)	99	129	1.35	22	412	-18.1

[a] Conditions: Ti = 20 μmol, Ti/B/Al = 1/1/1, solvent = toluene, total volume = 30 mL, T = 0 °C. [b] Calculated from the weight of the obtained copolymer and the total mass of monomer in feed. [c] Determined by GPC. [d] Number of copolymer chains (N) was calculated from the weights of the obtained copolymer and M_n. [e] Determined by TGA. [f] Determined by DSC, with T_g values calculated from the second heating curves. [g] Data from previous work. [h] Monomer mixture was added in drops over 7.5 min, total reaction time was 10 min. [i] Not determined. [j] Not detected.

corresponding gradient copolymer, except for a small shoulder corresponding to the prepolymer.

Figure 3-1b and c show the GPC curves of the gradient, diblock, and triblock copolymers synthesized by adding the same amount of NB/O in each stage. The main peak of copolymer was obviously shifted to a higher molar mass region after each stage of reaction. However, weak

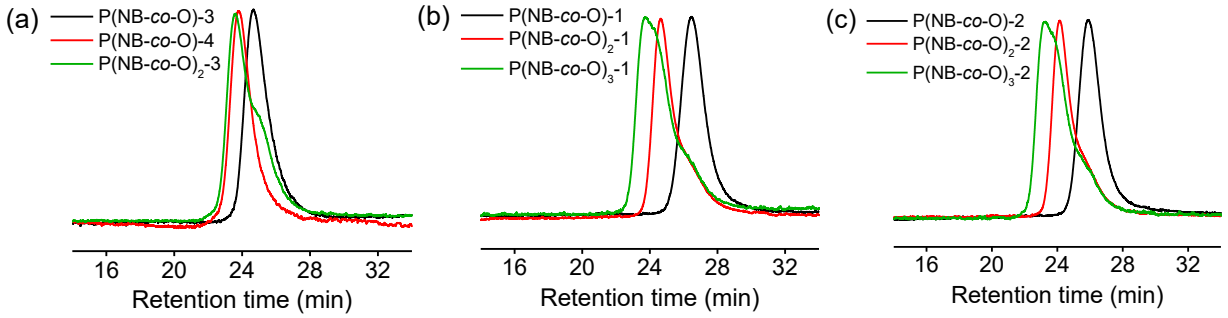

Figure 3-1. GPC curves of gradient and block NB/O copolymers obtained by **I**–[Ph_3C][$B(C_6F_5)_4$]/Oct_3Al/BHT: (a) P(NB-*co*-O)-3, P(NB-*co*-O)-4, P(NB-*co*-O)$_2$-3; (b) P(NB-*co*-O)-1, P(NB-*co*-O)$_2$-1, P(NB-*co*-O)$_3$-1; (c) P(NB-*co*-O)-2, P(NB-*co*-O)$_2$-2, P(NB-*co*-O)$_3$-2.

shoulder peaks still existed in the curves of the block copolymers, thus the diblock triblock copolymers had wider *Đ*s of 1.27 – 1.35 and 1.45 – 1.46, respectively. But the number of polymer chains (*N*) of the block copolymers (20–24 μmol) were close to those of the gradient polymers (19–22 μmol), indicating that chain transfer reactions were basically avoided during the block copolymerization. These results clearly indicate that the "pseudo-living" NB/O copolymerization were achieved **I**–[Ph_3C][$B(C_6F_5)_4$]/Oct_3Al/BHT to produce diblock and triblock NB/O copolymers with a gradient structure in each block in 100% yields at high speed.

Based on the results of NB/O block copolymerization, a diblock NB/Do copolymer was synthesized (**Table 3-1**, P(NB-*co*-Do)$_2$), and a diblock NB/O copolymer with the same NB wt.% with that of the NB/Do diblock copolymer (NB = 50 mol% and 36 wt.%) was also synthesized (**Table 3-1**, P(NB-*co*-O)$_2$-4). In addition, the corresponding pseudo-random copolymers of NB/O and NB/Do were prepared by the continuous addition of the monomer mixture during the copolymerization in a period of 7.5 min (**Table 3-1**, P(NB-*co*-O)$_n$ and P(NB-*co*-Do)$_n$). The small shoulder peak in the GPC curve of P(NB-*co*-O)$_n$ was considered as an experimental error for the erratical manual adding rate of the monomer mixture . The pseudo-random copolymers showed unimodal peaks in their GPC curves with narrow *Đ*s, which were 1.43 for P(NB-*co*-O)$_n$ and 1.35 for P(NB-*co*-Do)$_n$ (**Figure 3-2**). The weight fractions of the prepolymer and the block copolymer

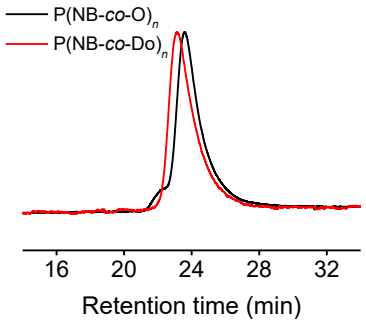

Figure 3-2. GPC curves of NB/O and NB/Do pseudo-random copolymers

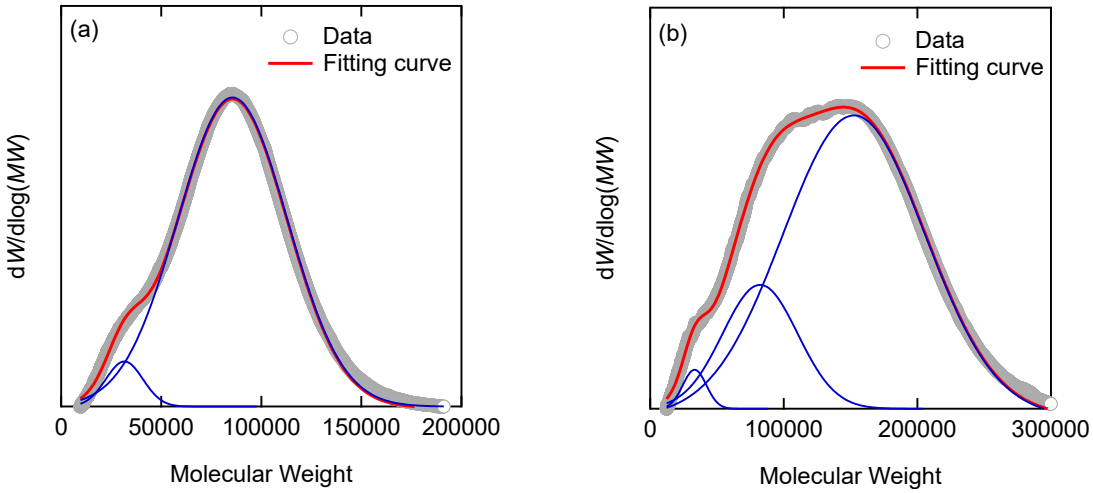

Figure 3-3. Fitting results of molecular weight distribution curves of P(NB-*co*-O)$_2$-1 (a) and P(NB-*co*-O)$_3$-1 (b). The red line represents the fitting curve from a sum of Gaussian functions (blue lines).

Table 3-2. Weight fractions of NB/*α*-olefin block copolymers in obtained post polymers [a]

sample	Gradient content (wt.%)	Diblock content (wt.%)	Triblock content (wt.%)
P(NB-*co*-O)$_2$-1	12	89	–
P(NB-*co*-O)$_2$-2	11	89	–
P(NB-*co*-O)$_2$-3	15	85	–
P(NB-*co*-O)$_2$-4	17	83	–
P(NB-*co*-O)$_3$-1	6	27	68
P(NB-*co*-O)$_3$-2	6	25	69
P(NB-*co*-Do)$_2$	17	83	–

[a] Determined from the relative peak area of each fraction after converting the x-axis of the molecular weight distribution curve back to logarithmic scale.

in the product were calculated from the relative areas of the fitting curves of the molecular weight distribution curve (**Figure 3-3**, **Table 3-2**). The diblock copolymer contents in the obtained polymers were about 83 to 89 wt.%, while the triblock polymer contents were 68 to 69 wt.%. Therefore, it was considered that the thermal and mechanical properties of the obtained copolymers were representative for those of the pure block copolymers.

Optical properties of copolymer films. Figure 3-4 showed the UV-vis spectra of the films prepared from the diblock and triblock NB/O copolymers. All films showed good transparency in the visible-light range (~ 80%).

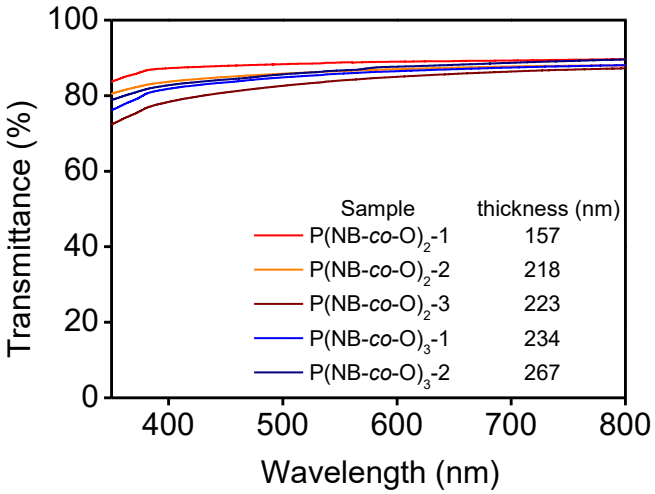

Figure 3-4. Visible light transmittance curves (350 – 800 nm) of diblock and triblock NB/O copolymer films.

Thermal properties of copolymer films. The decomposition temperature ($T_{d(10\%)}$) of the copolymer films listed in **Table 3-1** was determined by TGA, and the curves are shown in **Figure 3-5**. The NB/O copolymers with different molecular structures (gradient, diblock, triblock, and pseudo-random) and a NB molar content of 50 mol% had similar $T_{d(10\%)}$ values ranging from 408 to 418 °C. The NB/Do copolymers with different molecular structures (gradient, diblock, and pseudo-random) and a NB molar content of 50 mol% also had similar $T_{d(10\%)}$ values between 412 and 414 °C. The gradient and diblock NB/O copolymers with a NB molar content of 40 mol% had lower $T_{d(10\%)}$ around 395 – 400 °C (P(NB-*co*-O)-5 and P(NB-*co*-O)$_2$-4). These results indicate that the NB content of the NB/α-olefin copolymer influenced its thermal stability.

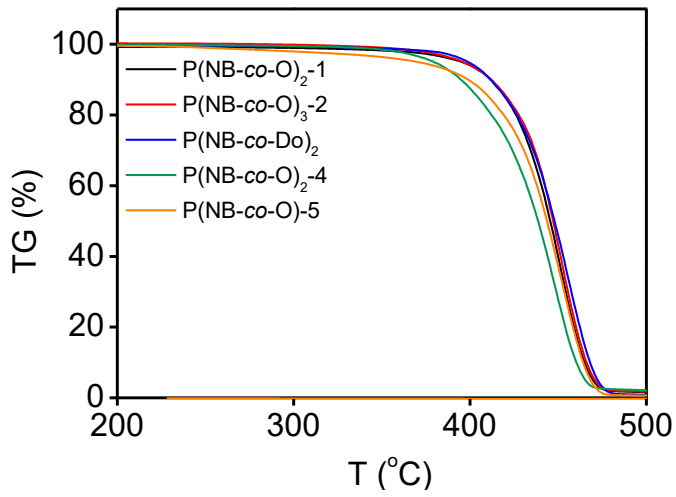

Figure 3-5. TGA curves of NB/α-olefin copolymers.

The T_g values of the NB/α-olefin copolymer films are also listed in **Table 3-1,** and the DSC curves are shown in **Figure 3-6**. The gradient and block NB/O copolymers with 50 mol% of NB had T_g values ranged from -18.0 to -11.1 °C, while those of the gradient (P(NB-*co*-O)-5) and diblock (P(NB-*co*-O)$_2$-4) copolymers with 40 mol% of NB were -18.4 °C and -13.2 °C, respectively. These results indicate that the T_g values over the observed ranges of NB content and block length were not strongly influenced by the block structures and the NB molar content. No clear glass transition point was observed in the DSC curve of pseudo-random NB/O copolymer (P(NB-*co*-O)$_n$). When Do was used as the comonomer instead of O, the T_g values of the gradient, block, and pseudo-random copolymer (P(NB-*co*-Do), P(NB-*co*-Do)$_2$, and P(NB-*co*-Do)$_n$) were -46.8 °C, -13.6 °C, and -18.1 °C , respectively. In addition, a melting point (T_m) probably derived from the side-chain crystallization of PDo segments appeared below 0 °C.

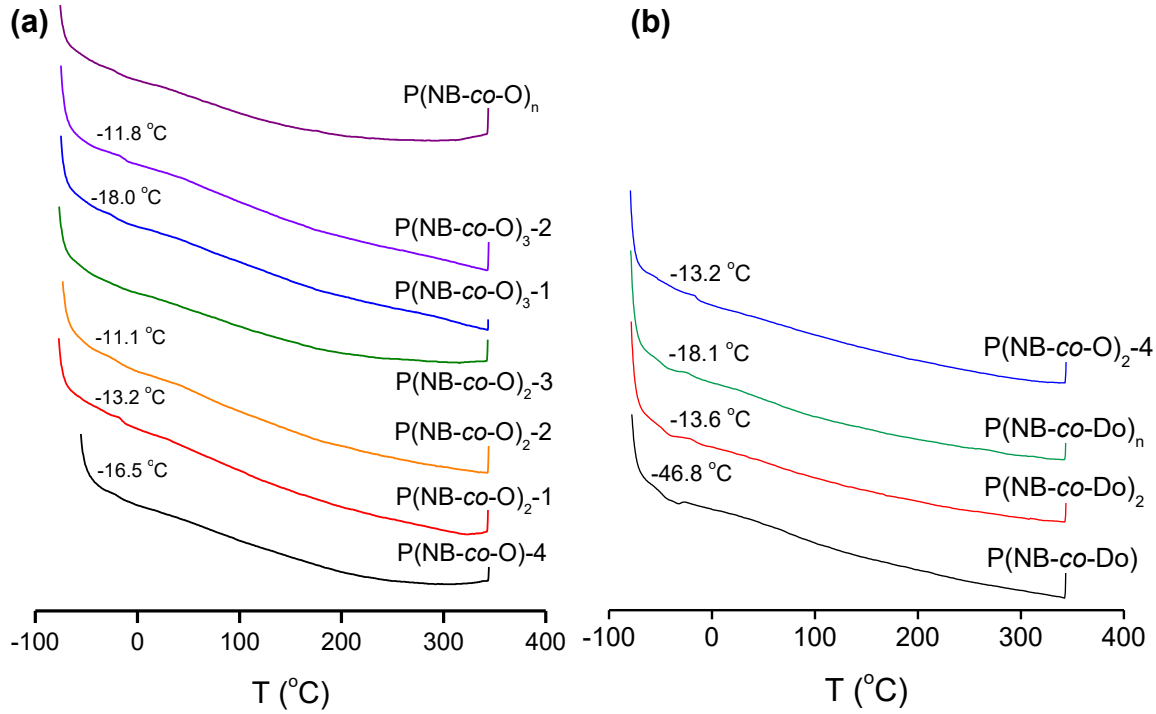

Figure 3-6. DSC curves of copolymers: (a) gradient, diblock and triblock NB/O copolymers; (b) gradient, diblock and pseudo-random NB/Do copolymers.

The DMA curves of the di- and triblock NB/O copolymer films are shown in **Figure 3-7** and **3-8**. Two single relaxation peaks at around -24 and 160 ºC (T_gs) were observed for all sample films, which were belonging to the O-rich and NB-rich segment, respectively. In the curve of diblock copolymer with the longest block length (P(NB-*co*-O)$_2$-3), the two relaxation peaks were clearly separated, more obvious than those in the curves of the other di- and triblock copolymers. To be mentioned that the lower relaxation peak in DMA coincided with the T_g detected by DSC. These results suggest that there must existed a phase-separated morphology in P(NB-*co*-O)$_2$-3, while the phase-separated morphology of the other copolymers was not clear.

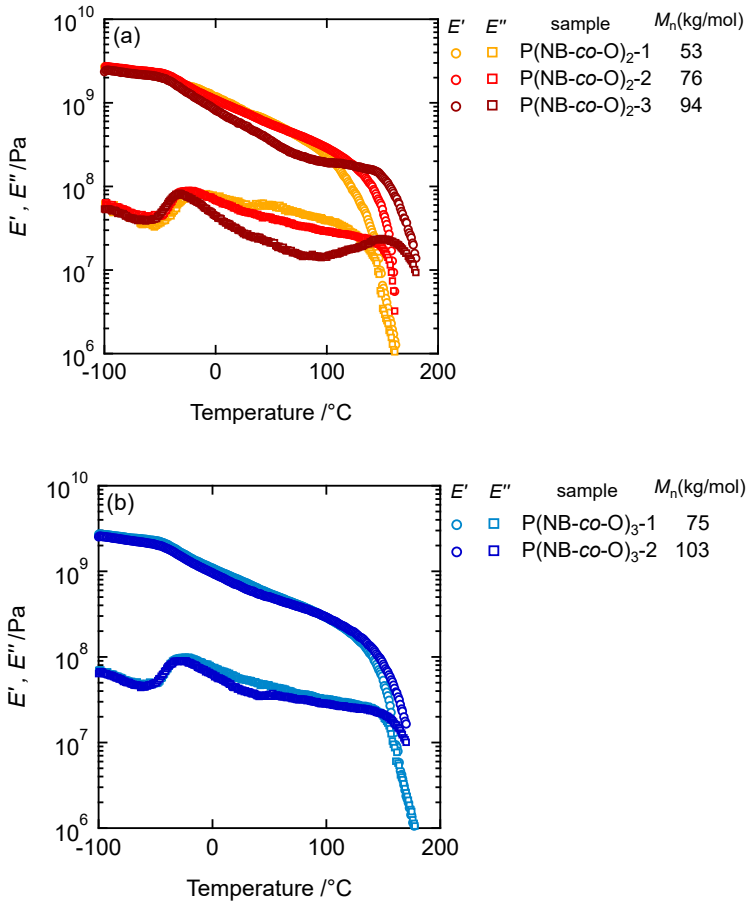

Figure 3-7. Temperature dependences of the storage and loss moduli (*E*' and *E*'') of NB/O copolymers: (a) diblock; (b) triblock.

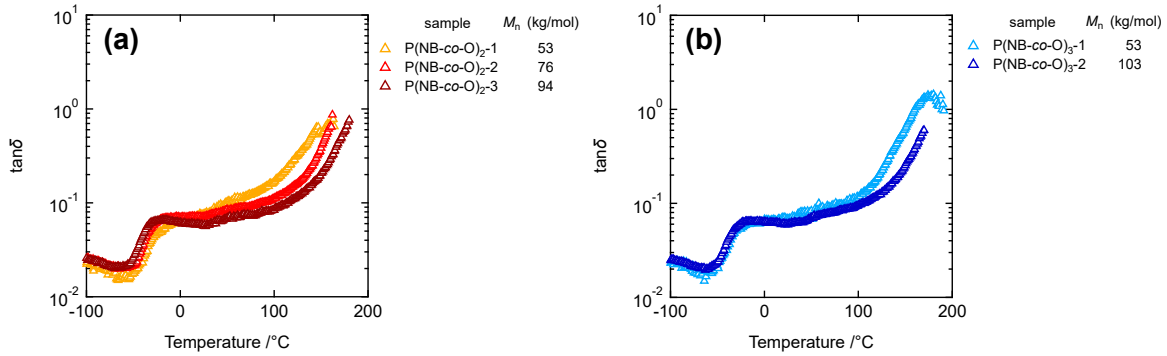

Figure 3-8. Temperature dependences of the tangent delt of NB/O copolymers: (a) diblock; (b) triblock.

The small-angle X-ray scattering (SAXS) of the NB/O copolymer films were also measured (**Figure 3-9**). In the SAXS curves of the gradient and block copolymers, a broad peak for the phase-separated morphology was observed, while in the curve of the pseudo-random copolymer, no obvious scattering peak was observed. Besides, the scanning probe microscopy (SPM) was measured to investigate the structures of the gradient and the diblock NB/O copolymers (**Figure 3-10**). Lamellar structures were observed in the image of the gradient copolymer film, while no distinct structure was observed in that of the diblock copolymer film. The DMA and SAXS results suggest that the gradient-block copolymers with shorter block length had smaller phase separation structures without obvious boundaries, which could not be identified in SPM images.

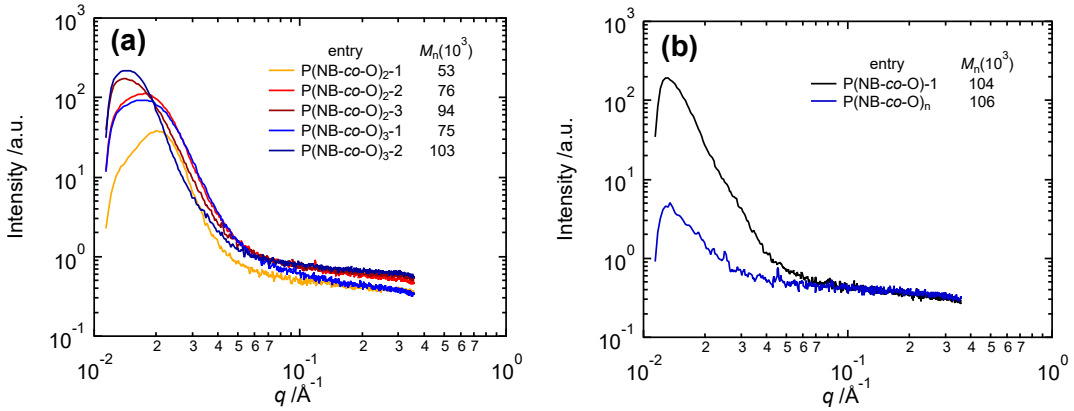

Figure 3-9 One-dimensional SAXS profiles of NB/O copolymers: (a) block; (b) gradient and pseudo-random.

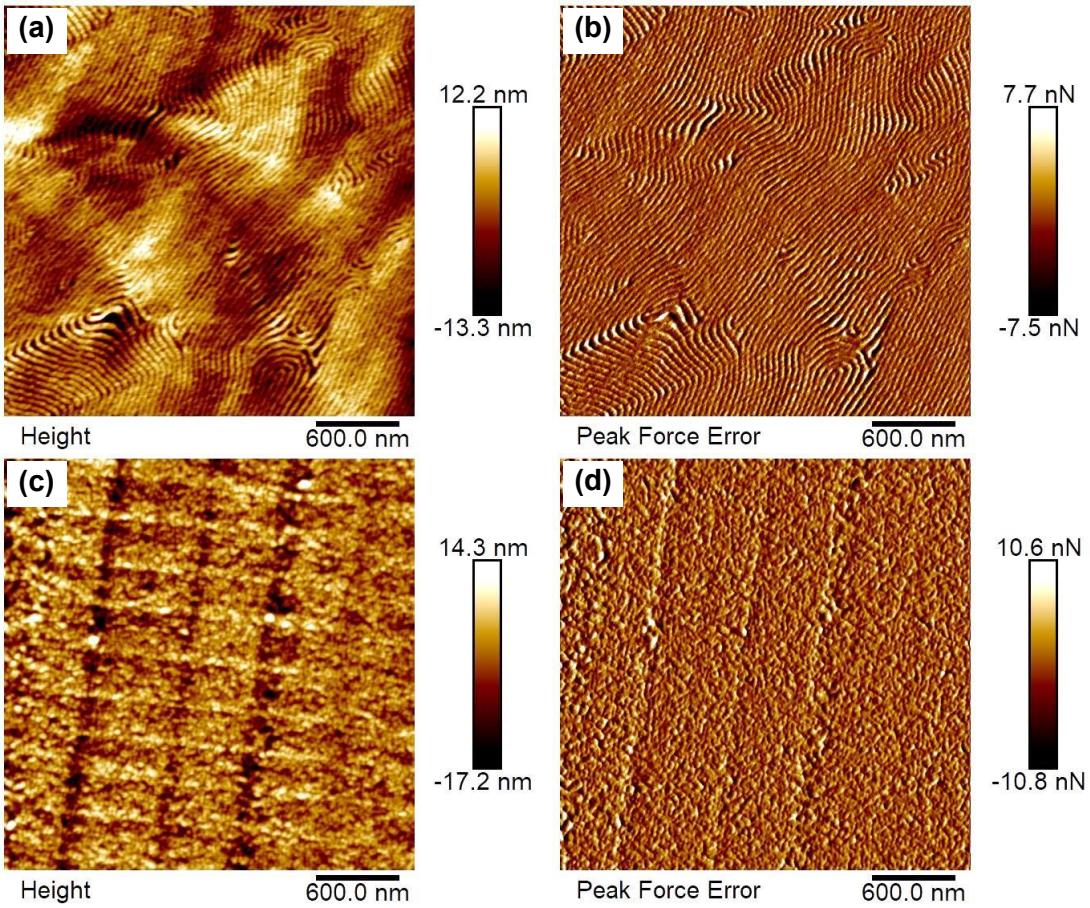

Figure 3-10. SPM images of gradient and block NB/O copolymer films: (a) gradient (M_n = 77000, $Đ$ = 1.18), height image; (b) gradient, peak force error image; (c) gradient-block (M_n = 73000, $Đ$ = 1.44), height image; (d) gradient-block, peak force error image.

Tensile properties and microstructure of copolymer films. The tensile properties and the stress-strain curves of NB/α-olefin copolymer films before annealing are shown in **Table 3-3** and **Figure 3-11,** respectively. **Figure 3-11**a and b indicate that only the strains at break of the di- and triblock with the shortest block length (P(NB-co-O)$_2$-1 and P(NB-co-O)$_3$-1) were tremendously improved among the NB/O copolymers with a NB molar content of 50 mol%, while those of the other block and pseudo-random NB/O copolymers were slightly improved compared to the gradient copolymer. The strength of the block copolymers was also improved in comparison to the gradient copolymer, but the pseudo-random copolymer showed the highest strength, which was about twice the strengths of the block copolymers. (**Figure 3-11**c shows that the improvement of strain at break of diblock NB/Do copolymer (NB = 50 mol% (36 wt.%), (P(NB-*co*-Do)$_2$) and diblock NB/O copolymer with a similar M_n and NB content (NB = xx mol% (36 wt.%), P(NB-*co*-O)$_2$-4) was obvious compared to that of the corresponding gradient copolymers (P(NB-*co*-O)-3

Table 3-3. Tensile properties of NB/α-olefin copolymer films prepared using melt-pressing procedure (without annealing)

Sample	M_n [a] (kg/mol)	Young modulus [b] (MPa)	strength [b] (MPa)	strain at break [b]
P(NB-*co*-O)-4	104	327 ± 14	6.5 ± 0.2	0.03 ± 0.01
P(NB-*co*-O)$_2$-1	53	441 ± 30	17.1 ± 0.2	0.83 ± 0.42
P(NB-*co*-O)$_2$-2	76	358 ± 9	16.2 ± 0.3	0.10 ± 0.01
P(NB-*co*-O)$_2$-3	94	366 ± 5	11.9 ± 1.9	0.06 ± 0.03
P(NB-*co*-O)$_3$-1	75	356 ± 10	16.4 ± 0.1	0.40 ± 0.31
P(NB-*co*-O)$_3$-2	103	335 ± 12	13.6 ± 1.5	0.06 ± 0.01
P(NB-*co*-O)$_n$	106	766 ± 5	21.8 ± 1.6	0.04 ± 0.01
P(NB-*co*-O)-3	141	312 ± 3	9.7 ± 0.3	0.11 ± 0.05
P(NB-*co*-O)$_2$-4	125	239 ± 6	10.0 ± 1.2	1.13 ± 0.05
P(NB-*co*-Do)	124	158 ± 15	4.8 ± 0.2	0.22 ± 0.10
P(NB-*co*-Do)$_2$	114	77 ± 2	7.5 ± 0.1	2.85 ± 0.15
P(NB-*co*-Do)$_n$	129	151 ± 3	6.1 ± 0.4	0.06 ± 0.02

[a] Determined by GPC (THF, 40 °C, polystyrene standards). [b] Determined by elongation test.

and P(NB-*co*-Do)). Moreover, P(NB-*co*-Do)$_2$ showed higher strain at break but lower strength than P(NB-*co*-O)$_2$-4, while the pseudo-random NB/Do copolymer (P(NB-*co*-Do)$_n$) was brittle.

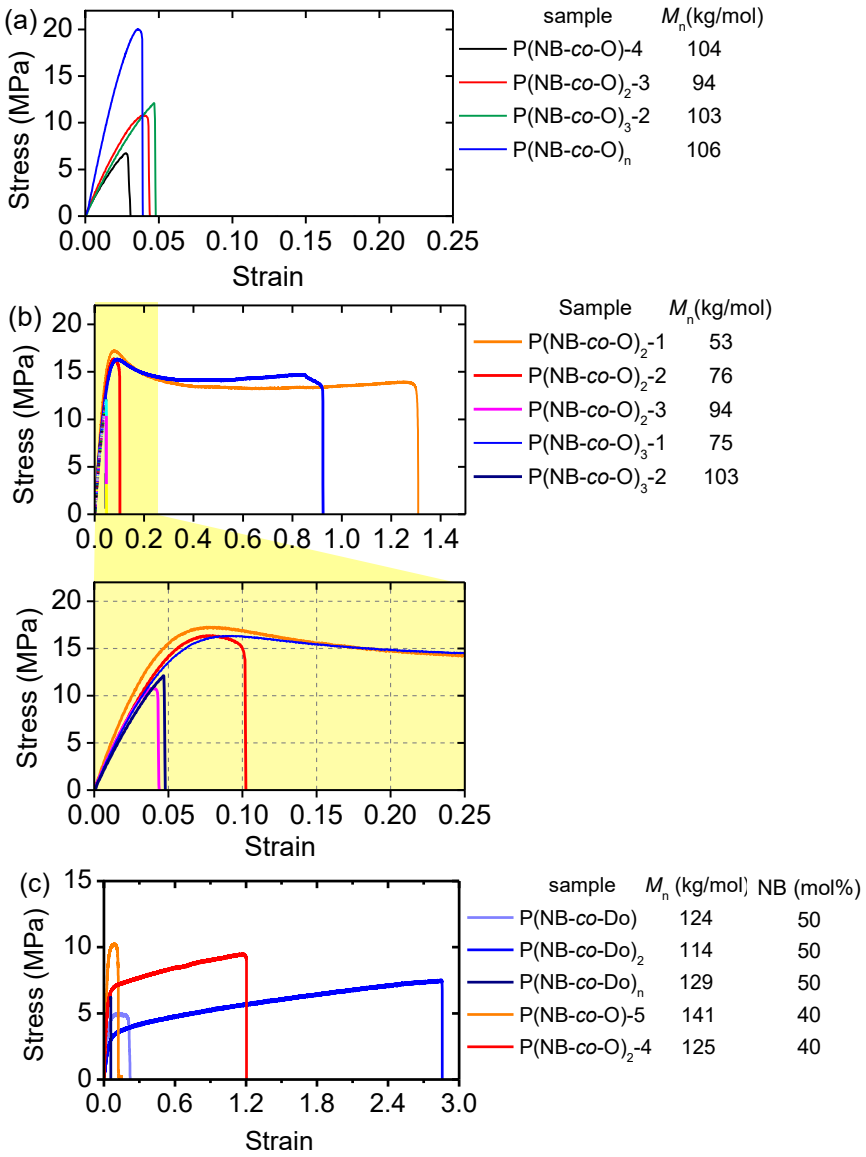

Figure 3-11. Stress-strain curves of NB/α-olefin copolymer films prepared without annealing procedure: (a) gradient, diblock, triblock and pseudo-random NB/O (NB = 50 mol%); (b) diblock and triblock NB/O with various block length (NB = 50 mol%, enlarged view in yellow color); (c) NB/Do and NB/O with the same NB wt.% (NB = 36 wt.%).

Since a phase-separation structure was observed in the copolymers by the DMA and SAXS tests, it was expected that the annealing procedure, which made the internal structure of the material more obvious and stable, would largely affect material's tensile properties. Therefore, the copolymer films were annealed and supplied for tensile tests.

The tensile properties and stress-strain curves of the NB/α-olefin copolymer films after annealing are shown in **Table 3-4** and **Figure 3-12**. As was introduced in Chapter 2, the NB/O gradient copolymer films with 50 mol% of NB were brittle under uniaxial deformation irrespective of the M_n value. The stress–strain curves of the NB/O copolymers with similar M_n values and 50 mol% of NB but different molecular structures, i.e., gradient (P(NB-*co*-O)-1), di- and triblock (P(NB-*co*-O)$_2$-3 and P(NB-*co*-O)$_3$-2), and pseudo-random (P(NB-*co*-O)$_n$) copolymers, are compared (**Figure 3-12**a). The pseudo-random copolymer and the diblock copolymer were brittle similarly to the gradient copolymer, while the triblock copolymer showed an obvious yielding

Table 3-4. Tensile properties of NB/α-olefin copolymer films prepared using melt-pressing and annealing procedure

sample	M_n [a] (kg/mol)	Young's modulus [b] (MPa)	strength [b] (MPa)	strain at break [b]
P(NB-*co*-O)-4	104	302 ± 13	9.1 ± 0.5	0.05 ± 0.01
P(NB-*co*-O)$_2$-1	53	509 ± 14	15.4 ± 0.6	0.97 ± 0.22
P(NB-*co*-O)$_2$-2	76	302 ± 2	16.8 ± 0.2	1.35 ± 0.11
P(NB-*co*-O)$_2$-3	94	318 ± 2	17.7 ± 0.1	0.09 ± 0.03
P(NB-*co*-O)$_3$-1	75	302 ± 3	11.9 ± 0.2	0.42 ± 0.12
P(NB-*co*-O)$_3$-2	103	302 ± 2	14.7 ± 0.1	1.17 ± 0.21
P(NB-*co*-O)$_n$	106	618 ± 12	27.3 ± 2.9	0.08 ± 0.02
P(NB-*co*-O)-5	141	318 ± 22	12.3 ± 1.1	0.21 ± 0.06
P(NB-*co*-O)$_2$-4	125	154 ± 6	11.8 ± 1.2	2.60 ± 0.97
P(NB-*co*-Do)	124	196 ± 24	7.0 ± 1.7	0.13 ± 0.05
P(NB-*co*-Do)$_2$	114	160 ± 6	8.4 ± 0.8	2.50 ± 0.58
P(NB-*co*-Do)$_n$	129	367 ± 57	10.3 ± 0.5	2.00 ± 0.34

[a] Determined by GPC (THF, 40 °C, polystyrene standards). [b] Determined by elongation tests.

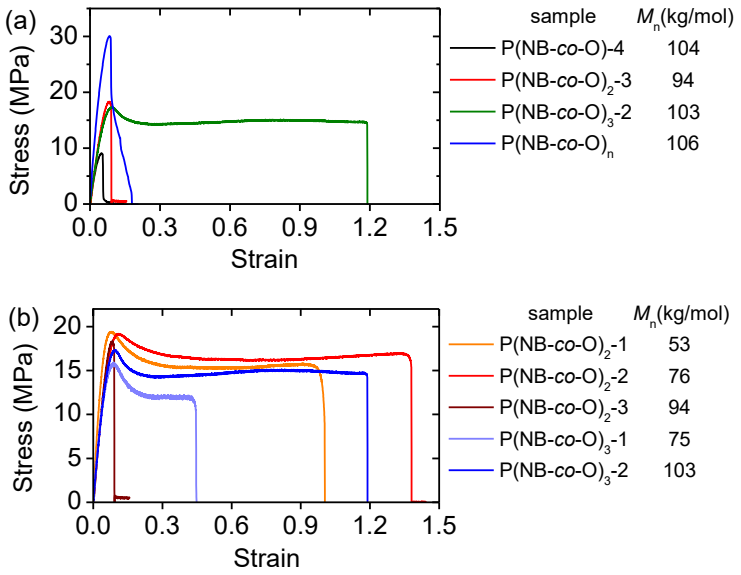

Figure 3-12. Stress–strain curves of copolymer films: (a) gradient, diblock, triblock, and multiblock NB/O (NB = 50 mol%); (b) diblock and triblock NB/O with different block lengths (NB = 50 mol%).

region observed was ductile. The results suggest that the strain at break behavior of the block copolymers is strongly related to the gradient-block length.

The stress–strain curves of di- and triblock NB/O copolymer films with different M_n values after annealing are shown in **Figure 3-12**b. All the annealed block NB/O copolymer films except P(NB-*co*-O)$_2$-3 had high strain at break values with a yield point in their curves. P(NB-*co*-O)$_2$-3 which had the longest block length had a low strain at break value of 0.09 and did not show a yield point. The DMA spectra of the block copolymers suggested that only P(NB-*co*-O)$_2$-3 had an obvious phase-separated morphology. Thus, the formation of a rigid phase mainly composed of NB-rich segments was considered as the reason for the brittleness of P(NB-*co*-O)$_2$-3. The M_n values and the block length did not affect the strength values of the copolymers, but the block length strongly influenced the strain-at-break values of of the copolymers. In addition, the diblock copolymers had larger strain at break values than the triblock copolymers with the same block length.

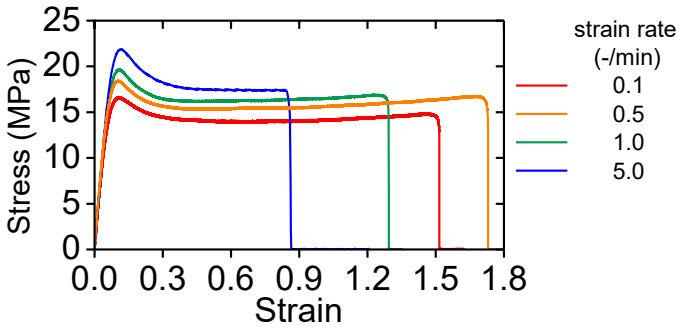

Figure 3-13. The effect of strain rate on the stress–strain curves of P(NB-*co*-O)$_3$-2.

The influence of the strain rate on the uniaxial deformation behavior was investigated to elucidate the structural origin of the yielding phenomena of the copolymer samples. **Figure 3-13**. shows the stress–strain curves of diblock copolymer of P(NB-*co*-O)$_3$-2 at different strain rates. The yielding stress monotonously increased with increasing the strain rates, which suggests that a flow process of some structural units is the origin of the yielding deformation. Thus, we applied the Eyring[11] equation to the strain-rate dependence of the yielding stress to obtain the activation volume of the yielding deformation. On the basis of the Eyring theory[11, 12], the strain rate $\dot{\varepsilon}$ is expressed as follows:

$$\dot{\varepsilon} = \dot{\varepsilon}_0 \exp\left(-\frac{\Delta H}{RT}\right) \exp\left(\frac{\sigma_y V^*}{2RT}\right) \qquad (3-1)$$

where $\dot{\varepsilon}$ is a constant, ΔH is the activation energy, R is the gas constant, T is the tensile temperature, σ_y is the yield stress, and V^* is the activation volume. The equation (3-1) can be rewritten as:

$$In\dot{\varepsilon} = V^* \frac{\sigma_y}{2RT} + b \qquad (3-2)$$

Here, $b = ln\dot{\varepsilon}_0 - \Delta H/RT$. **Figure 3-14** shows the plots of $ln\dot{\varepsilon}$ versus $\sigma_y/2RT$ for the di- and triblock copolymers. The values of V^* determined from the $ln\dot{\varepsilon}$ versus $\sigma_y/2RT$ plots are represented in **Figure 3-14**. It should be noted that the errors of V^* values were less than 0.18. V^* was very close for the copolymers with the same block length and different M_n. Considering that these copolymer samples form lamellar phase-separated morphology the size of which should depend on the block length, the yielding deformation is attributed to the fragmentation and slippage of the lamellar morphology.[12, 13]

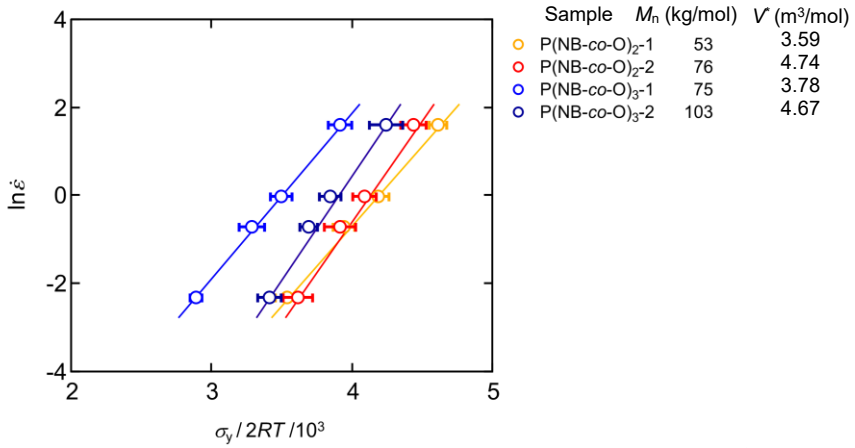

Figure 3-14. Strain-rate dependence of the yield stress for diblock and triblock NB/O copolymers at 25 ºC.

The stress–strain curves of NB/Do copolymers with similar M_n values but different structures, i.e., gradient, diblock and pseudo-random (P(NB-*co*-Do), P(NB-*co*-Do)$_2$, and P(NB-co-Do)$_n$, NB = 50 mol%), are shown in **Figure 3-15**. The gradient and diblock copolymers had almost the same strength values, but the strain-at-break value of the block copolymer increased to astonishing 2.50. The pseudo-random copolymer showed the highest strength and a strain at break value (2.0) larger than that of the gradient copolymer (0.13). The stress–strain curves of the gradient and diblock NB/O copolymers, P(NB-*co*-O)-5 and P(NB-*co*-O)$_2$-4, with the same NB wt.% (36 wt.%) and similar M_n values to the NB/Do copolymers are also shown in **Figure 3-15**. The

diblock NB/O copolymer also had strain-at-break value (2.60) much higher than that of the NB/O gradient copolymer (0.21). Moreover, the NB/O copolymers had higher strength compared to the NB/Do copolymers. The reason for the difference of the mechanical properties between the NB/O and NB/Do copolymers are considered to be their different gradient structures and the side-chain length of α-olefin units.

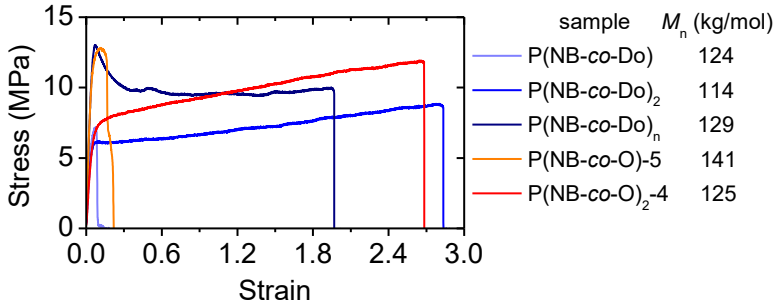

Figure 3-15. Stress–strain curves of gradient, diblock and pseudo-random NB/Do copolymer films (NB = 50 mol%, 36 wt.%), along with those for gradient and diblock NB/O copolymer films with the same NB wt.% (NB = 40 mol%, 36 wt.%) and similar M_n values.

The results in this work show that the strain-at-break behavior of NB/α-olefin copolymers can be improved by block copolymerization. The gradient NB/α-olefin copolymers had NB-rich "head" (hard segments) and O-rich "tail" (soft segments). And the movement between copolymer chains were restricted by the connection between the heads and tails in the block copolymers. The NB molar content and the choice of α-olefin can also influence the properties of NB/α-olefin block copolymers.

3.4. Conclusions

(^{t}BuNSi-Me$_2$Flu)TiMe$_2$ (**I**)–[Ph$_3$C][B(C$_6$F$_5$)$_4$] with 2,6-di-*tert*-butyl-4-methylphenol-treated tri-*n*-octylaluminium (Oct$_3$Al/BHT) scavenger was proven to have an ability for NB/higher α-olefin "pseudo-living" copolymerization. Di- and triblock NB/O or NB/Do copolymers with the gradient structure in each block segment were successfully synthesized with 100% monomer efficiency at high speed. The melt-pressed NB/O block copolymer films were highly transparent to visible light. The gradient and block copolymers with 50 mol% of NB had similar thermal properties. Only one T_g below 0 °C was detected by DSC for the block copolymers, and two T_gs, which should be ascribed to the α-olefin-rich and NB-rich segments, were detected by TMA. The block copolymers with suitable block length had strain-at-break values significantly larger and strength no less than the gradient copolymers. The improvement of the tensile properties was owning to the connections between hard and soft segments in the block copolymers. Moreover, the tensile properties of the block copolymers were also controlled by the comonomer type and comonomer composition. The block NB/α-olefin copolymers with better properties will certainly have a wider range of applications.

References

1 A. S. Rodrigues and J. F. Carpentier, *Coord. Chem. Rev.*, 2008, **252**, 2137-2154.
2 R. Ma, Y. Hou, J. Gao and F. Bao, *Polym. Rev.*, 2009, **49**, 249-287.
3 M. Jaymand, *Polym. Chem.*, 2014, **5**, 2663-2690.
4 N. Galdi, A. Buonerba and L. Oliva, *Polymers*, 2016, **8**, 405.
5 M. Atiqullah, M. Tinkl, R. Pfaendner, M. N. Akhtar and I. Hussain, *Polym. Rev.*, 2010, **50**, 178-230.
6 A. Hotta, E. Cochran, J. Ruokolainen, V. Khanna, G. H. Fredrickson, E. J. Kramer, Y. W. Shin, F. Shimizu, A. E. Cherian, P. D. Hustad, J. M. Rose and G. W. Coates, *Proc. Natl. Acad. Sci. U. S. A.*, 2006, **103**, 15327-15332.
7 K. Matyjaszewski, *Prog. Polym. Sci.*, 2005, **30**, 858-875.
8 J. M. Eagan, J. Xu, R. Di Girolamo, C. M. Thurber, C. W. Macosko, A. M. LaPointe, F. S. Bates and G. W. Coates, *Science*, 2017, **355**, 814-816.
9 E. Galanos, E. Grune, C. Wahlen, A. H. E. Müller, M. Appold, M. Gallei, H. Frey and G. Floudas, *Macromolecules*, 2019, **52**, 1577-1588.
10 H. Hagihara, T. Shiono and T. Ikeda, *Macromolecules*, 1998, **31**, 3184-3188.
11 G. Halsey, H. J. White and H. Eyring, *Text. Res. J.*, 1945, **15**, 295-311.
12 R. Gao, M. Kuriyagawa, K. H. Nitta, X. L. He and B. P. Liu, *J. Macromol. Sci., Part B*, 2015, **54**, 1196-1210.
13 I. M. Ward and J. Sweeney, *An Introduction to The Mechanical Properties of Solid Polymers*, John Wiley & Sons, New York, 2004.

Chapter 4. Norbornadiene Homopolymerization and Norbornene/Norbornadiene/1-Octene Terpolymerization by *ansa*-Fluorenylamidodimethyltitanium–based Catalyst Systems

4.1. Introduction

Cycloolefin copolymers (COCs) have attractive properties such as good heat and chemical resistance, low water absorption, high transparency, and low dielectric constants.[1, 2] Norbornene (NB)-based copolymers are one kind of COCs with high commercial value as thermoplastics.[3] With the development of single-site catalysts, not only the copolymerization of NB with ethylene (E) [3], but also with α-olefins[4-9], styrene[10], and functionalized olefins[11, 12] were achieved.

Recently, researches have become more interested in synthesizing pendant double bonds functionalized polyolefins, because the introduced pendant double bonds can be converted into various functional groups by further chemical reactions or be used for crosslinking reactions. The polyolefins bearing pendant double bonds can be synthesized by copolymerization of olefin with symmetric dienes[13-15] or asymmetric dienes[2, 16]. However, when symmetrical α, ω-dienes were used, undesirable cyclopolymerization and/or crosslinking reactions during the copolymerization were inevitable, thus the researches using symmetrical dienes are still limited. For example, when 1,5-hexadiene was polymerized with ethylene and propylene by *rac*-Et(Ind)$_2$ZrCl$_2$–methylaluminoxane (MAO), extensive crosslinking happened.[17] On the other hand, as asymmetric NB derivatives, such as dicyclopentadiene (DCPD),[18-20] 5-ethylidene-2-norbornene (ENB),[21, 22] 5-vinyl-2-norbornene (VNB),[23, 24] and other bulky cyclic diolefins[25] were used for copolymerization with α-olefins [26] or dienes [27].

In a previous work, copolymers of NB and 1,5-hexadiene with good solubility in tetrahydrofuran (THF) were successfully synthesized by (^{t}BuNSiMe$_2$Flu)TiMe$_2$ (**I**) with 2,6-di-*tert*-butyl-4-methylphenol (BHT)-treated modified MAO (MMAO/BHT) as a cocatalyst,[16, 28] and the pendant 3-butenyl groups were remained in the copolymers. When 1,7-octadiene was applied instead of 1,5-hexadiene, insoluble copolymer was obtained. There results suggest that the butenyl group in the NB chain could not be coordinated to the active center due to the steric hindrance and eventually prevent cross-linking reaction.

Norbornadiene (NBD), a symmetric NB derivative diene, can also be polymerized with NB and α-olefins to give copolymers with norbornenyl units in the chain.[29-32] The second double bond in the inserted NBD unit can be used for further functionalization or crosslinking reaction. It was expected that crosslinking reaction by the second double bond of the inserted NBD unit in the homopolymer or NBD/NB/1-alkene terpolymer chains would not be occurred due to the steric hindrance of the main chain, as was observed in the NB/1,5-hexadiene copolymerization by **I**–MMAO/BHT. Furthermore, cyclopolymerization of NBD is extremely unlikely to happen because of its rigidity.

In this chapter, NBD homopolymerization and NB/NBD/1-octene (O) terpolymerization were conducted by different combinations of an *ansa*-fluorenylamidodimethyltitanium complex **I** or [^{t}BuNSiMe$_2$(2,7-^{t}Bu$_2$Flu)]TiMe$_2$ (**II**), **Figure 4-1**) with a suitable cocatalyst (MMAO/BHT or [Ph$_3$C][B(C$_6$F$_5$)$_4$] with BHT-treated tri-*i*-butylaluminum (^{i}Bu$_3$Al/BHT, scavenger).

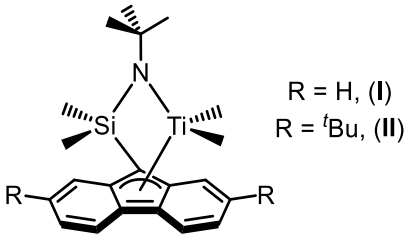

Figure 4-1. Chemical structures of *ansa*-fluorenylamidodimethyltitanium complex **I**, and **II**.

4.2. Experiment section

Materials. All operations were performed under nitrogen gas using standard Schlenk-line techniques. Titanium complex **I** and **II** were synthesized according to the literature.[33, 34] MMAO (6.5 wt.% Al in toluene), $[Ph_3C][B(C_6F_5)_4]$ and tri-*i*-butylaluminum ($^{i}Bu_3Al$; 13.6 wt.% Al; Tosoh Finechem Co.) were used as received. Toluene (Kanto Chemical Co. Inc.) was dried with sodium metal and distilled. BHT was made into a solution in toluene (0.50 M). NB, NBD and O were dried by CaH_2 and distilled. $^{i}Bu_3Al$/BHT mixture was made by adding 2 equivalents of BHT into $^{i}Bu_3Al$ in toluene.

Homopolymerization Procedure. The polymerization reactions were conducted in a 100-mL flask stirred by a magnetic stirrer bar. First, the flask was dried with a hot air gun and charged with nitrogen gas, followed by the addition of toluene (26 mL), MMAO (4.0 mmol), BHT (0.60 mmol) and NBD (5 mmol, 0.5 mL) in this order. The mixture was stirred for 30 min. The polymerization was started by adding the toluene solution of titanium catalyst **I** (20 mmol, 1 mL). After 5 min of polymerization at room temperature, the mixture was poured into 200 mL of methanol with 4 mL of concentrated HCl in a beaker. The precipitated polymer was filtrated followed by drying at 60 ºC under vacuum for 6 h. The white polymer was weighted as 54.3 mg.

Terpolymerization Procedure. The polymerization reactions were conducted in a 100-mL flask stirred by a magnetic stirrer bar. First, the flask was dried with a hot air gun and charged with nitrogen gas, followed by the addition of toluene (25 mL), MMAO (4.0 mmol), BHT (0.60 mmol) NB (6.6 mmol), NBD (1.7 mmol) and O (1.7 mmol) in this order. The mixture was stirred for 30 min. The polymerization was started by adding the toluene solution of titanium catalyst **I** (20 mmol, 1 mL). After 10 min of polymerization at room temperature, the mixture was poured into 200 mL of methanol with 4 mL of concentrated HCl in a beaker. The precipitated polymer was filtrated

followed by drying at 60 ºC under vacuum for 6 h. The white polymer was weighted as 292 mg.

Analytical Procedures. ^{1}H and ^{13}C NMR spectra were recorded with $CDCl_3$ as the solvent on a JEOL Lambda 500 NMR spectrometer. The obtained spectra were referenced to the signal of a residual trace of the partially protonated solvents for ^{1}H NMR [^{1}H: δ = 5.91 ppm (C_2HDCl_4), δ = 7.26 ppm ($CHCl_3$)] and solvents for ^{13}C NMR [^{13}C: δ = 77.1 ppm ($CDCl_3$)]. Molecular weights of polymers were determined by GPC on a Tosoh HLC-8320 chromatograph (40 ºC, $CHCl_3$, polystyrene standards). The polymer concentration was approximately 2 – 3 mg/mL, and the injection volume was 0.2 mL. Wide-angle X-ray diffraction spectra (WAXD) of the polymers were recorded by an X-ray spectrometer (PANalytical empyrean) with Cu$K\alpha$ radiation (λ = 1.54056 Å) with a 2θ testing range from 3 to 35º.

4.3. Results and discussion

NBD homopolymerization by different catalyst systems. Homopolymerization of NBD was conducted by complex **I** or **II** with MMAO/BHT or $[Ph_3C][B(C_6F_5)_4]/^iBu_3Al$/BHT under room temperature (25°C) for 10 min (**Table 4-1**, NBD-2, -4 to -6). The results indicated that the choice of complex and cocatalyst had a strong influence on the yield and M_n of the obtained polymer. The yield was depended on the catalyst system and decreased in an order of **II**-$[Ph_3C][B(C_6F_5)_4]/^iBu_3Al$/BHT > **II**-MMAO/BHT > **I**-$[Ph_3C][B(C_6F_5)_4]/^iBu_3Al$/BHT > **I**-MMAO/BHT. **II**–$[Ph_3C][B(C_6F_5)_4]/^iBu_3Al$/BHT gave the polymer with the highest M_n value and

Table 4-1. Results of NBD homopolymerization by different catalyst systems [a]

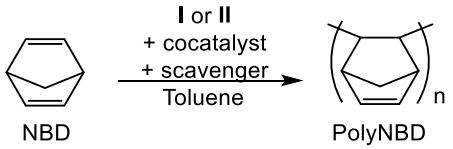

sample	cat.	cocat.	cat./cocat.	T (ºC)	t (min)	yield [b] (%)	M_n [c] (kg/mol)	$Đ$[c]	N[d] (μmol)
NBD-1	**I**	MMAO	100	25	10	10	1.4	2.6	34
NBD-2	**I**	MMAO	200	25	10	12	1.5	3.3	37
NBD-3	**I**	MMAO	400	25	10	17	1.7	3.2	47
NBD-4	**II**	MMAO	200	25	10	21	4.2	2.8	22
NBD-5	**I**	$[Ph_3C][B(C_6F_5)_4]$	10	25	10	19	2.6	2.2	32
NBD-6	**II**	$[Ph_3C][B(C_6F_5)_4]$	10	25	10	52	21.8	3.1	11
NBD-7	**II**	$[Ph_3C][B(C_6F_5)_4]$	10	0	10	62	34.4	3.9	8
NBD-8	**II**	$[Ph_3C][B(C_6F_5)_4]$	10	0	2	24	14.9	1.8	7
NBD-9	**II**	$[Ph_3C][B(C_6F_5)_4]$	10	0	5	55	32.8	2.0	8
NBD-10	**II**	$[Ph_3C][B(C_6F_5)_4]$	10	0	30	69	32.1	3.9	10
NBD-11	**II**	$[Ph_3C][B(C_6F_5)_4]$	10	0	60	82	34.1	4.4	11

[a] Conditions: Ti = 20 μmol, NBD = 5 mmol, total volume = 30 mL, BHT (0.6 mmol) was added with MMAO, $^iBu_3Al$/BHT (0.2 mmol) was added with $[Ph_3C][B(C_6F_5)_4]$. [b] Calculated from the weight of the obtained copolymer and the total mass of monomer in feed. [c] Determined by GPC ($CHCl_3$, 40 ºC, polystyrene standards). [c] Number of copolymer chain was calculated from the mass of obtained polymer and M_n value.

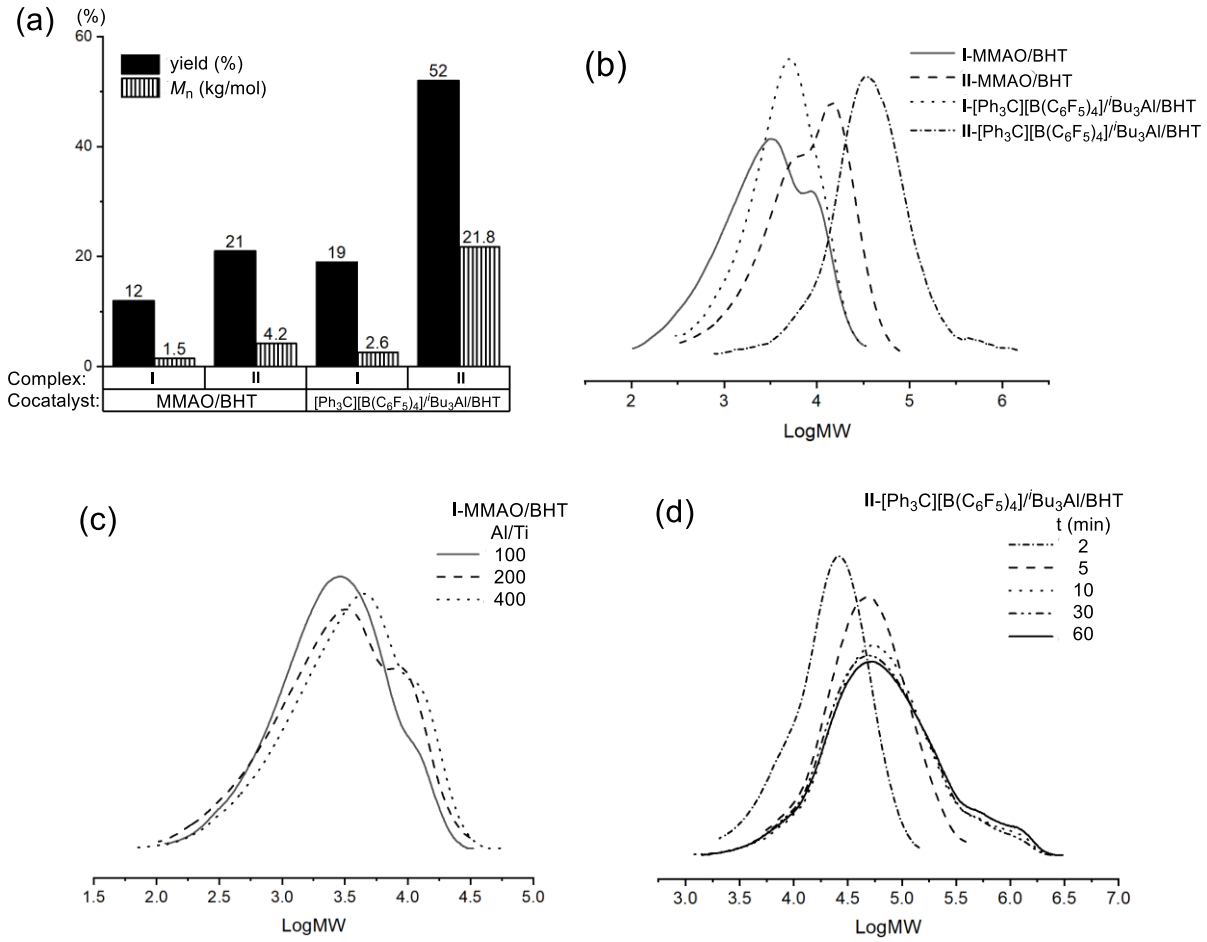

Figure 4-2. NBD homopolymerization results and GPC curves of NBD homopolymers obtained by different catalyst systems under different reaction conditions: (a) conversion and molecular weight of NBD homopolymer obtained by each catalytic system; (b) GPC curves of NBD homopolymer obtained by each catalytic system (**Table 4-1**, NBD-2, -4 to -6); (c) GPC curves of NBD homopolymer obtained by **I**–MMAO/BHT with different Al/Ti molar ratio (**Table 4-1**, NBD-1 to -3); (d) GPC curves of NBD homopolymer obtained by **II**–$[Ph_3C][B(C_6F_5)_4]/^{i}Bu_3Al$/BHT with different polymerization time (**Table 4-1**, NBD-7 to -11).

the lowest number of polymer chains (*N*) among the four catalyst systems employed. This was due to the high propagation rate of **II**–$[Ph_3C][B(C_6F_5)_4]$ and low chain transfer ability of $^{i}Bu_3Al$/BHT.[35] The GPC spectra of the NBD homopolymers obtained are shown in **Figure 2**b. When the MMAO/BHT was used as the cocatalyst, the NBD homopolymers showed bimodal distributions regardless of the complex used. On the contrary, the NBD homopolymers obtained by the systems with $[Ph_3C][B(C_6F_5)_4]/^{i}Bu_3Al$/BHT as a cocatalyst showed unimodal distributions.

The NBD homopolymerizations by **I**–MMAO/BHT with different Al/Ti ratio were also conducted (**Table 4-1**, NBD-1, 2, 3). All the yield, M_n and N of the obtained polymers increased by increasing the Al/Ti ratio from 100 to 400, indicating that excess MMAO could enhance the propagation rate.[36] The increase of the Al/Ti ratio also changed the shape of the bimodal distribution, the side peak in higher molar mass region became bigger accompanied by a shift to higher molar mass region (**Figure 4-2**c). The reason for the appearance of the side peak in the GPC curve of the NBD homopolymer obtained by the MMAO system was still unclear yet, but there existed a report about the formation of two active species in the zirconocene catalyst system during the ethylene/1-hexene copolymerization.[37]

When the NBD homopolymerization by **II**–$[Ph_3C][B(C_6F_5)_4]$ was conducted in a lower temperature (0 ºC), both the yield and M_n of the obtained NBD homopolymer increased (**Table 4-1**, NBD-7). It was speculated that both the deactivation of active center and the occurrence of chain transfer reactions were suppressed under low temperature. In the same system, when the polymerization time was extended from 2 min to 60 min, the polymer yield increased (**Table 4-1**, NBD-8 to 11). On the other hand, the M_n of the produced polymer reached the upper limit after 10 min of reaction, while the molecular weight distribution ($Đ$) value increased obviously. It can be seen in the GPC curves of this series of NBD homopolymers that the components with high molecular weight appeared from 10 minutes and continually increased to 60 minutes (**Figure 4-2**d), which was the reason for an increase of $Đ$ value of the obtained polymer in the late stage of the polymerization reaction. In addition, it is worth noting that all the obtained polymers, including that obtained in an 82% yield, had excellent solubility in $CHCl_3$ at room temperature.

In the typical ^1H and ^{13}C NMR spectra of NBD homopolymer (**Table 4-1**, NBD-4) shown in **Figure 4-3**, both the peaks belonging to the olefinic carbons (140 ppm) and aliphatic carbons

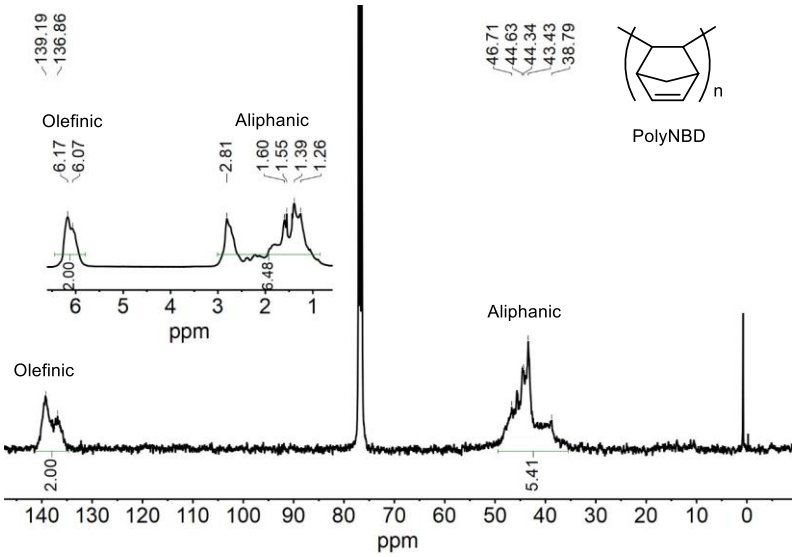

Figure 4-3. ^{13}C and ^{1}H NMR spectra of NBD homopolymer obtained by **II**–MMAO/BHT (**Table 4-1**, NBD-4).

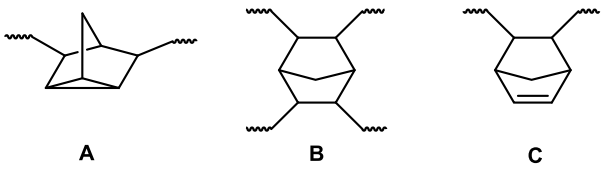

Figure 4-4. Possible structure of monomer units in the cationic NBD homopolymer.

(35-50 ppm) were observed. In the previous work about the cationic polymerization of NBD, both double bonds in NBD reacted to form the polymer with half-substituted type (A) and fully-substituted type (B) structures shown in **Figure 4-4**.[38, 39] The resonance peaks attributed to these structures appeared in a range from 50 to 55 ppm in the ^{13}C NMR spectrum. Despite the integral ratio of the olefinic and aliphatic protons (2/6.48) in the corresponding ^{1}H NMR spectrum suggested that a small part of the second double bonds in the incorporated NBD units may also have taken part in the polymerization, no identical peak was observed in the 50-55 ppm range even in the ^{13}C NMR spectra of the NBD homopolymer obtained in the late stage of polymerization (**Figure 4-5**). In other words, the existence of B-type structure in the NBD homopolymer obtained

in this work was negligible. Thus, almost all the pendant double bonds were retained in the NBD homopolymer obtained by the present catalyst probably because of the steric hindrance of the neighboring NBD units.

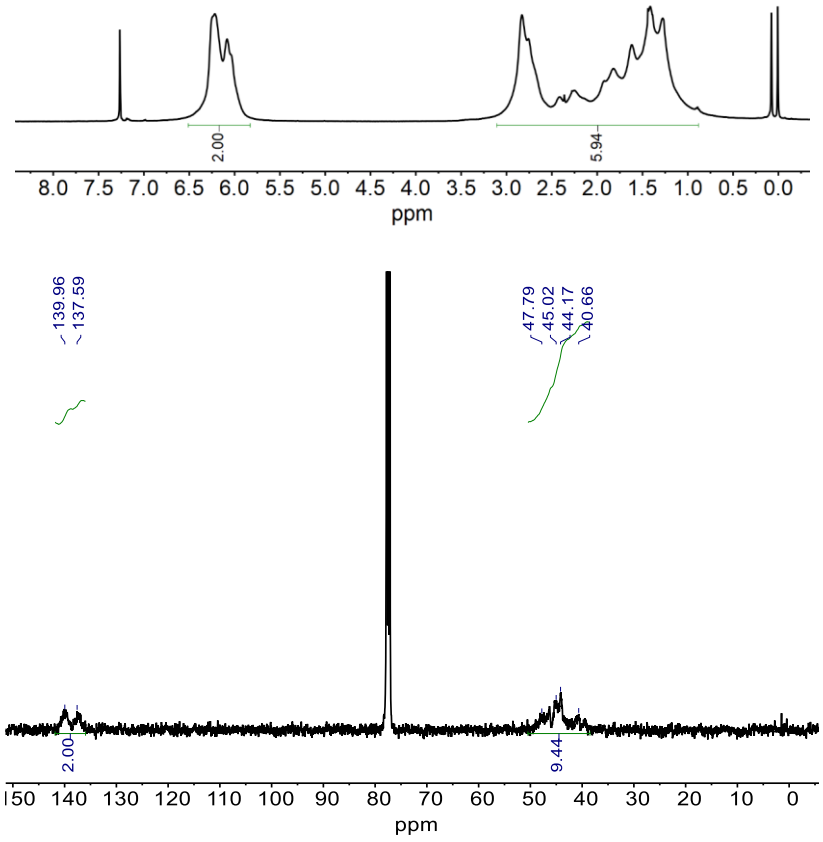

Figure 4-5. ^{1}H and ^{13}C NMR spectra of NBD homopolymer obtained by **II**–$[Ph_3C][B(C_6F_5)_4]/^{i}Bu_3Al$/BHT (**Table 4-1**, NBD-11).

NB/NBD/O terpolymerization using I- or II-MMAO/BHT catalyst system. The NB/NBD/O terpolymerizations by **I**-MMAO/BHT were conducted with a NB/NBD/O feed ratio of 4/1/1 at 0 ºC or 25 ºC, and terpolymer was obtained only at 25 ºC (**Table 4-2**, Ter-1 and 2). Thus, terpolymerizations were conducted by **I**-MMAO/BHT at 25 ºC with different monomer feed ratios while keeping the total monomer amount constant (Ter-1, -3 to -6). The GPC curves of the obtained terpolymers shown in **Figure 4-6**a had bimodal distributions. With the increase of the NB ratio in feed, the whole curve shifted to higher molar mass region accompanied by the shrinking of the peak in lower molar mass region and enlarging the peak in higher molar mass. The extension of polymerization time also caused the shift of the GPC curve to higher molar mass region with the appearance of a third peak (**Table 4-2**, Ter-1, -7 to -9, **Figure 4-6**b). The third peak

Table 4-2. Terpolymerization of NB/NBD/O using **I-** or **II**-MMAO/BHT [a]

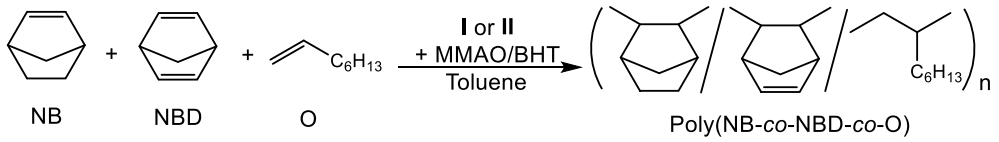

sample	cat.	NB/NBD/O (mmol)	*T* (ºC)	*t* (min)	yield [b] (%)	NB/NBD/O [c] (mol%)	M_n [d] (kg/mol)	*Đ* [d]
Ter-1	**I**	6.6/1.7/1.7	25	10	21	59/24/15	4.7	3.3
Ter-2	**I**	6.6/1.7/1.7	0	10	trace	-	-	-
Ter-3	**I**	2.0/2.0/6.0	25	10	10	38/34/28	2.7	2.6
Ter-4	**I**	3.3/3.3/3.3	25	10	9	45/40/15	2.8	2.9
Ter-5	**I**	4.4/1.2/4.4	25	10	19	53/26/21	4.6	3.0
Ter-6	**I**	7.3/1.0/1.7	25	10	14	73/17/10	7.1	3.1
Ter-7	**I**	6.6/1.7/1.7	25	5	7	62/30/8	4.3	2.4
Ter-8	**I**	6.6/1.7/1.7	25	60	25	62/28/10	10.1	3.6
Ter-9	**I**	6.6/1.7/1.7	25	120	28	64/29/7	11.4	4.6
Ter-10	**II**	2.0/2.0/6.0	25	10	18	39/34/27	14.3	2.2
Ter-11	**II**	4.4/1.2/4.4	25	10	28	54/22/24	31.3	2.3
Ter-12	**II**	6.6/1.7/1.7	25	10	39	64/24/12	36.4	5.0

[a] Conditions: Ti =20 μmol, Al/Ti = 200, BHT = 0.6 mmol, total volume = 30 mL. [b] Calculated from the weight of the obtained copolymer and the total mass of monomer in feed. [c] Monomer molar contents calculated by ^{1}H NMR. [d] Determined by GPC ($CHCl_3$, 40 °C, polystyrene standards).

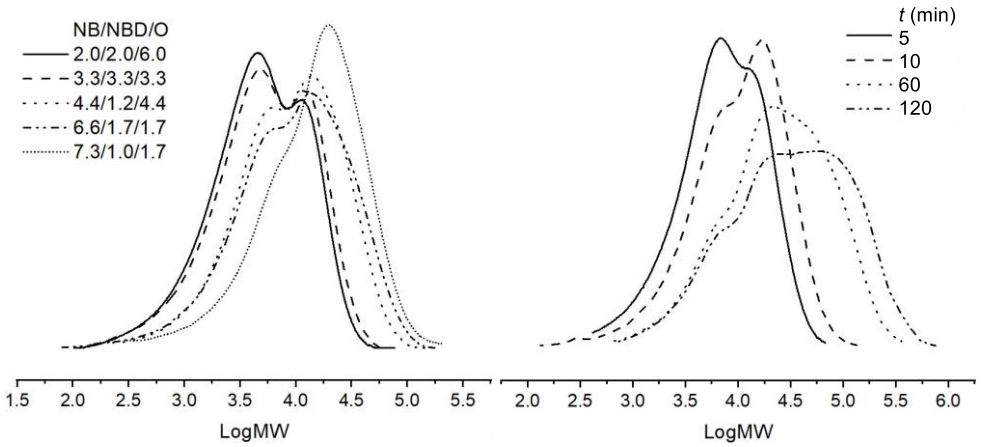

Figure 4-6. GPC curves of NB/NBD/O) terpolymers obtained by **I**–MMAO/BHT at 25 ºC: (a) Different NB/NBD/O feed ratio (**Table 4-2**, Ter-3 to -6); (b) Different terpolymerization time.

should belong to the production of the interconnected terpolymer via copolymerization of the NBD units.

When **II**-MMAO/BHT was applied, terpolymers were obtained in higher conversions (39% *vs*. 21%; Ter-1 and -12). The M_n value of the terpolymer obtained by **II** was 7 times higher than that by **I** (36.7 kg/mol *vs*. 4.7 kg/mol). When the NB/NBD/O feed ratio was changed from 1/1/3 to 4/1/1, the yield as well as the M_n value of the obtained terpolymer increased (**Table 4-2**, Ter-10 to -12).

The ^{13}C NMR spectra of NB/NBD/O terpolymers obtained by **I**–MMAO/BHT and **II**–MMAO/BHT are shown in **Figure 4-7**. The signals corresponding to the olefinic carbons of NBD units (137–139 ppm) and the signals corresponding to the last two carbon atoms on the side chain of O units (14 and 22 ppm) can be used for the calculation of monomer contents in the NB/NBD/O terpolymers.[44] The monomer contents were calculated from the integral area of these characteristic peaks by the following equations:

$$\text{Cont.}_{\text{O}} = \frac{8 \times (I_{\text{O1}} + I_{\text{O1}})/2}{I_{\text{tot.}}} \times 100\% \text{ (mol\%)} \quad (4-1)$$

$$\text{Cont.}_{\text{NBD}} = \frac{7 \times (I_{\text{NBD1}} + I_{\text{NBD2}})}{I_{\text{tot.}}} \times 100\% \text{ (mol\%)} \quad (4-2)$$

$$\text{Cont.}_{\text{NB}} = 100 - \text{Cont.}_{\text{O}} - \text{Cont.}_{\text{NBD}} \text{ (mol\%)} \quad (4-3)$$

where the Cont._{O}, $\text{Cont.}_{\text{NBD}}$ and Cont._{NB} represent the molar content of O, NBD, and NB in NB/NBD/O terpolymers, respectively. The I_{O1}, I_{O2} and I_{NBD1}, I_{NBD2} represent the integral area of characteristic peaks of O units and NBD units, respectively, and the $I_{\text{tot.}}$ represents the total integral area.

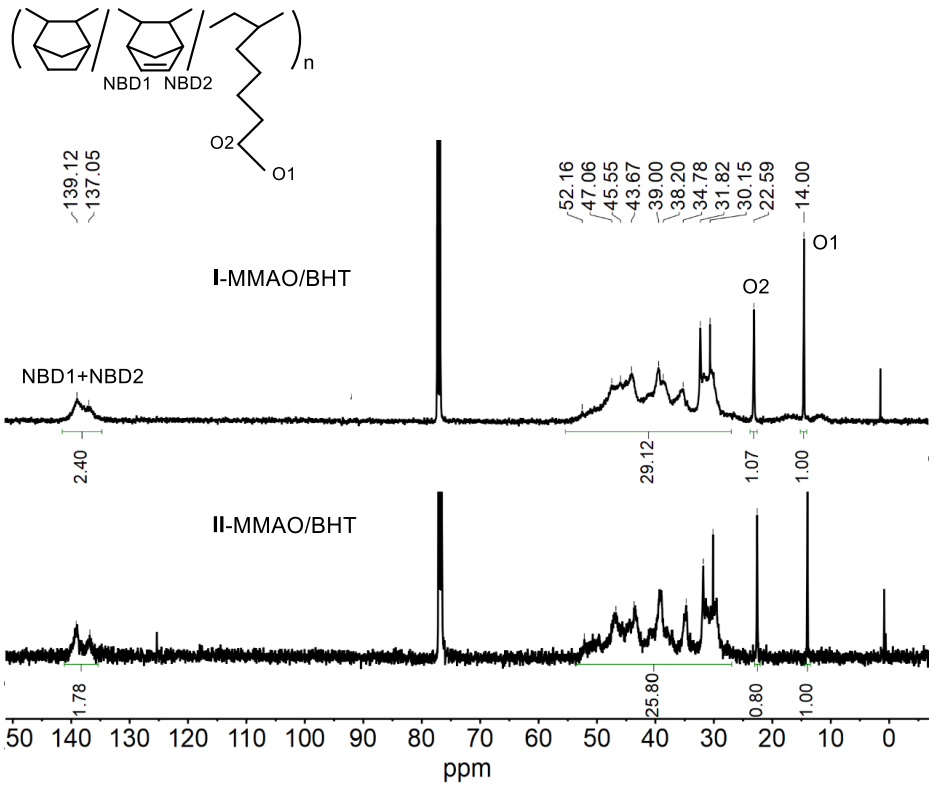

Figure 4-7. ^{13}C NMR spectra of NB/NBD/O terpolymers obtained by **I**-MMAO/BHT or **II**-MMAO/BHT (NB/NBD/O = 4.4/1.2/4.4 (mmol)).

In the ^{13}C NMR spectra of the terpolymers shown in **Figure 4-7**, the peaks between 50 to 55 ppm, a signature of B-type NBD units which was absent in the spectra of NBD homopolymers, appeared.[38, 39] The result indicates that some of the second double bonds in the inserted NBD units also took part in the polymerization. This can be explained by the less-hindered NBD unit neighboring to O unit and/or less hindered incoming O comonomer. The value of each monomer molar content did not depend on the polymerization time, but the signals for B-type NBD units became stronger (**Figure 4-8**). This is consistent with the appearance of the third peak in the highest molar mass region in GPC curves of these terpolymers shown in **Figure 4**b.

Although the above experimental results clearly showed that the second double bonds of the inserted NBD units were also involved in the polymerization reaction in NB/NBD/O terpolymerization by **I**–MMAO/BHT or **II**–MMAO/BHT, all the obtained terpolymers had good solubility and no gelation was observed during the polymerization.

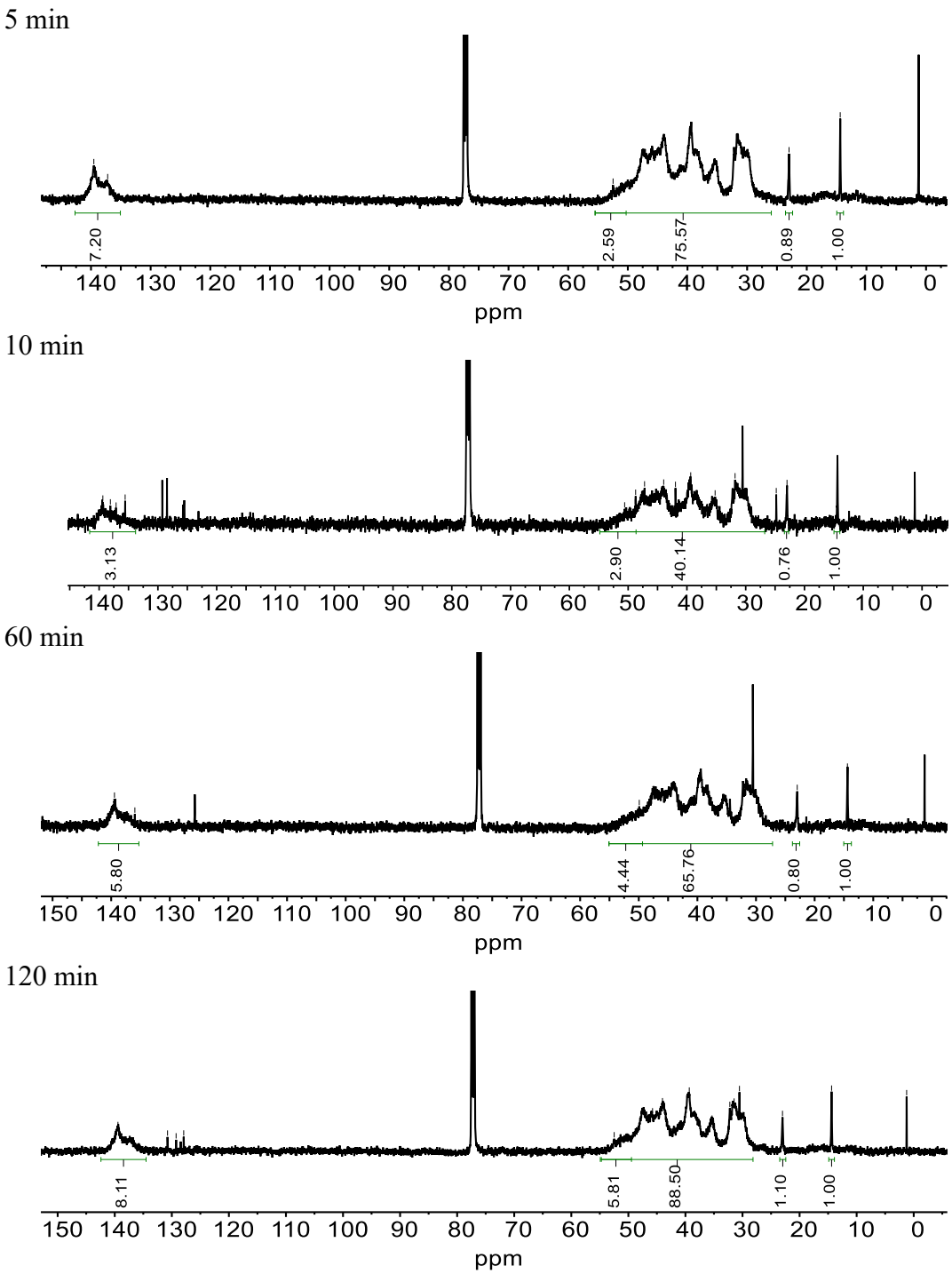

Figure 4-8. ^{13}C NMR spectra of NB/NBD/O terpolymers obtained by **I**–MMAO/BHT with different polymerization time.

Terpolymerization of NB/NBD/O with I- or II-[Ph$_3$C][B(C$_6$F$_5$)$_4$]/^{i}Bu$_3$Al/BHT. Terpolymerization of NB/NBD/O was also conducted with **I-** or **II**-[Ph$_3$C][B(C$_6$F$_5$)$_4$]/^{i}Bu$_3$Al/BHT at 0 and 25 ºC (**Table 4-3**). When the reaction was conducted at 25 ºC, **II**-[Ph$_3$C][B(C$_6$F$_5$)$_4$]/^{i}Bu$_3$Al/BHT showed a polymer yield 5 times higher than **I**-[Ph$_3$C][B(C$_6$F$_5$)$_4$]/^{i}Bu$_3$Al/BHT: the result was consistent with that of the NBD homopolymerization. Then, the terpolymerization was conducted by **II**-[Ph$_3$C][B(C$_6$F$_5$)$_4$]/^{i}Bu$_3$Al/BHT at 0 °C in different monomer feed ratios. The increase of the NB feed from 2.0 to 6.6 mmol increased the polymer yield, the M_n value of the polymer, and the NBD molar content, while the GPC curve of the polymer changed from unimodal to bimodal (**Figure 4-9**a).

Table 4-3. Terpolymerization of NB/NBD/O by **I-** or **II**-[Ph$_3$C][B(C$_6$F$_5$)$_4$]/^{i}Bu$_3$Al/BHT [a]

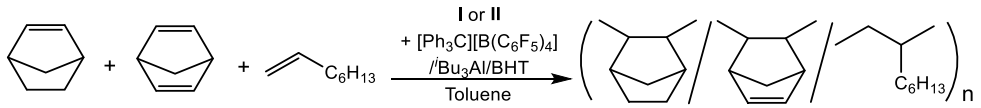

sample	cat.	NB/NBD/O (mmol)	T (°C)	t (min)	yield [b] (%)	NB/NBD/O [c] (mol%)	M_n [d] (kg/mol)	$Đ$ [d]
Ter-13	**I**	6.6/1.7/1.7	25	10	11	57/30/13	5.2	2.2
Ter-14	**II**	6.6/1.7/1.7	25	10	56	60/22/18	96.5	5.5
Ter-15	**II**	6.6/1.7/1.7	0	10	64	63/13/24	66.3	4.0
Ter-16	**II**	2.0/2.0/6.0	0	10	41	34/26/40	38.3	2.5
Ter-17	**II**	3.3/3.3/3.3	0	10	49	30/33/37	54.1	4.1
Ter-18	**II**	4.4/1.2/4.4	0	10	59	38/18/44	56.5	5.2
Ter-19	**II**	6.6/1.7/1.7	0	2	33	77/13/10	59.6	4.0
Ter-20	**II**	6.6/1.7/1.7	0	5	35	67/21/12	85.7	4.4
Ter-21	**II**	6.6/1.7/1.7	0	60	72	-[e]	-[e]	-[e]

[a] Conditions: Ti = 20 μmol, Ti/B/Al = 1/1/10, total volume = 30 mL. [b] Calculated from the weight of the obtained copolymer and the total mass of monomer in feed. [c] Monomer molar contents calculated from ^{1}H NMR. [d] Determined by GPC (CHCl$_3$, 40 °C, polystyrene standards). [e] Not determined due to the insolubility of the product.

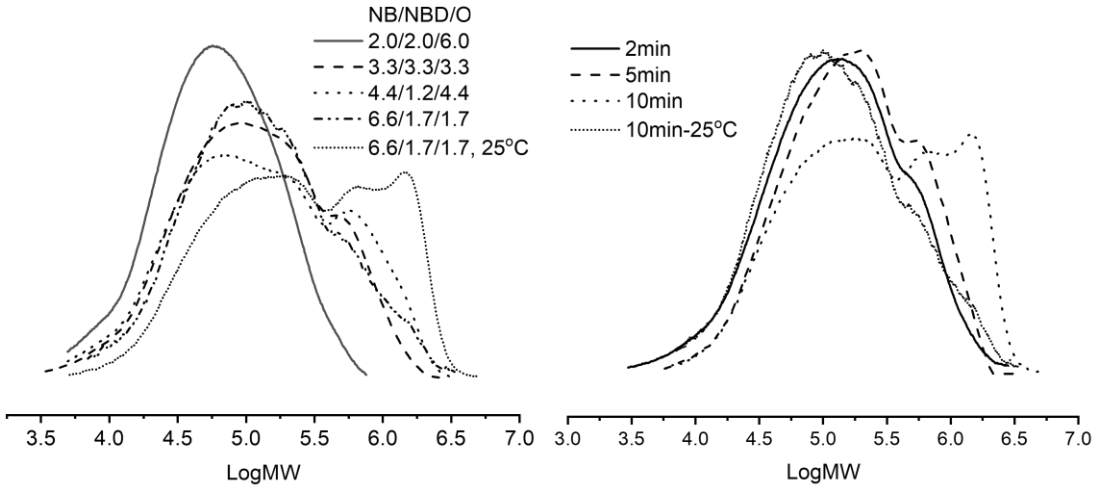

Figure 4-9. GPC curves obtained by **II**–$[Ph_3C][B(C_6F_5)_4]$/$^{i}Bu_3Al$/BHT at 0 ºC with (a) different monomer feed ratio (Table 3, Run 2–6) or (b) different polymerization time.

Terpolymerization by **II**–$[Ph_3C][B(C_6F_5)_4]$/$^{i}Bu_3Al$/BHT was further conducted at 0 ºC in different polymerization time. The polymer yield increased from 33 % to 72 % as the polymerization time being extended from 2 min to 60 min. And the increase of the M_n values can be clearly seen in **Figure 4-9**b. The solubility (in $CHCl_3$) of the terpolymers was depended on the polymerization time and the terpolymer obtained in the 60-min polymerization did not dissolve in the NMR and GPC solvent. The result indicates that cross-linking occurred at the late stage of the terpolymerization.

Microstructure of NBD homopolymer and NB/NBD/O terpolymer. The wide-angle X-ray diffraction (WAXD) analysis of the NBD homopolymer and NB/NBD/O terpolymer obtained with **II-**$[Ph_3C][B(C_6F_5)_4]$/$^{i}Bu_3Al$/BHT showed two broad peaks (**Figure 4-10**), which was consistent with the previously report.[38, 40] The WAXD result indicates that both the NBD homopolymer and NB/NBD/O terpolymer were predominantly amorphous.[35, 38, 39]

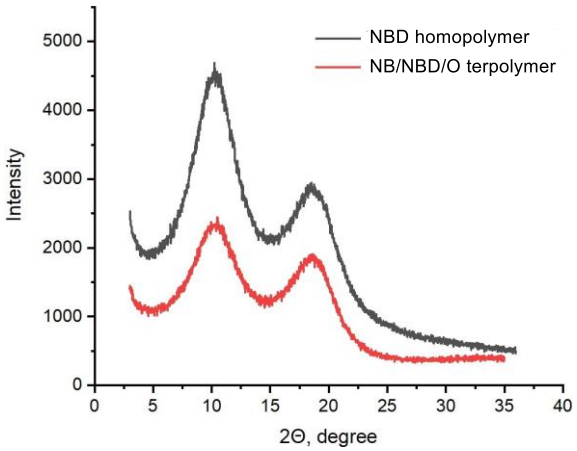

Figure 4-10. WAXD curves of NBD homopolymer and NB/NBD/O terpolymer obtained with **II**–$[Ph_3C][B(C_6F_5)_4]$.

4.4. Conclusions

Pendant double bonds functionalized polymers——NBD homopolymer and NB/NBD/O terpolymers with good solubility were successfully synthesized by using *ansa*-fluorenylamidodimethyltitanium complex **I** or **II** with MMAO/BHT or $[Ph_3C][B(C_6F_5)_4]/^iBu_3Al$/BHT. Most of the second double bonds of the inserted NBD units in all NBD homopolymers and the NB/NBD/O terpolymers obtained by **I**- or **II**-MMAO/BHT system were remained intact, which was proved by ^1H and ^{13}C NMR spectra. More NBD units were introduced into the NB/NBD/O terpolymer by **I**- or **II**-$[Ph_3C][B(C_6F_5)_4]/^iBu_3Al$/BHT due to the higher activity of the catalyst system. Gelation was observed in the late stage of the NB/NBD/O terpolymerization by **II**-$[Ph_3C][B(C_6F_5)_4]/^iBu_3Al$/BHT. The catalytic activity, the NBD molar content, the M_n and $Đ$ values of the polymers were depended on the catalyst system used as well as the experimental conditions. These pendant double bonds in the NBD homopolymers and NB/NBD/O terpolymers obtained in this work can be used for further functionalization or crosslinking reaction.

References

1 J. Y. Shin, J. Y. Park, C. Liu, J. He and S. C. Kim, *Pure Appl. Chem.*, 2005, **77**, 801-814.
2 X. Li and Z. Hou, *Coord. Chem. Rev.*, 2008, **252**, 1842-1869.
3 I. Tritto, L. Boggioni and D. R. Ferro, *Coord. Chem. Rev.*, 2006, **250**, 212-241.
4 H. Jung, S. Hong, M. Jung, H. Lee and Y. Park, *Polyhedron*, 2005, **24**, 1269-1273.
5 T. Shiono, M. Sugimoto, T. Hasan, Z. Cai and T. Ikeda, *Macromolecules*, 2008, **41**, 8292-8294.
6 Z. Cai, R. Harada, Y. Nakayama and T. Shiono, *Macromolecules*, 2010, **43**, 4527-4531.
7 Y. Xing, Y. Chen, X. He and H. Nie, *J. Appl. Polym. Sci.*, 2012, **124**, 1323-1332.
8 X. He, Y. Deng, Z. Han, Y. Yang and D. Chen, *J. Polym. Sci., Part A: Polym. Chem.*, 2016, **54**, 3495-3505.
9 W. Zhao and K. Nomura, *Macromolecules*, 2016, **49**, 59-70.
10 S. I. Chowdhury, R. Tanaka, Y. Nakayama and T. Shiono, *Polymers*, 2019, **11**, 1100.
11 T. Shiono, M. Sugimoto, T. Hasan and Z. Cai, *Macromol. Chem. Phys.*, 2013, **214**, 2239-2244.
12 X. Song, L. Yu, T. Shiono, T. Hasan and Z. Cai, *Macromol. Rapid Commun.*, 2017, **38**, 1600815.
13 S. Song, A. Wu, Y. Yu, P. Yang, Z. Fu and Z. Fan, *J. Polym. Sci., Part A: Polym. Chem.*, 2017, **55**, 1900-1909.
14 I. Belaid, V. Monteil and C. Boisson, in *Handbook of transition metal polymerization catalysts*, John Wiley & Sons, Inc., 2018, ch. 18, pp. 661-692.
15 O. Železník and J. Merna, *Polymer*, 2019, **175**, 195-205.
16 T. Hasan, T. Ikeda and T. Shiono, *J. Polym. Sci., Part A: Polym. Chem.*, 2007, **45**, 4581-4587.
17 W. Kaminsky and H. Drägemüller, *Makromol. Chem., Rapid Commun.*, 1990, **11**, 89-94.
18 X. F. Li and Z. M. Hou, *Macromolecules*, 2005, **38**, 6767-6769.
19 C.-S. Lu, Y.-T. Zhang and Y. Mu, *Chem. Res. Chin. Univ.*, 2007, **23**, 31-34.
20 M. Hong, L. Pan, W. P. Ye, D. P. Song and Y. S. Li, *Journal of Polymer Science Part a-Polymer Chemistry*, 2010, **48**, 1764-1772.
21 H. Li, J. Li, Y. Zhang and Y. Mu, *Polymer*, 2008, **49**, 2839-2844.
22 I. N. Meshkova, A. N. Shchegolikhin, E. V. Kiseleva and L. A. Novokshonova, *Polymer Science Series B*, 2015, **57**, 77-84.
23 S. Marathe and S. Sivaram, *Macromolecules*, 1994, **27**, 1083-1086.
24 F. Blank, J. K. Vieth, J. Ruiz, V. Rodríguez and C. Janiak, *J. Organomet. Chem.*, 2011, **696**, 473-487.
25 M. Hong, L. Cui, S. Liu and Y. Li, *Macromolecules*, 2012, **45**, 5397-5402.
26 X. Li, M. Nishiura, K. Mori, T. Mashiko and Z. Hou, *Chem. Commun. (Camb.)*, 2007, DOI: 10.1039/b708534f, 4137-4139.
27 B. Commarieu, J. Potier, M. Compaore, S. Dessureault, B. L. Goodall, X. Li and J. P. Claverie, *Macromolecules*, 2016, **49**, 920-925.
28 R. Tanaka, A. Sasaki, T. Takenaka, Y. Nakayama and T. Shiono, *Polymer*, 2018, **136**, 109-113.
29 K. Monkkonen and T. T. Pakkanen, *Macromol. Chem. Phys.*, 1999, **200**, 2623-2628.
30 K. Radhakrishnan and S. Sivaram, *Macromol. Chem. Phys.*, 1999, **200**, 858-862.
31 M. J. Yanjarappa and S. Sivaram, *Macromol. Chem. Phys.*, 2004, **205**, 2055-2063.
32 J.-Y. Lee and J.-C. Tsai, *J. Polym. Sci., Part A: Polym. Chem.*, 2011, **49**, 3739-3750.

33 K. Nishii, H. Hagihara, T. Ikeda, M. Akita and T. Shiono, *J. Organomet. Chem.*, 2006, **691**, 193-201.
34 R. Tanaka, C. Yanase, Z. Cai, Y. Nakayama and T. Shiono, *J. Organomet. Chem.*, 2016, **804**, 95-100.
35 Z. Cai, T. Ikeda, M. Akita and T. Shiono, *Macromolecules*, 2005, **38**, 8135-8139.
36 T. Shiono, *Polym. J.*, 2011, **43**, 331-351.
37 K. Soga, T. Uozumi, T. Arai and S. Nakamura, *Macromol. Rapid Commun.*, 1995, **16**, 379-385.
38 J. T. G. Huckfeldt and W. Risse, *Macromol. Chem. Phys.*, 1998, **199**, 861-868.
39 M. V. Bermeshev, B. A. Bulgakov, A. M. Genaev, J. V. Kostina, G. N. Bondarenko and E. S. Finkelshtein, *Macromolecules*, 2014, **47**, 5470-5483.
40 T. Hasan, T. Ikeda and T. Shiono, *Macromolecules*, 2004, **37**, 7432-7436.

Chapter 5. Synthesis of Star Polymers with Norbornene/*α*-Olefin Gradient Copolymer Arms by *ansa*-Fluorenylamidodimethyltitanium–based Catalysts

5.1. Introduction

Star polymers have unique rheological and thermal properties, some of which can even self-assemble due to their amphipathic microstructures.[1] Star polymer can be synthesized by three methods: the "arm-first" strategy, which is to synthesize the arm segments first followed by adding monomers with multifunctional groups; the "core-first" strategy, which is to synthesized the cross-linking core first followed by the propagation of arm segments; the "grafting-onto" strategy, which is to link the end functional groups of the pre-prepared arm polymers. The first two strategies usually require living polymerization systems.

Our group have explored the synthesis of star-shaped NB/*α*-olefin copolymers using the "grafting-onto" strategy. Boronic acid group end functionalized NB/1-octene (O) copolymers were successfully synthesized by (^{t}BuNSiMe$_2$Flu)TiMe$_2$ (**I**)-B(C$_6$F$_5$)$_4$/^{i}BuAl(OAr)$_2$ (Ar = 2,6-di-*tert*-butyl-4-methylphenyl) system.[2, 3] After further treatment, the boronic acid groups in the copolymers can be connected to form star shaped copolymers. Furthermore, it was expected that a gradient structure, which was observed in the copolymers obtained by **I**-[Ph$_3$C][B(C$_6$F$_5$)$_4$]/^{i}Bu$_3$Al/BHT system in Chapter 2, also exists in the arms of these star polymers. Specifically, the star polymers obtained by the **I**-B(C$_6$F$_5$)$_3$/^{i}BuAl(OAr)$_2$ system possessed the arms with NB-rich segments close to the cores and O-rich segments far from the cores.

In Chapter 2, pseudo-living copolymerization was achieved by **I**-[Ph_3C][$B(C_6F_5)_4$]/BHT-treated trialkylaluminum (R_3Al/BHT) system at higher speed, which quantitatively gave NB/α-olefin gradient copolymers. In Chapter 3, the catalyst system was applied for the synthesis of NB/α-olefin block copolymers with a gradient structure in each block segment. The strain at break of the gradient-block NB/α-olefin copolymers was massively improved without losing strength compared to the corresponding gradient copolymers. In Chapter 4, polynorbornadiene (polyNBD) with good solubility in THF was obtained by **II**-[Ph_3C][$B(C_6F_5)_4$]/$^{i}Bu_3Al$/BHT system, where the second double bonds in the NBD units was intact because of the steric hindrance of the neighboring NBD units. The catalytic system also gave the soluble NB/NBD/O terpolymer, but the gelation was observed at the late stage of the terpolymerization, indicating the NBD units in the terpolymer took part in the polymerization.

Thus, in this chapter, taking the advantage of the pseudo-living nature of the **I**-[Ph_3C][$B(C_6F_5)_4$]/Oct_3Al/BHT system for NB/α-olefin copolymerization, star polymers with NB/O gradient copolymer arms were synthesized in one pot by adding NBD with E or 1,11-dodecadiene (DoD) to form cores with cross-linked structures after living NB/O copolymerization had been completed, the "arm-first" strategy. To be mentioned that the gradient structure in the arms of star polymers synthesized in this work was opposite compared to the previous work [2, 3]. Specifically, the NB-rich segments were far away from the cores, and the O-rich segments were close to the cores (**Figure 5-1**). The thermal and mechanical properties of the star polymers were investigated and compared with the results of the previous work.

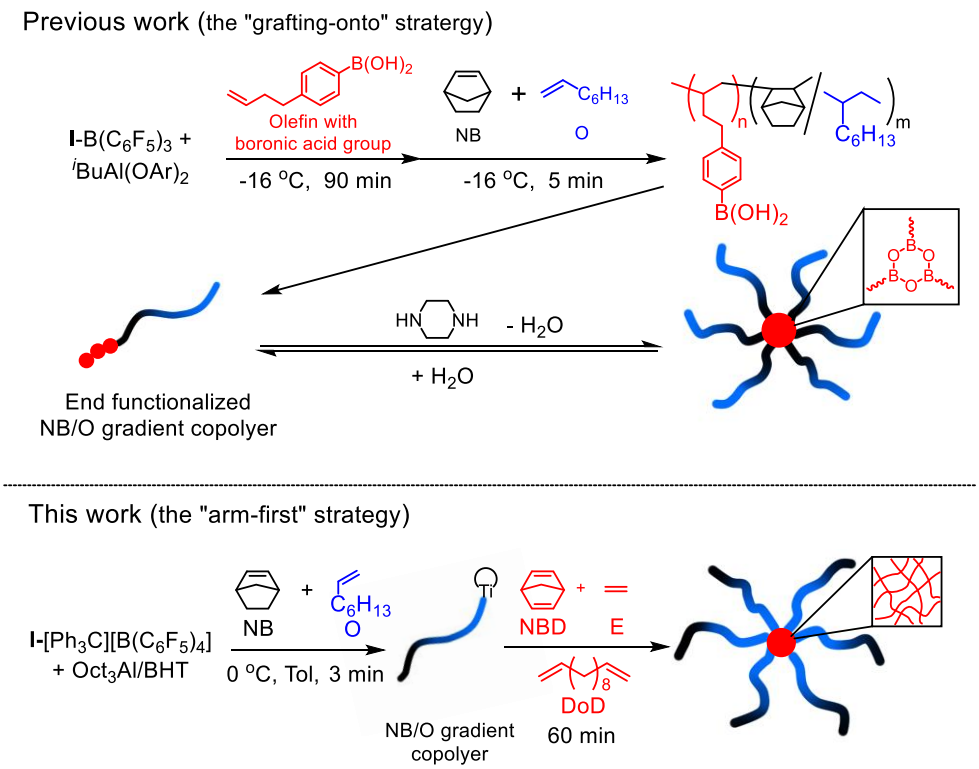

Figure 5-1. Synthesis and structures of star polymers with NB/O copolymer arms in the previous work[2,3] and this work.

5.2. Experimental section

Materials. All operations were performed in nitrogen gas using standard Schlenk-line techniques. Titanium complex **1** was synthesized according to the previously reported method.[4] $[Ph_3C][B(C_6F_5)_4]$ (Tosoh Finechem Co.), Oct_3Al (7.3 wt.% Al; Tosoh Finechem Co.), and BHT (Fujifilm Wako Pure Chemical Co.) were used as received. Oct_3Al/BHT toluene solution (0.4 mol/L) was prepared by adding two equivalents of BHT into Oct_3Al in toluene. Toluene (Kanto Chemical Co.) was dried with sodium metal and distilled before use. NB, O, and 1,7-octadiene (OD) (Tokyo Chemical Industry Co.) were dried over CaH_2, distilled, and made into toluene solutions (1 mol/L) before use. DoD (Tokyo Chemical Industry Co.) made into toluene solution (1 mol/L) and treated with 6 $mmol_{Al}$/L Oct_3Al/BHT before use. Ethylene gas was passed through purification columns (drycolumn DC-A4 and gascolumn GC-RP, NIKKA SEIKO CO., LTD.) before use.

Star polymer synthesis. All the polymerization reactions were performed in a 100-mL glass reactor with a magnetic stirrer bar under the nitrogen atmosphere. First, the reactor was heated with hot air gun under reduced pressure to remove a trace of moisture and then charged with nitrogen gas. Then prescribed amounts of toluene, NB, O and Oct_3Al/BHT solutions were added in this order into the reactor. The solution was stirred at room temperature for 30 min and then cooled down to 0 °C by an ice-water bath. Finally, the $[Ph_3C][B(C_6F_5)_4]$ (18.6 mg, 20 μmol in 4 mL toluene) and **I** (7.4 mg, 20 μmol in 1 mL toluene) were added successively to start the polymerization. After the NB/O copolymerization was complete, the DoD solution was added to start the synthesis of the cores of star polymer. When NBD and E was added instead of DoD, the E gas was added with NBD solution separately by syringe. The total volume of the solution was 15 mL. After the polymerization was complete, the solution was quenched by methanol with 5 wt.%

of concentrated hydrochloric acid. The polymer was washed with methanol, filtered, and dried at 60 °C under reduced pressure for 3 h. The yields (%) were calculated from the polymer weights and the weight of the monomer used.

Preparation of Sample Films. Polymer films were made by a melt-pressing procedure under 210 °C. After the copolymers were pressed under 20 MPa for 5 min, they were quenched in ice water and separated from the mold. The polymer films with a thickness about 200 μm were used for thermal and tensile measurements.

Analytical Procedures. The number-average molecular weights (M_ns) and molecular weight distributions ($Đ$s) were determined by gel permeation chromatography (GPC HLC-8320, Tosoh Co., Tokyo, Japan) at 40 °C with THF as the solvent. Polystyrene standards were used for calibration. ^{1}H NMR (500 MHz) spectra were recorded at 25 °C by a Varian system500 spectrometer, 16 scans were accumulated with a pulse repetition time of 5.0 s. The copolymer solutions were prepared with chloroform-*d* as the solvent. The central peak (7.26 ppm) of the solvent was used as the internal reference. Thermal gravimetric analysis (TGA) (30–500 °C; 10 °C/min) was performed using a SII TG/DTA 6300 (Hitachi High-technologies Co., Tokyo, Japan). Differential scanning calorimetry (DSC) was performed in nitrogen gas using a SII DSC 6220 (Hitachi High-technologies Co., Tokyo, Japan) with a heating rate of 10 °C/min and a cooling rate of 20 °C/min. The T_g values were determined from the middle point of the phase transition of the second heating scan. Stress–strain curves were recorded using a tensile-testing machine (Model 4466, Instron Japan, Kanagawa, Japan) at 25 °C with an elongation rate of 10 mm/min. Dumbbell-shaped specimens with a width of 4 mm and a gauge length of 10 mm were cut from the sample sheets. Young's modulus values were determined as the slope of the straight line in the first 2 to 5% of elastic region of the stress-strain curve, and the strength and strain at break were determined

from the strain at break point of the sample.

5.3. Results and discussion

Synthesis of star polymers with NB/O gradient segment arms. The star polymers were synthesized by the NB/O copolymerization by **I**-[Ph_3C][$B(C_6F_5)_4$]/Oct_3Al/BHT for 3 min to form the arms first, followed by the post polymerization of dienes for another 60 min or more to form the cores with cross-linked structures. The NB/O copolymerization was almost completed within 3 min (**Table 5-1**, NB/O) to produce the copolymer with a M_n of 38 kg/mol and a $Đ$ of 1.18.

At the beginning, NBD was added alone as the cross-linking agent after NB/O copolymerization (NB/O/NBD adding ratio was 5/5/2, **Table 5-1**, NBD-$(NB/O)_n$). However, the M_n of the obtained polymer only increased to 50 kg/mol, and the GPC curve of the obtained polymer was similar to that of the corresponding arm polymer (**Table 5-1**, NB/O) except a small shoulder peak appeared in the high molar mass region (**Figure 5-1**a,). This result indicated that star polymer was not formed. However, the peaks belonging to the second double bonds of NBD

Table 5-1. Synthesis results of NB/O copolymer arm and star polymers by adding NBD or NBD/E after NB/O copolymerization using **I**-[Ph_3C][$B(C_6F_5)_4$]/Oct_3Al/BHT [a]

sample	NBD/E (mmol/mmol)	t (min)	yield [b] (%)	M_n [c] (kg/mol)	$Đ$ [c]	$M_{n(star)}/M_{n(arm)}$
NB/O	-/-	3	100	34	1.19	-
NBD-$(NB/O)_n$	1.1/-	3 + 60	92	50	1.28	1
(NBD/E)-$(NB/O)_n$-1	1.1/1.6	3 + 60	95	54 (190/36)	2.14	5
(NBD/E)-$(NB/O)_n$-2	1.1/1.6	3 + 120	94	75 (224/38)	2.34	6
(NBD/E)-$(NB/O)_n$-3	2.2/1.6	3 + 60	88	66 (243/39)	2.45	6
(NBD/E)-$(NB/O)_n$-4	1.1/3.2	3 + 60	97	68 (259/34)	2.95	7
(NBD/E)-$(NB/O)_n$-5	1.1/1.6	2.5 + 90	99	73 (226/37)	2.37	6
(NBD/E)-$(NB/O)_n$-6 [d]	1.1/1.6	3 + 120	94	63 (197/36)	2.25	6

[a] Conditions: Ti = 20 μmol, Ti/B/Al = 1/1/1, solvent = toluene, NB/O = 2.7/2.7 mmol/mmol, total volume = 15 mL, T = 0 ºC. [b] Calculated from the weight of the obtained copolymer and the total mass of monomer in feed. [c] Determined by GPC (THF, 40 ºC, polystyrene standards), the M_n values of star polymer and arm polymer were shown in the parentheses. [d] NB/O = 1.8/4.5 mmol/mmol.

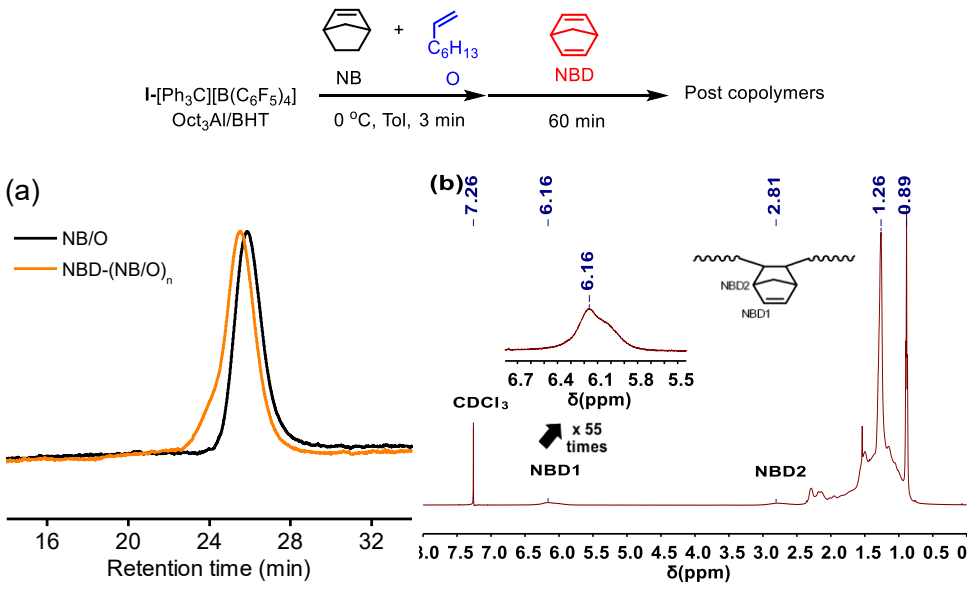

Figure 5-1. (a) GPC curves of NB/O copolymer arm and polymer obtained by adding NBD after NB/O copolymerization using **I**-$[Ph_3C][B(C_6F_5)_4]$/Oct_3Al/BHT; (b) ^1H NMR spectrum of polymer obtained by adding NBD after NB/O copolymerization using **I**-$[Ph_3C][B(C_6F_5)_4]$/Oct_3Al/BHT.

units were detected in the ^1H NMR spectrum of the obtained copolymer (**Figure 5-1**b), which suggested that NBD units was successfully inserted at the end of the NB/O copolymer. The reason why the crosslinking NBD could not be formed should be the steric hindrance of the adjacent NBD units as was expected from the result of NBD homopolymerization with this catalyst.

Then, E was added with NBD as the cross-linking agents after NB/O copolymerization (**Table 5-1**, (NBD/E)-$(NB/O)_n$-1 to -4). In the GPC curves of the obtained polymers (**Figure 5-2**a, b), a new peak bigger than that of the NB/O copolymer arm appeared in high molar mass region, which indicates the formation of star polymers. Moreover, in the typical ^1H NMR spectrum of the obtained polymer (**Figure 5-2**c), the intensity of the peak assignable to the second double bonds in the inserted NBD units became weaker, indicating that the double bonds were involved in the cross-linking reaction. In addition, the weight contents of the star polymer in the product were calculated from the relative integral areas of the fitting curves of the molecular weight distribution curve by the same method applied in Chapter 3, and are shown in **Figure 5-2**a and b. A typical

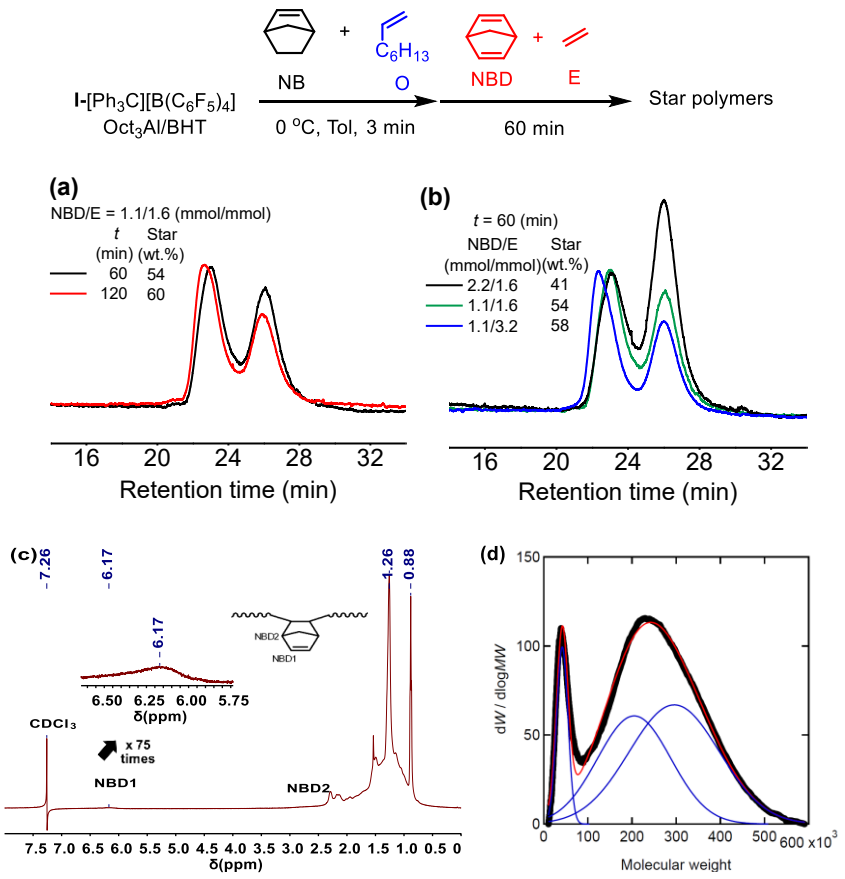

Figure 5-2. GPC curves of star polymers with cross-linked NBD/E copolymer cores and NB/O gradient copolymer arms obtained by **I**-[Ph_3C][$B(C_6F_5)_4$]/Oct_3Al/BHT: (a) different NBD/E copolymerization time; (b) different NBD/E adding ratios. (NB = O =2.7 mmol); (c) typical ^1H NMR spectrum of the obtained star polymer; (d) typical fitting result of GPC curve of the obtained star polymer, where the red line represents the fitting curve from a sum of Gaussian functions (blue lines).

fitting result of the GPC curve of the obtained polymer ((NBD/E)-$(NB/O)_n$-2) is shown in **Figure 5-2**d. When the post polymerization time of NBD/E was extended from 60 min to 120 min, the content of the star polymer increased from 54 wt.% to 60 wt.% (**Figure 5-2**a). The increase of the E/NBD feed ratio from 3/4 to 3/1 also increased the content of star polymer from 41 wt.% to 58 wt.% (**Figure 5-2**b). The M_ns of star polymers increased as the reaction time or E/NBD feed ratio increasing. The ratios of the M_n values of the star polymer and the arm polymer ($M_{n(star)}/M_{n(arm)}$), were also calculated as an approximate of the number of arms in the star polymer (N_{arm}). All the star polymers obtained with different reaction time and different NBD/E feed ratios had similar

$M_{n(star)}/M_{n(arm)}$s of 5 – 7. The star polymer with a NB/O ratio of 2/5 in arms was also synthesized for comparison with the star polymer synthesized in the previous work (**Table 5-1**, (NBD/E)-(NB/O)$_n$-6).

Long chain dienes can also work as the cross-linking agents for the synthesis of star polymers. However, when the 1,7-octadiene (OD) was added after NB/O copolymerization by **I**-[Ph_3C][$B(C_6F_5)_4$]/Oct_3Al/BHT, the M_n of the obtained polymer only increased to 49 kg/mol (**Table 5-2**, OD-(NB/O)$_n$), which was close to that of the arm polymer (38 kg/mol, **Table 5-1**, NB/O). The GPC curve of the obtained polymer shown in **Figure 5-3**a was similar to that of the corresponding arm polymer (**Table 5-1**, NB/O) except the appearance of a shoulder peak in the high molar mass region of the former. This result indicated that only a small fraction of the arms took part in the

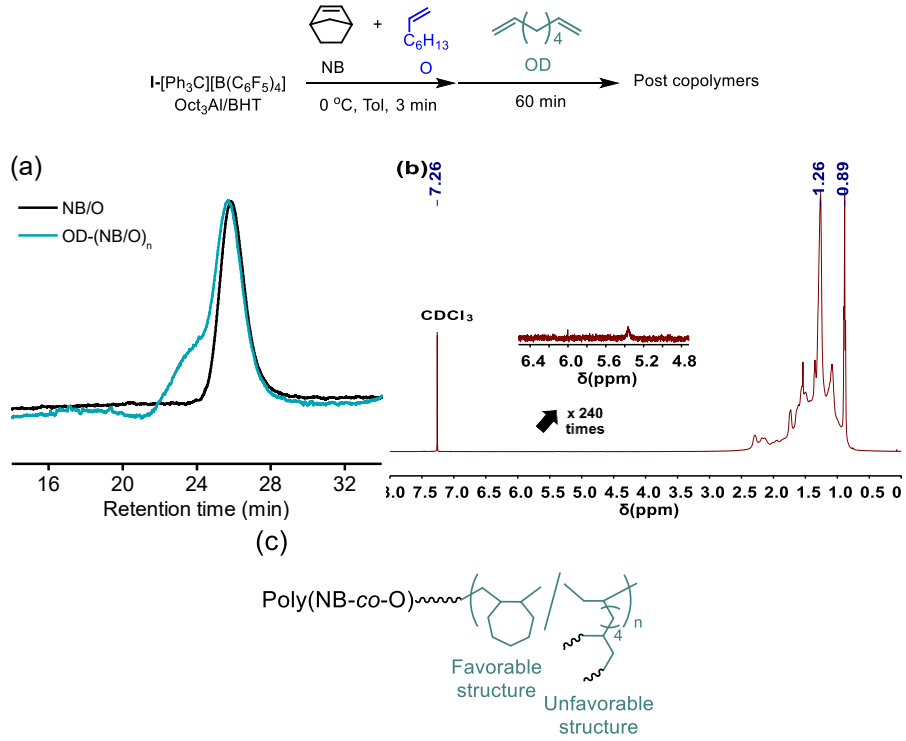

Figure 5-3. (a) GPC curves of NB/O copolymer arm and polymer obtained by adding OD after NB/O copolymerization using **I**-[Ph_3C][$B(C_6F_5)_4$]/Oct_3Al/BHT; (b) ^{1}H NMR spectrum of polymer obtained by adding OD after NB/O copolymerization using **I**-[Ph_3C][$B(C_6F_5)_4$]/Oct_3Al/BHT, and (c) predicted molecular structure of polyOD segment in obtained polymer.

formation of the star polymer. However, in the ^{1}H NMR spectrum of the obtained polymer shown in **Figure 5-3**b, no peak belonging to the C=C double bonds was identified. According to a previous research about the NB/1,5-hexadiene (HD) copolymerization by 1-MMAO/BHT, cyclic structural units formed by HD were detected in the obtained copolymers by ^{13}C NMR.[5] In the research about the polymerization of OD by metallocene-MAO systems, the cycloaddition units of OD were detected by ^{1}H and ^{13}C NMR in the obtained polymers.[6] Thus, the low efficiency of OD for the star polymer formation should be ascribed to the consumption of the pendant vinyl groups by intra cyclization (**Figure 5-3**c).

Therefore, DoD was added instead of OD as the cross-linking agents after NB/O copolymerization (**Table 5-2**, DoD-(NB/O)$_n$-1 to -6). A peak belonging to the star polymer clearly appeared in the GPC curves of the obtained copolymers, of which molecular weight was significantly larger than that of the arm polymer (**Figure 5-4**a, b), indicating that the obtained polymers had high star polymer contents. Only a small peak belonging to the vinyl groups of DoD units was detected by ^{1}H NMR (**Figure 5-4**d). The weight contents of the star polymer in the

Table 5-2. Synthesis results of star polymers by adding OD or DoD after NB/O copolymerization using **I**-[Ph_3C][$B(C_6F_5)_4$]/Oct_3Al/BHT [a]

sample	NB/O (mmol/mmol)	t (min)	yield [b] (%)	M_n [c] (kg/mol)	$Đ$ [c]	$M_{n(star)}/M_{n(arm)}$
OD-(NB/O)$_n$	2.7/2.7	3 + 60	98	49	1.72	1
DoD-(NB/O)$_n$-1	2.7/2.7	3 + 60	100	81 (488/32)	5.10	15
DoD-(NB/O)$_n$-2	2.7/2.7	3 + 120	100	85 (450/35)	5.11	13
DoD-(NB/O)$_n$-3	2.7/2.7	3 + 720	100	130 (500/31)	5.15	16
DoD-(NB/O)$_n$-4	2.7/2.7	3 + 120	100	95 (469/37)	4.73	13
DoD-(NB/O)$_n$-5	2.2/3.3	3 + 120	100	83 (468/34)	5.12	14
DoD-(NB/O)$_n$-6	1.8/3.6	3 + 120	100	90 (467/36)	5.05	13

[a] Conditions: Ti = 20 μmol, Ti/B/Al = 1/1/1, solvent = toluene, DoD = 1.1 mmol, total volume = 15 mL, T = 0 ºC. [b] Calculated from the weight of the obtained copolymer and the total mass of monomer in feed. [c] Determined by GPC (THF, 40 ºC, polystyrene standards), the M_n values of star polymer and arm polymer were shown in the parentheses.

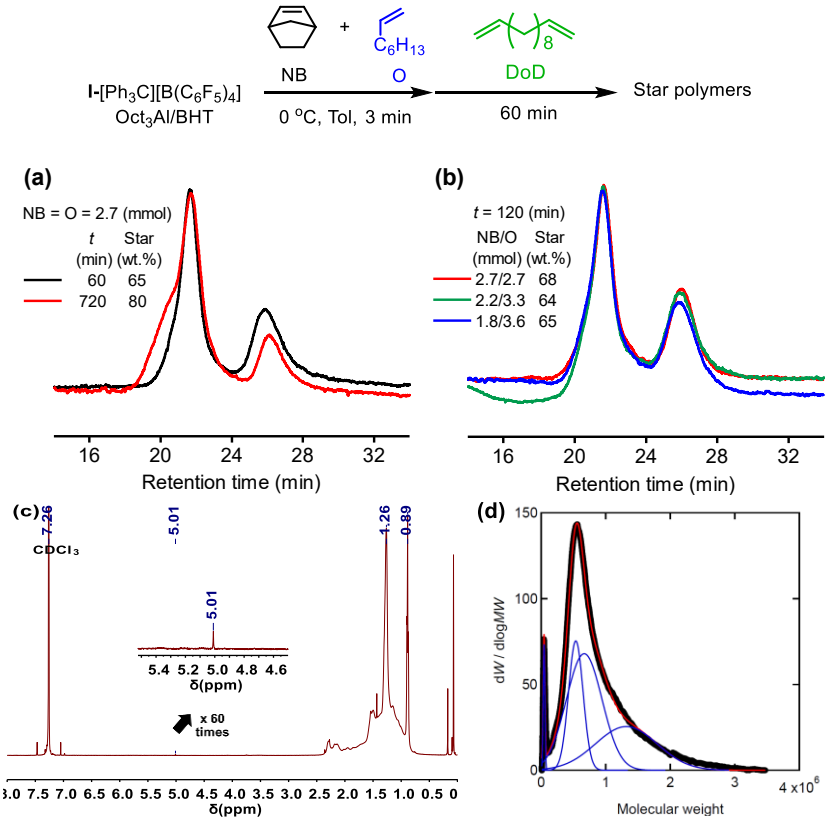

Figure 5-4. GPC curves of star polymers with cross-linked DoD homopolymer cores and NB/O gradient copolymer arms obtained by **I**-[Ph_3C][$B(C_6F_5)_4$]/Oct_3Al/BHT: (a) different DoD polymerization time; (b) different NB/O adding ratios. (DoD = 1.1 mmol); (c) typical ^1H NMR spectrum of the obtained star polymer; (d) typical fitting result of GPC curve of obtained star polymer, where the red line represents the fitting curve from a sum of Gaussian functions (blue lines).

product are shown in the **Figure 5-4**a and b, and a typical fitting result of the GPC curve of the obtained polymer (DoD-(NB/O)$_n$-2) is shown in **Figure 5-4**d. The star polymers obtained by DoD had a $M_{n(star)}/M_{n(arm)}$ value between 13 and 16. When the polymerization time for DoD was extended from 60 min to 720 min, the star polymer content in the obtained copolymer increased from 65 wt.% to 80 wt.%. Meanwhile, a new shoulder peak appeared in higher molar mass region beside the peak of the first star polymer, indicating a possibility for the connection between the cores of the star polymers in the late stage of the reaction (**Figure 5-4**a), and the star polymer had the highest $M_{n(star)}/M_{n(arm)}$ value (16). When the NB/O feed ratio was changed from 1/1 to 1/2 for the synthesis of arm polymer, the weight contents of the star polymer remained unchanged (~ 65

wt.%), indicating that changing the composition of the arm polymer did not affect the $M_{n(star)}/M_{n(arm)}$ in star polymer.

Thermal properties of the star polymers. The DCS curves of the (NBD/E)-$(NB/O)_n$ and DoD-$(NB/O)_n$ star polymers are shown in **Figure 5-5**. Only one T_g in a range from -22 to -18 °C was identified in the curves of all the star polymers. Besides, the DoD-$(NB/O)_n$ star polymers with different NB molar content in the arm segments had similar T_g values. In Chapter 2 and 3, the same DSC results were obtained for the gradient and block NB/O copolymers, but another T_g around 160 °C was detected in DMA test. Thus, it was expected that the star polymers also possessed another T_g higher than 0 °C.

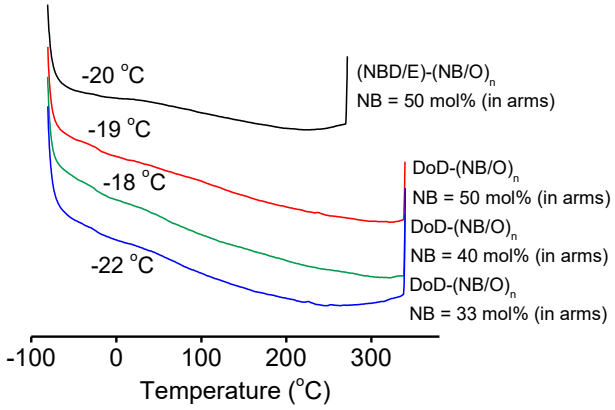

Figure 5-5. Second heating scan of the DSC curves of the (NBD/E)-$(NB/O)_n$ and DoD-$(NB/O)_n$ star polymers (heating rate = 10 °C/min, cooling rate = 20 °C/min).

Mechanical properties of the star polymers. The stress-strain curves of (NBD/E)-$(NB/O)_n$ star polymers (**Table 5-1**, (NBD/E)-$(NB/O)_n$-5 and -6) are shown in **Figure 5-6**. Note that the film of the NB/O gradient polymer corresponding to the NB/O gradient copolymer arms in the star polymer was too brittle for the elongation test. However, the film of (NBD/E)-$(NB/O)_n$-5 (M_w = 173 kg/mol) showed better toughness, and both the strain at break and strength of the (NBD/E)-$(NB/O)_n$-5 were improved compared to the NB/O gradient copolymer with a M_w value

of 76 kg/mol (**Figure 5-6**a). When the NB molar content in the arms of star polymer was decreased from 50 mol% to 29 mol%, the strength of the star polymer ((NBD/E)-(NB/O)$_n$-6) decreased while the strain at break was improved to astonishing 4.5 (**Figure 5-6**a. red line and b. green line). More interestingly, both the strain at break and strength values of the star polymer obtained this work ($M_{n(star)}/M_{n(arm)}$ = 6, M_w = 142 kg/mol) were higher than that of the star polymer with the opposite gradient structure in the NB/O copolymer arms obtained in the previous work[3] (NB = 29 mol%, N_{arm} = 5, M_w = 127 kg/mol) (**Figure 5-6**b).

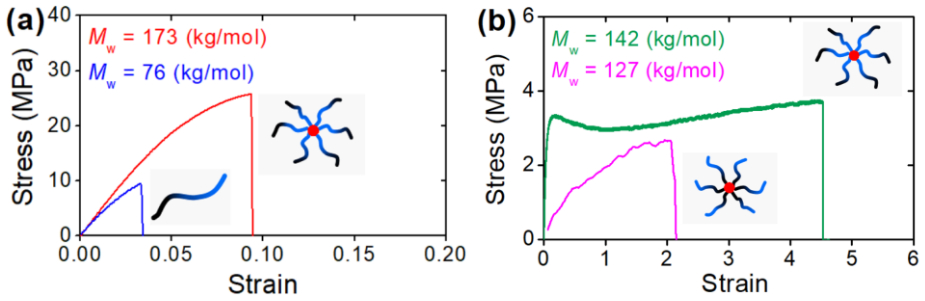

Figure 5-6. Comparation of the stress-strain curves of the (NBD/E)-(NB/O)$_n$ star polymers: (a) the NB/O gradient copolymer with similar M_n value (NB = 50 mol%); (b) the star polymer with similar arm numbers but opposite gradient structure in NB/O copolymer arms obtained in the previous work [3] (NB = 29 mol%).

5.4. Conclusions

Star polymers with gradient norbornene (NB)/1-octene (O) copolymer arms were successfully synthesized by adding 1,11-dodecadiene (DoD) or norbornadiene (NBD)/ethylene (E) as a cross-linking agent after NB/O copolymerization by using (^{t}BuNSiMe$_2$Flu)TiMe$_2$ (**I**)-[Ph$_3$C][B(C$_6$F$_5$)$_4$] with 2,6-di-tert-butyl-4-methylphenol (BHT)-treated tri-*n*-octylaluminium (Oct$_3$Al/BHT). The NB-rich segments were far from the cores of the star polymers, and the O-rich segments were close to the cores. The polymers obtained by adding NBD/E after NB/O copolymerization contained 41 wt.% to 58 wt.% of star polymers, which had approximately 5 – 7 arms. Meanwhile, those polymers obtained by adding DoD after NB/O copolymerization

contained over 64 wt.% of star polymers, which had approximately 13 – 16 arms. Only one T_g below 0 °C was detected by DSC irrespective of the core structures. The mechanical properties of the star polymer were improved compared to the precursor arm and the star polymer possessing opposite NB/O gradient structure with a similar number of arms reported previously. The pure star polymer will be separated from the obtained polymer for further investigation in the future.

References

1 J. M. Ren, T. G. McKenzie, Q. Fu, E. H. Wong, J. Xu, Z. An, S. Shanmugam, T. P. Davis, C. Boyer and G. G. Qiao, *Chem. Rev.*, 2016, **116**, 6743-6836.
2 R. Tanaka, N. Tonoko, S.-i. Kihara, Y. Nakayama and T. Shiono, *Polym. Chem.*, 2018, **9**, 3774-3779.
3 T. Kida, R. Tanaka, K.-h. Nitta and T. Shiono, *Polym. Chem.*, 2019, **10**, 5578-5583.
4 H. Hagihara, T. Shiono and T. Ikeda, *Macromolecules*, 1998, **31**, 3184-3188.
5 R. Tanaka, A. Sasaki, T. Takenaka, Y. Nakayama and T. Shiono, *Polymer*, 2018, **136**, 109-113.
6 N. Naga, T. Shiono and T. Ikeda, *Macromol. Chem. Phys.*, 1999, **200**, 1466-1472.

Chapter 6. Summary

In this thesis, a mixture of trialkylaluminum (R_3Al) with 2 equivalents of 2,6-di-tert-butyl-4-methylphenol (BHT) in toluene (R_3Al/BHT), the average composition formula of $RAl(OAr)_2$ (Ar = 2,6-bis(1,1-dimethylethyl)-4-methylphenyl, R = ^{i}Bu or Oct), was used as a new scavenger with (^{t}BuNSiMe$_2$Flu)TiMe$_2$ (**I**)-[Ph_3C][$B(C_6F_5)_4$] for the synthesis of tailor-made norbornene (NB)/*α*-olefin copolymers.

In Chapter 2, the **I**-[Ph_3C][$B(C_6F_5)_4$]/R_3Al/BHT (R = ^{i}Bu or Oct) system was discovered for a high-speed pseudo-living copolymerization of NB/*α*-olefin. A series of NB/*α*-olefin copolymers (*α*-olefin = 1-octene (O), 1-decene (De) or 1-dodecene (Do)) with controllable molecular weights were quantitatively synthesized at high speed, and the gradient structures of the copolymers were confirmed. Transparent films were made from the copolymers by melt-pressing, and the mechanical properties of these copolymer films were controlled by the choice of *α*-olefin, the monomer molar content and the molecular weight.

In Chapter 3, NB/*α*-olefin (O or Do) block copolymers with a gradient structure in each isometric block were quantitatively synthesized at high speed through NB/*α*-olefin pseudo-living copolymerization by the **I**-[Ph_3C][$B(C_6F_5)_4$]/Oct_3Al/BHT system. The strain at break of the NB/*α*-olefin block copolymer with moderate block length was massively improved without losing strength compared to the corresponding gradient copolymer.

In Chapter 4, norbornadiene (NBD) homopolymerization and NB/NBD/O terpolymerization were conducted by different combinations of **I** or [^{t}BuNSiMe$_2$(2,7-^{t}Bu$_2$Flu)]TiMe$_2$ (**II**) with MMAO/BHT or [Ph_3C][$B(C_6F_5)_4$]/^{i}Bu$_3$Al/BHT. As a result, pendant NBD homopolymers and NB/NBD/O terpolymers with good solubility were obtained in high yield

without cross-linking. The double bonds in the inserted NBD units in these polymers can be used for further functionalization and cross-linking reactions.

In Chapter 5, star polymers with the arms of NB/O gradient copolymer and the core of cross-linked NBD/E copolymer or cross-linked 1,11-dodecadiene (DoD) polymer were synthesized by the "arm-first" strategy in one pot using the **I**-[Ph_3C][$B(C_6F_5)_4$]/Oct_3Al/BHT system. The NB-rich segments were far from the cores of star polymer, and the O-rich segments were closed to the cores. The number-average molecular weight ratios ($M_{n(star)}/M_{n(arm)}$s) of the star polymers and arm polymers and the contents of the star polymers in the products were depended on the choice of monomer (NBD/E or DoD) used for the synthesis of cross-linked cores. When DoD was used, the star polymers with higher $M_{n(star)}/M_{n(arm)}$ values were obtained in higher contents. Both the strain at break and strength of the star polymer were improved compared to the precursor arm copolymer. And the star polymers with opposite gradient structures in the NB/O copolymer arms were found to have totally different mechanical properties.

The NB/α-olefin gradient, block and star copolymers with improved mechanical properties synthesized in this thesis will broaden the application range of COCs.

List of Publications

Chapter 2:

Synthesis and Properties of Gradient Copolymers Composed of Norbornene and Higher *α*-Olefins Using an *ansa*-Fluorenylamidodimethyltitanium-[Ph_3C][$B(C_6F_5)_4$] Catalyst System

Haobo Yuan, Takumitsu Kida, Hyunchul Kim, Ryo Tanaka, Zhengguo Cai, Yuushou Nakayama and Takeshi Shiono

Macromolecules **2020**, *53* (11), 4323-4329

Chapter 3:

Synthesis and Properties of Block Copolymers Composed of Norbornene/Higher -Olefin Gradient Segments Using *ansa*-Fluorenylamidodimethyltitanium–[Ph_3C][$B(C_6F_5)_4$] Catalyst System

Haobo Yuan, Takumitsu Kida, Ryo Tanaka, Zhengguo Cai, Yuushou Nakayama and Takeshi Shiono

Polymer Chemistry, accepted.

Chapter 4:

Norbornadiene Homopolymerization and Norbornene/norbornadiene/1-octene Terpolymerization by *ansa*-Fluorenylamidodimethyltitanium–based Catalysts

Hongyi Suo, Haobo Yuan, Ryo Tanaka, Yuushou Nakayama, Wen-Hua Sun and Takeshi Shiono

Polymer Chemistry **2020**, *11* (42), 6803-6810

Presentations in International Conferences:

Ring-opening polymerization of macrocyclic oligocarbonates with phosphazene superbase

Haobo Yuan, Ryo Tanaka, Yuushou Nakayama, Takeshi Shiono

The 8th Joint Conference on Renewable Energy and Nanotechnology (JCREN), **2019**, GI 4. (Makassar, Indonesia)

Synthesis and Properties of Gradient Copolymers Composed of Norbornene and Higher *α*-olefins Using *ansa*-Fluorenylamidodimethyltitanium / $Ph_3CB(C_6F_5)_4$ Catalyst System

Haobo Yuan, Takumitsu Kida, Ryo Tanaka, Yuushou Nakayama, Takeshi Shiono

The 8th Asia Polyolefin Workshop (APO), **2019**, P061. (Hiroshima, Japan)

Presentations in Domestic Conferences:

Synthesis and Properties of Gradient Copolymers Composed of Norbornene and Higher α-olefins Using *ansa*-Fluorenylamidodimethyltitanium/$Ph_3CB(C_6F_5)_4$ Catalyst System

Haobo Yuan, Ryo Tanaka, Yuushou Nakayama, Takeshi Shiono

The 49th Petroleum-Petrochemical Symposium of Jpn. Petrol. Inst. (Yamagata Convention) 2019

Volume 2019f 2G03

Synthesis and Properties of Block Copolymers Composed of Norbornene/*α*-Olefin Gradient Segments Using *ansa*-Fluorenylamidodimethyltitanium–$[Ph_3C][B(C_6F_5)_4]$

Haobo Yuan, Takumitsu Kida, Ryo Tanaka, Yuushou Nakayama and Takeshi Shiono

The 69th Symposium on Macromolecules of Society Polymer Science, Japan (SPSJ), **2020**, 3ESA05.

Synthesis and Properties of Star Polymers with Norbornene/*α*-olefins Gradient Copolymer Arms Using *ansa*-Fluorenylamidodimethyltitanium-$Ph_3CB(C_6F_5)_4$ Catalyst System

Haobo Yuan, Ryo Tanaka, Yuushou Nakayama, Takeshi Shiono

The 50th Petroleum-Petrochemicals Symposium of Jpn. Petrol. Inst. (Kumamoto Convention), **2020**, 2B11.

Acknowledgments

Here, the author gives the greatest thanks to Prof. Shiono Takeshi, Prof. Yuushou Nakayama and Prof. Ryo Tanaka for the theoretical and experimental guidance, and Dr. Takumitsu Kida and Dr. Hongyi Suo (Chinese Academy of Sciences) for their cooperation. This thesis was successfully completed with their dedicated help.

The author is also grateful to Tosoh Finechem Co. Ltd. for their donation of chemicals, such as borate, aluminoxanes and trialkylaluminums, and Daicel Corporation for their experimental support with the SPM tests. Thank Prof. Kohhei Nitta from Kanazawa University for the experimental support with the tensile tests and the DMA tests.

The author also gratefully acknowledges Prof. Zhengguo Cai for giving the recommendation to Prof. Shiono Takeshi in the first place, and again Prof. Shiono Takeshi and Prof. Yuushou Nakayama for the financial support during the hole PhD program. It has been a great honor.

At last, the author wants to express gratitude to the lab members, friends, and family for their daily and mental support.